2007-04-01

Characterisation of the Aldo Keto Reductase from Helicbacter pylori.

Denise Cornally
Technological University Dublin, denisecornally@yahoo.com

Recommended Citation

Cornally, D. (2007). *Characterisation of the Aldo Keto Reductase from Helicbacter pylori*. Doctoral thesis. Technological University Dublin. doi:10.21427/D7X89R

Characterisation of the Aldo Keto Reductase from *Helicobacter pylori*

A THESIS SUBMITTED TO DUBLIN INSTITUTE OF TECHNOLOGY IN FULLFILMENT OF THE REQUIREMENTS FOR THE DEGREE OF

DOCTOR OF PHILOSOPHY

Denise Cornally B.Sc.

School of Food Science and Environmental Health
Dublin Institute of Technology,
Marlborough St.,
Dublin 1.

April 2007
(Volume 1 of 1)

Research Supervisors: Dr. Gary Henehan, Dr. Henry Windle and Dr. Ciaran McDonnell

Abstract

Aldo keto reductases reversibly reduce toxic aldehydes to their corresponding alcohol products. The aldo-keto reductase from *Helicobacter pylori* (HpAKR) was cloned and expressed in *Escherichia coli* as a His-tag fusion protein and purified using nickel chelate chromatography. The enzyme is a monomer with a molecular mass of approximately 39 kDa. It reduces a broad range of aldehyde substrates with a high catalytic efficiency and exhibits dual co-factor specificity for both NADH and NADPH. HpAKR can function over a broad pH range (pH 4-9) with a pH optimum of 5.5. Inhibition of AKR activity was observed with sodium valproate.

Generation of an isogenic HpAKR negative mutant of *H. pylori* demonstrated that HpAKR is required for growth under acidic conditions, suggesting a role in acid adaptation.

This study also examines the growth of a cinnamyl alcohol dehydrogenase (HpCAD) knockout mutant under acid conditions. It was surprising that despite previous reports that HpCAD is upregulated under acid growth conditions, that the knockout showed enhanced growth at acid pH.

Taken together these data indicate that these aldehyde metabolising enzymes may have an important role in *H. pylori* in acid adaptation in addition to their role as aldehyde metabolising enzymes.

Preliminary studies on a short chain alcohol dehydrogenase from *H. pylori* (HpSCADH) are also presented.

I certify that this thesis which I now submit for examination for the award of Doctor of Philosophy, is entirely my own work and has not been taken from the work of others save and to the extent that such work has been acknowledged within the text of my work.

This thesis was prepared according to the regulations for postgraduate study by research of the Dublin Institute of Technology and has not been submitted in whole or in part for an award in any other Institute or University.

The work reported in this thesis conforms to the principles of the Institutes guidelines for ethics in research.

The Institute has permission to keep, to lend or to copy this thesis in whole or in part, on condition that any use of the material of the thesis is acknowledged.

Signature Denise Carney **Date** 4/4/07

Acknowledgements

I would like to thank Gary Henehan and Henry Windle for their tremendous amount of guidance and tireless effort through out my research. A huge thanks to Keith Tipton for all of his help with the enzyme kinetic analysis and Ciaran McDonnell for his continuously positive attitude and support. Thanks to Dermot Kelleher for the use of his laboratory and facilities.

I would also like to thank my parents and sisters for all of their support over the years. A special thanks to Ian Brooks for his exceptional IT skills and patience since the start of my studies.

I am extremely grateful to all of the laboratory technicians in DIT (Marlborough Street), especially Noel Grace who is the best Lab Tech in the world! To all of the Post Grads in DIT, thank you for all the craic and I wish you the best of luck in completing your research. I am going to miss you guys.

A special thank you to Carmel Cremin for bringing more humour to the protein chemistry lab in St. James's hospital. Thanks also to all of the Post Grads and Post Docs in the Trinity Centre for Health Sciences, St. James Hospital, for all of their help, support and endless laughter at lunch breaks. It is sad to say goodbye.

Finally, a huge thanks to Blanaid Mee for the unbelievable amount of guidance throughout my project. Without your help, I would have been lost! The craic we had in the lab made it one of the best places to work in, which I will always remember.

Abbreviations

ADH:	Alcohol dehydrogenases
AKR:	Aldo keto reductases
APS:	Ammonium persulfate
Asp:	Aspartate
BSA:	Bovine Serum Albumin
CagA:	Cytotoxin associated protein
Cag PAI:	Cag pathogenicity island
CAD:	Cinnamyl alcohol dehydrogenase
CFU:	Colony forming units
DENT:	*H. pylori* antibiotic media supplement
DTT:	Dithiothreitol
DL-Gly:	D,L glyceraldehyde
E.coli:	*Escherichia coli*
EDTA:	Ethylenediaminetetraacetic acid
H. pylori:	*Helicobacter pylori*
HCl:	Hydrochloric acid
His:	Histidine
HSD:	Hydroxysteroid dehydrogenases
IEF:	Ioselectric focusing
IPTG:	Isopropyl β-D-thiogalactoside
kDa:	Kilo dalton
Lys:	Lysine
MALT:	mucosa-associated lymphoid tissue
MeGly:	Methylglyoxal

NADH:	Nicotinamide adenine dinucleotide, reduced form
NADPH:	Nicotinamide adenine dinucleotide phosphate, reduced form
NMA:	No measurable activity
4-NBA:	4-nitrobenaldehyde
OD:	Optical density
ORF:	Opening reading frame
PBS:	Phosphate buffered saline
PCR:	Polymerase chain reaction
PPI:	Protein pump inhibitor
9,10 PQ:	9,10 phenanthrenequinone
PVDF:	Polyvinylidene Fluoride
RPM:	Rotations per minute
SCADH:	Short chain alcohol dehydrogenase
SDS-PAGE	Sodium dodecyl sulphate polyacrylamide gel electrophoresis
SEM:	Standard error of the mean
TIGR:	The Institute of Genomic Research
VacA:	Vacuolating cytotoxin

Table of Contents

List of Figures

List of Tables

Chapter 1

Introduction

1.0 Introduction

1.1 Aldo Keto Reductase (AKR)

1.1.1 Introduction

Aldo keto reductases (AKR) are a class of enzymes that reversibly reduce toxic aldehydes and ketones to their corresponding alcohol product. The catalysed reaction favours alcohol formation whereas the reverse reaction only occurs to a limited extent (Kuhn *et al.*, 1995)

$$\text{Aldehyde or Ketone} + \text{NADPH} + H^+ \rightleftharpoons RCH_2OH + NADP^+$$

The AKRs are proteins, approx 35kDa in size, that utilise a nicotinamide co-factor but are lacking a Rossmann-fold motif that is present in the related alcohol dehydrogenases (Fig. 1.1) (Jez *et al.*, 1997). These proteins are generally monomeric with the exception of the dimeric mammalian AKR7 enzymes and some dimeric xylose reductases (Ellis, 2002). AKRs are found in mammals, amphibians, plants, yeast, protozoa and bacteria. These proteins break down a diverse range of substrates including aliphatic and aromatic aldehydes, monosaccharides, steroids, prostaglandins, polycyclic aromatic hydrocarbons and isoflavinoids (Jez *et al.*, 1997, Hyndman *et al.*, 2003).

Aldehydes, ketones and quinones are present in synthetic compounds and are produced through normal oxidative and deamination reactions, which occur in all living organisms. A build-up of aldehydes within the cell can have a potentially toxic and/or mutagenic effect. Aldehydes have been shown to react with and modify the nucleophilic centres of nucleic acids and proteins leading to their inactivation (Matsunaga *et al.*, 2006). However, the presence of detoxifying enzymes such as members of the AKR

family can protect cells from these compounds (Ellis *et al.*, 1995). There is usually more than one member of the AKR superfamily present in a cell suggesting these proteins have evolved to perform specific roles in different cells (Ellis., 2002).

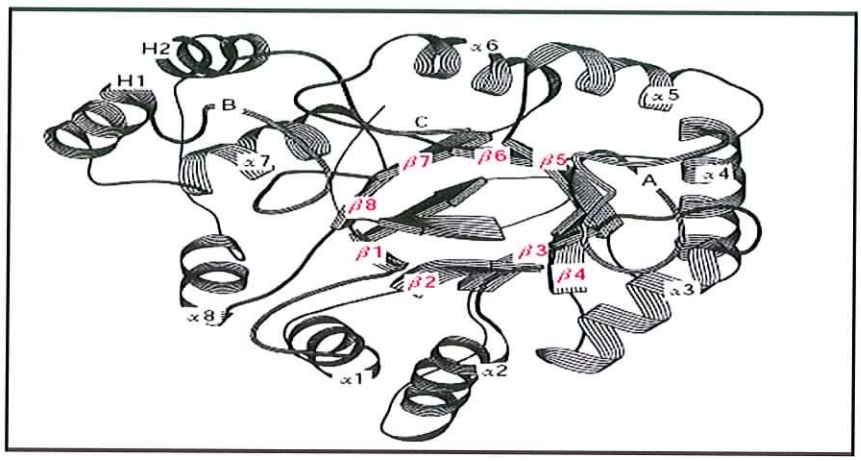

Fig. 1.1: A representative three-dimensional structure for AKRs (Jez *et al.*, 1997).

1.1.2 AKR Superfamily Nomenclature

The aldo keto reductases are a family of related enzymes, which share structural and functional features. Originally, members were identified based on substrate specificity. However the overlap in substrate activity, led to some confusion. Following expansion of the family, a nomenclature was established in 1997 (Jez *et al.*, 1997), which was updated in 2001 (Jez *et al.*, 2001). The nomenclature is based on amino acid sequence similarity. The AKR superfamily is divided into 15 families, named AKR1-AKR15, and within these, subfamilies are denoted by a letter, and each individual enzyme is assigned a number for unique identification (Ellis. 2002). To become a member, an enzyme has to be shown to have been expressed and possess aldehyde reductase activity. Each family must have at least 40% amino acid identity with other family members. Within a given family, subfamilies are defined as possessing greater than 60% identity in amino

acid sequence among subfamily members. In 2003, a website (www.med.upenn.edu/akr) was established to allow for submission of AKR sequences so assign membership to a specific family (Hyndman *et al.*, 2003). An overview of the information available on the website is shown in Fig. 1.2.

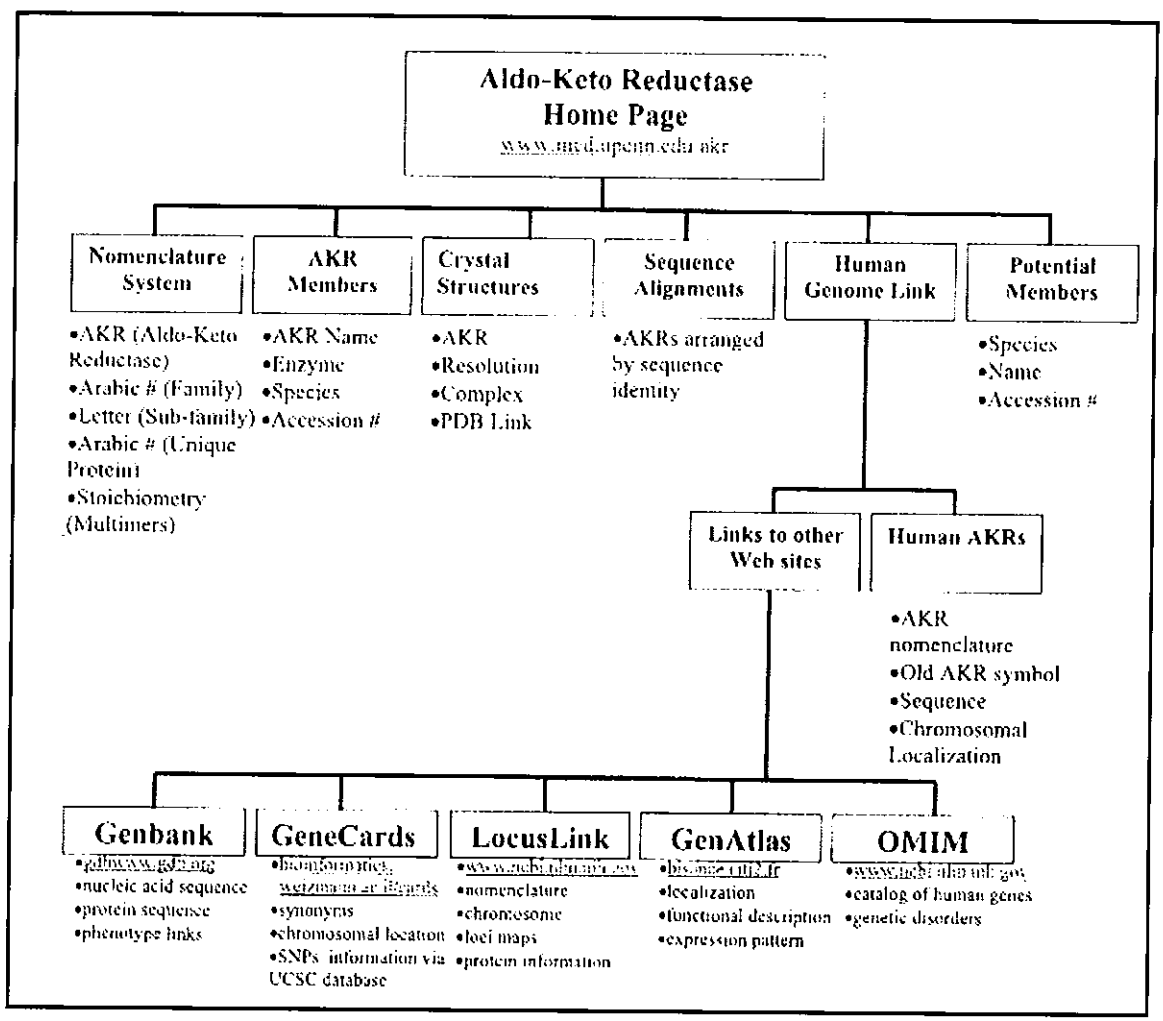

Fig. 1.2: Flowchart of information available on the AKR website (Hyndman *et al.*, 2003).

Specific information regarding single AKR family members is also available once an AKR sequence has been submitted to the AKR website. For example, Fig. 1.3 illustrates the data for the human aldehyde reductase or AKR1A1.

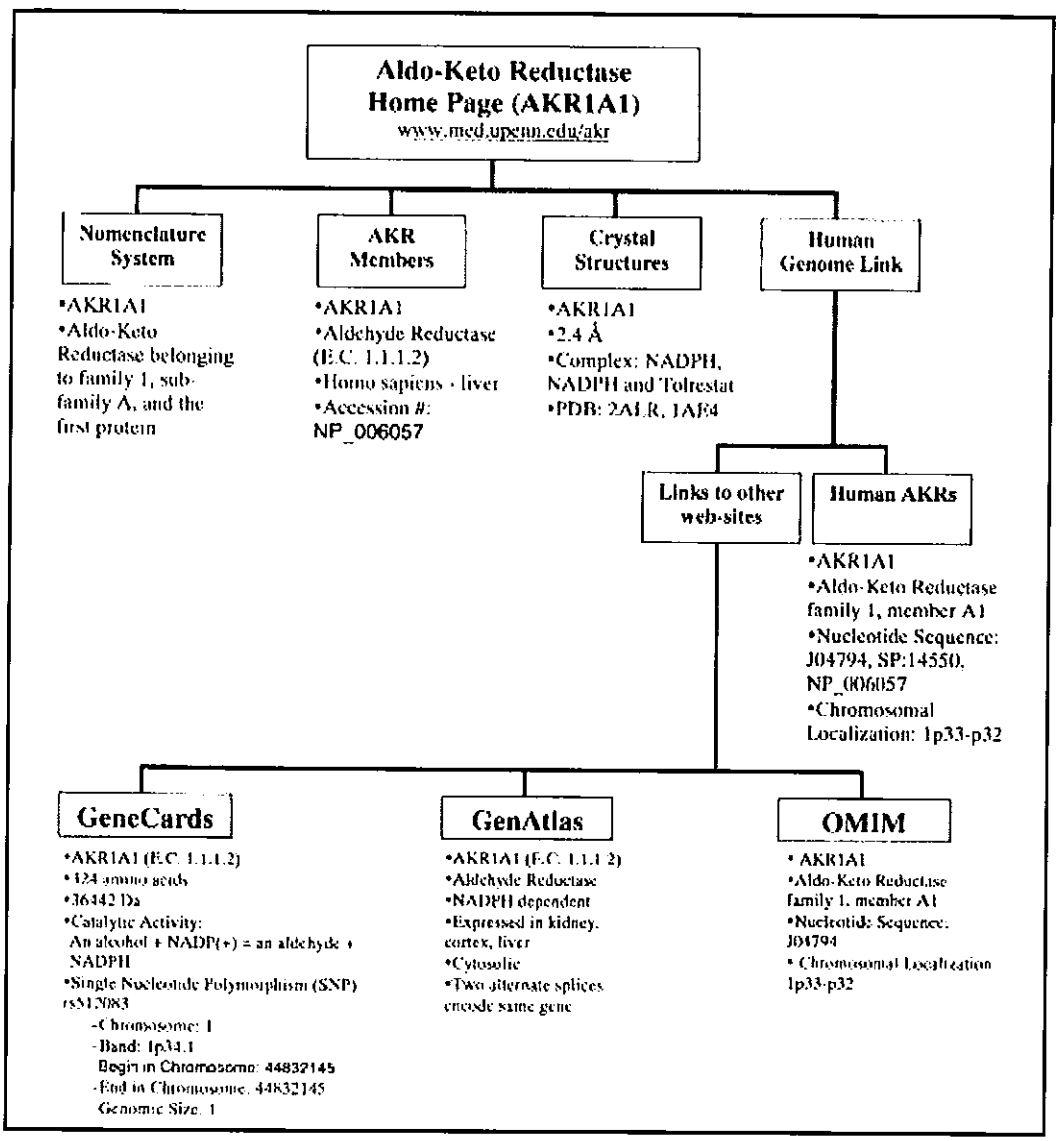

Fig. 1.3: Flowchart of information available specifically for AKR1A1 from the AKR website. This level of information is available for all AKRs submitted to the AKR superfamily website.

As stated above, there are 15 AKR families of which AKR1 is the largest. This family comprises a wide variety of members including: the aldose reductases, the aldehyde reductases, the hydroxysteroid dehydrogenases and steroid 5β- reductases. There is considerable diversity among AKR amino acid sequences meaning that family classification generally includes AKRs from more than one species. For example, microbial AKRs span 10 families: AKR2, AKR3, AKR5 and AKR8-14 (Ellis EM., 2002). Table 1.1 is a summary of all characterised AKRs however, there are a further 200 putative AKRs that have been identified through genome sequencing (Hyndman *et al.*, 2003) which, once characterised, can then be assigned membership.

AKR	Enzyme	Species
1A1	aldehyde reductase	*Homo sapiens* – liver
1A2	aldehyde reductase	*Sus scrofa*
1A3	aldehyde reductase	*Rattus norvegicus* – liver
1A4	murine liver aldehyde reductase	*Mus musculus*
1B1	aldose reductase	*Homo sapiens* – placenta
1B2	aldose reductase	*Oryctolagus cuniculus* – kidney
1B3	aldose reductase	*Mus musculus*
1B4	aldose reductase	*Rattus norvegicus* – lens
1B5	aldose reductase (bovine 20α-HSD)	*Bos taurus* – lens/testis
1B6	aldose reductase	*Sus scrofa* – lens
1B7	aldose reductase related protein 1androgen-dependent vas deferens protein	*Mus musculus*
1B8	fibroblast growth factor induced protein	*Mus musculus*
1B9	inducible-aldo-keto reductase from CHO cells	*Cricetulus griseus*
1B10	small intestine reductase	*Homo sapiens* – small intestine *Homo sapiens* – liver
1B12	chicken aldo-keto reductase	*Gallus domesticus* – eye, tongue, esophagus
1B13	aldose reductase-like gene	*Rattus norvegicus*
1C1	20 α -HSD	*Homo sapiens* – liver
1C2	3 α -HSD type III	*Homo sapiens* – liver
1C3	3 α -HSD type II	*Homo sapiens* – liver

Table 1.1 continued...

AKR	Enzyme	Species
1C4	3 α -HSD type I	*Homo sapiens* – liver
1C5	Prostaglandin E2 reductase;	*Oryctolagus cuniculus* – ovary
1C6	Estradiol 17β-HSD	*Mus musculus* – liver
1C7	Prostaglandin F synthase 1	*Bos taurus* – lung
1C8	20 α -HSD	*Rattus norvegicus* – ovary
1C9	3 α -HSD	*Rattus norvegicus* – liver
1C10a	rho-crystallin	*Rana temporaria* – lens
1C10b	rho-crystallin	*Rana temporaria* – lens
1C11	prostaglandin F synthase 2	*Bos taurus* – liver
1C12	aldo-keto reductase 1C12	*Mus musculus*
1C13	interleukin-3-regulated AKR	*Mus musculus*
1C14	AKR	*Mus musculus*
1C15	rat AKR C	*Rattus norvegicus*
1C16	rat AKR B	*Rattus norvegicus*
1C17	rat AKR D	*Rattus norvegicus*
1C18	murine 20 α -HSD	*Mus musculus*
1C19	murine 3(20 α)-HSD	*Mus musculus*
1C20	murine dihydrodiol dehydrogenase	*Mus musculus*
1C21	HSD	*Mus musculus*
1C22	dihydrodiol dehydrogenase	*Mus musculus*
1C23	17b(20 α)-hydroxysteroid dehydrogenase	*Equine*
1C24	17b-hydroxysteroid dehydrogenaset butyl-2, 3-epoxy-5-cyclohexene-1 4-dionereductase	*Rattus norvegicus*
1D1	D4-3-ketosteroid-5b-reductase	*Homo sapiens* – liver
1D2	D4-3-ketosteroid-5b-reductase	*Rattus norvegicus* – liver
1D3	D4-3-ketosteroid-5b-reductase	*Oryctolagus cuniculus*
1E1	mouse liver keto-reductase	*Mus musculus*
1G1	Aldo-keto reductase	*Caenorhabditis elegans*
2A1	NADP+-dependent sorbitol-6-phosphate reductase	*Malus domestica*
2A2	NADPH-dependent mannose -6-phosphate reductase	*Apium graveolens*
2B1	NAD(P)H dependent xylose reductase	*Pichia stipitis*
2B2	NAD(P)H dependent xylose reductase	*Kluyveromyces lactis*
2B3	NAD(P)H dependent xylose reductase	*Pachysolen tannophilus*
2B4	NAD(P)H dependent xylose reductase	*Candida tropicalis*
2B5	NAD(P)H dependent xylose reductase	*Candida tenuis*
2B6	Gre3p	*Saccharomyces cerevisiae*
2B7	xylose reductase	*Candida tropicalis*
2B8	xylose reductase	*Pichia guilliermondii*

Table 1.1 continued...

AKR	Enzyme	Species
2C1	4-dihydromethyltrisporate dehydrogenase	*Mucor mucedo*
2D1	D-xylose reductase	*Aspergillus niger*
2E1	3-dehydroecdysone 3b-reductase	*Spodoptera littoralis*
2E2	3-dehydroecdysone 3b-reductase	*Trichoplusia ni*
2E3	DL-glyceraldehyde reductase	*Drosophila melanogaster*
3A1	Gcy1p	*Saccharomyces cerevisiae*
3A2	2-methylbutyraldehyde reductase: Ypr1p	*Saccharomyces cerevisiae*
3B1	NADPH dependent aldehyde reductase	*Sporidiobolus salmonicolor*
3B2	erthyrose reductase ½	*Trichosporonoides megachilieni*
3B3	erthyrose reductase 3	*Trichosporonoides megachilieni*
3C1	Ara1p - arabinose dehydrogenase	*Saccharomyces cerevisiae*
3C2	isatin reductase	*Saccharomyces pombe*
3C3	polyketone reductase	*Candida parpsilosis*
3D1	aldose reductase	*Magnaporthe grisea*
3E1	b-ketoester reductase	*Pencillium citrinum*
3F1	D,L-glyceraldehyde reductase	*Thermotoga maritime*
3F2	2,5-diketo-D-gluconic acid reductase B	*Escherichia coli*
3F3	isatin reductase	*Sinorhizobium meliloti*
4A1	NAD(P)H dependent 6'- eoxychalcone synthase	*Glycine max*
4A2	chalcone polyketide reductase	*Medicago sativa*
4A3	chalcone polyketide reductase	*Glycyrrhiza echinata*
4A4	chalcone polyketide reductase	*Glycyrrhiza glabra*
4B1	chalcone polyketide reductase	*Sesbania rostrata*
4B2	NADPH-dependent codeine reductase	*Papaver somniferum*
4B3	codeinone reductase	*Papaver somniferum*
4B4	D-galacturonate reductase	*Fragaria ananassa*
4B5	deoxymugineic acid synthase1	*Zea mays*
4B6	deoxymugineic acid synthase1	*Oryza sativa*
4B7	deoxymugineic acid synthase1	*Hordeum vulgare*
4B8	deoxymugineic acid synthase1	*Triticum aestivum*
4C1	aldehyde reductase	*Hordeum vulgare*
4C2	aldehyde reductase	*Bromus inermis*
4C3	aldehyde reductase	*Avena fatua*
4C4	aldehyde reductase	*Xerophyta viscose*
4C5	aldose reductase	*Digitalis purpurea*
4C6	aldose reductase	*Digitalis purpurea*
4C7	aldehyde reductase	*Zea mays*
4C8	reductase	*Arabidopsis thaliana*
4C9	reductase	*Arabidopsis thaliana*
4C10	reductase	*Arabidopsis thaliana*

Table 1.1 continued...

AKR	Enzyme	Species
4C11	reductase	*Arabidopsis thaliana*
5A1	reductase	*Leishmania major*
5A2	prostaglandin F synthase	*Trypanosoma brucei*
5B1	morphine dehydrogenase	*Pseudomonas putida*
5C1	2,5-diketo-D-gluconic acid reductase	*Corynebacterium sp*
5C2	2,5-diketo-D-gluconic acid reductase	*E. coli*
5D1	2,5-diketo-D-gluconic acid reductase	*Corynebacterium sp*
5E1	2,5-diketo-D-gluconic acid reductase	*Zymomonas mobilis*
5F1	2,5-diketo-D-gluconic acid reductase	*Klebsiella*
6A1	Shaker channel β-subunit	*Bos Taurus*
6A2	Shaker channel β -subunit	*Rattus norvegicus*
6A3	Shaker channel β -subunit	*Homo sapiens*
6A4	Shaker channel β -subunit	*Mus musculus*
6A5	Shaker channel β -subunit	*Homo sapiens*
6A6	Shaker channel β -subunit	*Oryctolagus cuniculus*
6A7	Shaker channel β -subunit	*Oryctolagus cuniculus*
6A8	Shaker channel β -subunit	*Mus musculus*
6A9	Shaker channel β -subunit	*Homo sapiens*
6A10a	Shaker channel β -subunit	*Mustela putorius*
6A10b	Shaker channel β -subunit	*Oryctolagus cuniculus*
6A11	Shaker channel β -subunit	*Xenopus laevis*
6A12	Shaker channel β -subunit	*Rattus norvegicus*
6B1	Shaker channel β -subunit	*Drosophila melanogaster*
6C1	Shaker channel β -subunit	*Arabidopsis thaliana*
6C2	Shaker channel β -subunit	*Egeria densa*
7A1	Rat aflatoxin aldehyde reductase	*Rattus norvegicus – liver*
7A2	Human aflatoxin aldehyde reductase	*Homo sapiens – liver*
7A3	Human aflatoxin aldehyde reductase	*Homo sapiens – liver*
7A4	Rat aflatoxin aldehyde reductase	*Rattus norvegicus*
7A5	Mouse aflatoxin aldehyde reductase	*Mus musculus*
8A1	pyridoxal reductase	*Schizosaccharomyces pombe*
8A2	pyridoxal reductase	*Schizosaccharomyces pombe*
9A1	sterogmatocystin dehydrogenase	*Aspergillus nidulans*
9A2	norsolorinic acid reductase	*Aspergillus flavus*
9A3	aryl-alcohol dehydrogenase	*Phanerochaete chrysosporium*
9B1	aryl-alcohol dehydrogenase	*Saccharomyces cerevisiae*
9B2	aryl-alcohol dehydrogenase	*Saccharomyces cerevisiae*
9B3	aryl-alcohol dehydrogenase	*Saccharomyces cerevisiae*
9B4	aryl-alcohol dehydrogenase	*Saccharomyces cerevisiae*
9C1	reductase	*Haloferax volcanii*
10A1	bluensomycin aldo keto reductase	*Streptomyces bluensis*

Table 1.1 continued...

AKR	Enzyme	Species
10A2	streptomycin akr	*Streptomyces glaucescens*
11A1	vegetative protein 147	*Bacillus subtilis*
11B1	general stress protein 69	*Bacillus subtilis*
11B2	methylgloxal reductase	*E. coli*
11B3	methylglyoxal reductase	*Synechococcus sp*
11C1	aldo-keto reductase	*Bacillus halodurans*
12A1	NDP-hexose-2,3-enoyl-reductase TylCII	*Streptomyces fradiae*
12B1	mycarose/desosamine reductase EryBII	*Saccharopolyspora erythraea*
12C1	dTDP-4-keto-6-deoxy-L-hexose-2,3-reductase	*Streptomyces avermitilis*
13A1	YakC aldo-keto reductase	*Schizosaccharomyces pombe*
13B1	Phenylacetaldehyde dehydrogenase	*Xylella fastidiosa*
13C1	Aldehyde reductase	*Helicobacter pylori*
14A1	*E. coli* aldehyde reductase	*Escherichia coli*
15A1	Pyridoxal dehydrogenase	*Microbacteriun luteolum*

Table 1.1: Characterised members of the aldo keto reductase superfamily adapted from the AKR superfamily website dated January 2007 (www.med.upenn.edu/akr).

1.1.3 Classes of Aldo Keto Reductases

Four distinct subfamilies exhibit the properties typical of the aldo keto reductases:

(i) Aldose reductases which catalyse the reduction of aldehydes, but especially glycoaldehydes and polyolaldehydes

(ii) Aldehyde reductases which catalyse the reduction of a variety of aldehydes

(iii) Carbonyl reductases, which catalyse the reduction of quinones, other ketones and aldehydes to their corresponding alcohols

(iv) Hydroxysteroid dehydrogenases, which catalyse the reduction of various steroid hormones

(i.) Aldose Reductase

Aldose reductases, members of the AKR superfamily, exhibit properties similar to other AKRs. These enzymes fall into the general category of aldehyde reductase but are specifically referred to as aldose reductases since their substrate preference is for aldo sugars, unlike other aldehyde reductases (Cromlish *et al.*, 1983). These proteins were first identified in 1956 as glucose reducing enzymes but later were reported to be present in the rat lens during severe diabetic onset (Srivastava *et al.*, 2005).

In mammals, aldose reductases play a key role in the polyol pathway (Fig. 1.4) where they catalyse the reduction of D-glucose to D-sorbitol. The accumulation of D-sorbitol in the eye is believed to contribute to diabetic complications (Kubiseski *et al.*, 1995). The polyol pathway requires the presence of two enzymes: aldose reductase and sorbitol dehydrogenase (a short chain alcohol dehydrogenase). Research linking an enhanced polyol pathway to diabetes has been mainly carried out in animals where the severity of the disease can be altered by pharmacologic blockage or genetic enhancement of aldose

reductase activity. Even though there has been great success with these studies using aldose inhibitors as a method of prevention/cure for diabetes in animals, the translation to humans has proven very difficult. In humans the intervention using aldose inhibitors is required in the early stages following the onset of the illness (Chang *et al.*, 2003).

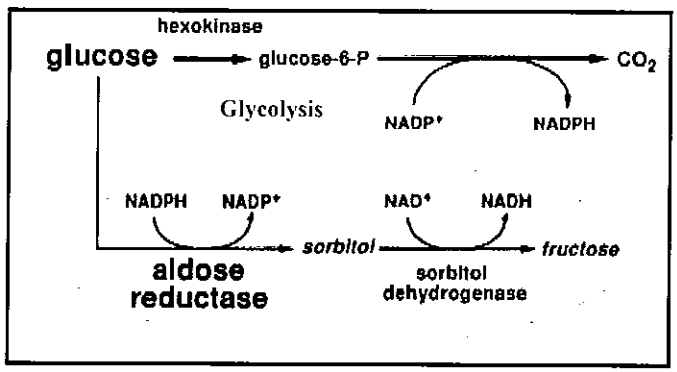

Fig. 1.4: Polyol Pathway shaded in grey. (Yabe-Nishimura., 1998)

Other members of the aldose reductases are involved in the reduction of D-xlyose to xylitol, which is a commercially important artificial sweetener (Lee *et al.*, 2003). In yeast, xylose may also be converted by two oxidoreductases, xylose reductase and xylitol dehydrogenase, to produce xylulose, which can be further channelled to produce ethanol (Zhang *et al.*, 1997, Verduyn *et al.*, 1985).

(ii.) Aldehyde Reductase

The aldehyde reductases are one of the largest sub-groups of the aldo keto reductases. These enzymes can reduce a wide range of aldehyde substrates making it difficult to determine their exact substrate preference and therefore to assign them a specific role within a particular organism. As a result, the use of the umbrella heading, aldehyde reductase is generally used for classifying these proteins.

Among the most studied members of the aldehyde redutase family are the aflatoxin B1-aldehyde reductases. They were first isolated from rat liver in 1993 (Judah *et al.*, 1993) following the administration of the antioxidant ethoxyquin. Aflatoxin B1 AKRs are different from other aldo keto reductases, such as the aldose reductases, since they have a high affinity for the dicarbonyl 9,10-phenanthrenequinone and other aromatic and aliphatic aldehydes including succinic semialdehyde. However, they are inactive with sugar substrates such as glucose, galactose and xylose. This enzyme is believed to be involved in protecting the liver, in both humans and rats, from the toxic and carcinogenic effects of aflatoxin B_1 by reducing aflatoxin B_1 dialdehyde to a dialcohol. Enhancement of this reaction is believed to result in a decreased formation of protein adducts which in turn protect the liver from the toxic affect of aflatoxin. However, experimental evidence supporting this hypothesis is still lacking. (Ellis *et al.*, 1993, Ellis *et al.*, 1995, Judah *et al.*, 1993, Knight *et al.*, 1999).

(iii.) Carbonyl Reductase

Certain members of the aldo-keto reductase superfamily have a specific role in catalysing the reduction of carbonyl group-containing xenobiotics. These enzymes are believed to participate in phase I metabolism, accelerating the elimination of potential toxins. Carbonyl group reduction provides the hydroxy group necessary for conjugation reactions, and the resulting hydrophillic molecules can be excreted via the bile and/or urine (Martin *et al.*, 2006).

(iv.) Hydroxysteroid Dehydrogenase

Hydroxysteroid dehydrogenases (HSD) interconvert active and inactive steroid hormones and neurosteroids in specific tissues. They are also involved in the

metabolism of bile acids (Matsumoto *et al.*, 2006). Even though the HSDs generally belong to the short-chain dehydrogenases/reductase superfamily, some enzymes (for example 17β-HSD, cytosolic 3α-HSD and 20α–HSD) are members of the aldo-keto reductase superfamily. These enzymes have high sequence homology with each other and unlike other aldo keto reductases, they have a narrow substrate preference with the exception of 3α(17β)-HSD, which may also function as a reductase for α-dicarbonyl compounds (Matsumoto *et al.*, 2006). Inhibition of certain HSD may represent a potential therapeutic target. For example, 3α-Hydroxysteroid dehydrogenase is believed to be involved in regulating the levels of inflammatory prostaglandins and is therefore a target for nonsteroidal anti-inflammatory drugs (Sanli *et al.*, 2003).

1.1.4 Microbial Aldo Keto Reductases

As mentioned earlier, AKRs are present in all organisms including microbial cells. Table 1.2 outlines the characterised microbial AKRs, which span 10 families.

Division	Organism	Enzyme name	AKR name
Archaebacteria		Oxidoreductase	AKR9C
Bacteria			
	Escherichia coli	2,5-diketo-D-gluconic acid reductase B	AKR3F2
	Pseudomonas putida	morphine-6-dehydrogenase	AKR5B1
	Cornyebacterium sp.	2,5-diketo-gluconic acid reductase	AKR5C1
	E. coli	2,5-diketo-gluconic acid reductase	AKR5C2
	Cornyebacterium sp.	2,5-diketo-gluconic acid reductase	AKR5D1
	Zymomonas mobilis	2,5-diketo- gluconic acid reductase	AKR5E1
	Klebsiella	2,5-diketo-gluconic acid reductase	AKR5F1
	Streptomyces glaucescens	StrT	AKR10A1
	Streptomyces bluensis	BlmT	AKR10A2
	Bacillus subtilis	Iols	AKR11A1
	Bacillus subtilis	general stress protein 69	AKR11B1
	E. coli	methylgloxal reductase	AKR11B2
	Bacillus halodurans	aldo-keto reductase	AKR11C1
	Streptomyces fradiae	2,3-enoyl reductase	AKR12A1
	Streptomyces avermitilis	2,3-reductase	AKR12C1
	Xylella fastidiosa	Phenylacetaldehyde dehydrogenase	AKR13B1
	*Helicobacter pylori**	Aldo Keto Reductase	AKR13C1
	Escherichia coli	aldo-keto reductase	AKR14A1
Yeasts			
	Candida tenius	xylose reductase	AKR2B5
	Candida tropicalis	xylose reductase	AKR2B4
	Kluveromyces lactis	xylose reductase	AKR2B2
	Saccharomyces cerevisae	Gre3p: YHR104w	AKR2B6
	Saccharomyces cerevisae	Gcy1p; YOR120w	AKR3A1
	Saccharomyces cerevisae	Yrp1p; YDR368w	AKR3A2
	Saccharomyces cerevisae	arabinose dehydrogenase	AKR3C
	Saccharomyces cerevisae	YDL124w	AKR5E
	Saccharomyces cerevisae	YJR096w	AKR5F
	Saccharomyces cerevisae	Aad14p; YNL331c	AKR9B1
	Saccharomyces cerevisae	Aad3p	AKR9B2
	Saccharomyces cerevisae	Aad4p	AKR9B3
	Saccharomyces cerevisae	Aad10p	AKR9B4
	Schizosacharomyces pombe	pyridoxal reductase	AKR8A1
	Schizosacharomyces pombe	pyridoxal reductase	AKR8A
Fungi			
	Mucor mucedo	4-dimethyltrisporate dehydrogenas	AKR2
	Pichia stipitis	NAD(P)H xylose reductase	AKR2B1
	Candida tropicalis	NAD(P)H xylose reductase	AKR2B4
	Candida tenuis	NAD(P)H xylose reductase	AKR2B5
	Saccharomyces cerevisiae	Gre3p	AKR2B6
	Candida tropicalis	xylose reductase	AKR2B7
	Pichia guilliermondii	xylose reductase	AKR2B8
	Aspergillus niger	D-xylose reductase	AKR2D1
	Saccharomyces cerevisiae	Gcy1p	AKR3A1
	Saccharomyces cerevisiae	2-methylbutyraldehyde reductase	AKR3A2
	Sporidiobolus salmonicolor	NADPH dependent reductase	AKR3B1
	Saccharomyces cerevisiae	Ara1p - arabinose dehydrogenase	AKR3C1

Table 1.2 continued...

Division	Organism	Enzyme name	AKR name
	Saccharomyces pombe	isatin reductase	AKR3C2
	Candida parpsilosis	polyketone reductase	AKR3C3
	Pencillium citrinum	b-ketoester reductase	AKR3E1
	Schizosaccharomyces pombe	pyridoxal reductase	AKR8A1
	Schizosaccharomyces pombe	pyridoxal reductase	AKR8A2
	Aspergillus nidulans	sterogmatocystin dehydrogenase	AKR9A1
	Aspergillus parasiticus	norsolorinic acid reductase	AKR9A2
	Saccharomyces cerevisiae	aryl-alcohol dehydrogenase	AKR9B1
	Saccharomyces cerevisiae	aryl-alcohol dehydrogenase	AKR9B2
	Saccharomyces cerevisiae	aryl-alcohol dehydrogenase	AKR9B3
	Saccharomyces cerevisiae	aryl-alcohol dehydrogenase	AKR9B4
	Schizosaccharomyces pombe	YakC aldo-keto reductase	AKR13A1

Table 1.2: Microbial members of the aldo keto reductase family (Ellis., 2002 & AKR superfamily website: www.med.upenn.edu/akr)

* This manuscript focuses on this enzyme.

As with the mammalian AKRs, the range of substrates that microbial AKRs can break down is usually quite broad, however, their affinities for different substrates differs greatly. This broad substrate specificity makes it difficult to assign these enzymes a specific function in the microbe. Table 1.3 shows a list of microbial AKRs for which detailed substrate specificity studies have been carried out. The majority of these enzymes have a preference for NADPH as a co-factor however some exhibit dual co-factor specificity. For example, aflatoxin-metabolising aldehyde reductase, AKR7A5, AKR1C19 and thermostable alcohol dehydrogenase from *E. coli* (Ellis *et al.*, 1995, Hinshelwood *et al.*, 2003, Ishikura *et al.*, 2005, Machielsen *et al.*, 2006). For the aldehyde substrates, the specificity shows a high degree of variation. Thus, it is difficult to predict the substrate specificity based on the sequence data alone.

Enzyme	Organism	AKR	Km (mM)					
			4-NBA	Dxylose	D,L-GA	9,10-PQ	NADPH (μM)	NADH (μM)
Xylose reductase	*P. stipitis*	AKR2B1	-----	42	18	------	9	21
Xylose reductase	*P. tannophilus*	AKR2B3	0.37	25	18	-----	16	NMA
Xylose reductase	*C. tropicalis*	AKR2B4	-----	37	----	----	18	NMA
Xylose reductase	*C. tenuis*	AKR2B5	0.38	76	2	------	16	195
Aldose reductase	*S. cerevisae*	AKR2B6	0.12	17	1.44	0.3	0.013	-----
Xylose reductase	*C.tropicalis*	AKR2B7	-----	30	----	------	14	NMA
Gcy1p	*S. cerevisae*	AKR3A1	0.13	NMA	11	------	28.5	NMA
Yrp1p	*S. cerevisae*	AKR3A2	1.1	418	1.1	0.3	8.8	-----
Aldehyde reductase	*S. salmonicolor*	AKR3B	0.8	403	-----	------	-----	------
D-arabinose dehydrogenase	*S. cerevisae*	AKR3C	-----	------	------	-----	-----	------
Morphine dehydrogenase	Pseudo-monas	AKR5B	-----	------	-----	-----	------	-----
2,5-DKGR-A	Coryne-bacterium	AKR5C	-----	-----	-----	-----	10	------
Pyridoxal reductase	*S. pombe*	AKR8A1	0.012	-----	-----	NMA	16	NMA
Aad14p	*S. cerevisae*	AKR9B1	0.95	NMA	-----	0.02	-----	------
AKR	*E.coli*	AKR14A1	1.06	------	------	------	------	------

Table 1.3: Substrate affinities of some microbial AKRs

4-NBA: 4-nitrobenaldehyde; 9,10 PQ 9,10 phenanthrenequinine; DL-Gla: D,L glyceraldehydes; NMA: no measurable activity (Ellis, 2002).

Microbial xylose reductases have been comprehensively characterised. These enzymes catalyse the reduction of xylose to xylitol, which can feed into the pentose phosphate, Embden-Meyerhof or phosphoketolase pathways. These enzymes are found in for example *Pichia stipitis, Candida tropicalis* and *Kluveromyces lactis*. The substrate specificity profile for these yeast organisms shows that they are capable of reducing other substrates such as benzaldehydes suggesting that they may have additional roles in the cell (Verduyn *et al.*, 1985, Zhang *et al.*, 1997, Lee *et al.*, 2003, Billard *et al.*, 1995). Several bacterial AKRs have also been characterised such as the *YqhE* from *E. coli*, which has been shown to play an important role in the detoxification of methylglyoxal by its reduction to acetol. Methylglyoxal is a highly toxic electrophile that is formed by lipid peroxidation, metabolism of acetone and amino acetone (Murata- Kamiya *et al.*, 2001). It reacts with cellular macromolecules, including DNA and proteins. Detoxification of this compound seems to be through multiple pathways as evidenced by the broad substrate specificities of the AKRs (Ko *et al.*, 2005, Habrych *et al.*, 2002 and Yum *et al.*, 1999).

The previously mentioned AKR6 potassium channel β-subunit has activity towards a range of substrates including methylglyoxal and may therefore be able to contribute to methylglyoxal detoxification *in vivo* (Grant *et al.*, 2002).

1.1.5 Aldo Keto Reductase of *H. pylori* and the "Toxic Aldehyde Theory"

The complete genome sequence of *H. pylori* 26695 (Tomb *et al.*, 1997) harbours a single putative aldo keto reductase (Hp1193) protein. This protein will be referred to as HpAKR henceforth. The HpAKR was of interest in light of the proposed contribution by aldehyde metabolising enzymes to the pathogenesis of the bacterium.

It has been reported that alcohol dehydrogenase activity of *H. pylori* could be important in the pathogenesis of *H. pylori* associated gastric damage (Salmela *et al.*, 1997, Roine *et al.*, 1992, Salmela *et al.*, 1993, Kaihovarra *et al.*, 1994 and Salaspuro *et al.*, 2004). These workers suggested that aldehydes derived from the oxidation of ingested alcohols could be exported from *H. pylori* growing in the gastric mucosa. It was suggested that the secreted aldehydes would react with thiol and amino groups of proteins in the gastric mucosa causing inflammation leading to gastritis. This "toxic aldehyde theory" was supported by several lines of evidence:

(i) Studies on homogenised rat gastric mucosa after incubation with labelled acetaldehyde demonstrated that the acetaldehyde interacted with proteins on the gastric mucosa resulting in the development of acetaldehyde adducts. Incubation of the mucosa with ethanol also resulted in the formation of acetaldehyde adducts. This study suggested that gastric mucosal acetaldehyde production and consequent adduct formation could be a pathogenic factor in ethanol-associated gastric damage (Salmela *et al.*, 1997, Roine *et al.*, 1992 & Salmela *et al.*, 1993).

(ii) Previously, aldehyde production had been observed in cytosolic extracts of *H. pylori* (Roine *et al.*, 1992 and Salmela *et al.*, 1993). Kaihovarra *et al.* (1994) estimated that the alcohol dehydrogenase protein made up 0.5 % of the total cytosolic protein.

(iii) No measurable aldehyde dehydrogenase activity was detected in *H. pylori* extracts indicating the absence of a pathway for the oxidation of toxic aldehydes (Kaihovarra *et al.*, 1994).

At the outset of this current study, it was noted that the *H. pylori* genome did not have a putative gene encoding an aldehyde dehydrogenase or aldehyde oxidase annotated in the database (www.TIGR.org). Moreover, measurements in cytosolic extracts showed no evidence of these activities (Kaihovarra *et al.*, 1994). Kaihovarra *et al.* (1994) reported the purification of an alcohol oxidising enzyme from *H. pylori* soluble proteins. They reported that this enzyme was highly abundant (0.5% of total cell protein) and suggested it was involved in the generation of toxic aldehydes. The generation of toxic aldehydes by alcohol dehydrogenases had previously been suggested to explain the pathogenesis of alcohol related liver disease. Sequencing of the *H. pylori* genome showed that there were three oxidoreductases potentially capable of oxidising alcohols and reducing toxic aldehydes. These were: aldo keto reductase, cinnamyl alcohol dehydrogease and short chain alcohol dehydrogenase. Since Kaihovarra *et al.* (1994) did not obtain an N-terminal sequence of the purified oxidoreductase, it is not possible to ascertain which gene product the group purified. One possibility apparently overlooked by these researchers was the possibility that "toxic aldehydes" might be reduced to their corresponding alcohols by aldo keto reductases or other aldehyde reducing enzymes in the cytosol of *H. pylori*. In this regard, the specificity of aldehyde reducing enzymes in *H. pylori* assumed a new and higher level of importance.

1.1.6 Other Aldehyde Reducing Enzymes of *H. pylori*

Besides the aldo keto reductase, HpAKR, two other enzymes annotated in the TIGR database are potentially capable of reducing toxic aldehydes.

(i) Cinnamyl alcohol dehydrogenase (HpCAD).

This enzyme has been extensively studied in this laboratory and it was found to be an enzyme with a broad specificity but displaying a

preference for aromatic aldehydes and alcohols. The HpCAD had a preference for the co-enzyme NADP(H), with little or no activity with NAD(H). The enzyme was capable of dismutating benzaldehyde to benzyl alcohol thus providing an important means of reducing the concentration of reactive aldehydes within the bacterium (Mee *et al.*, 2005).

(ii) Short chain alcohol dehydrogenase (HpSCADH)

This protein has not been previously characterised and therefore no information is available on its substrate specificity. This enzyme is currently being purified to obtain sufficient quantities to examine its substrate specificity profile. However, preliminary analysis of the HpSCADH showed it to have activity towards benzyl alcohol (results presented in this thesis).

1.2 *Helicobacter pylori*

1.2.1 Introduction

Helicobacter are spiral, flagellated, gram-negative bacteria (Fig. 1.5) that colonise the gastrointestinal tract of humans and animals.

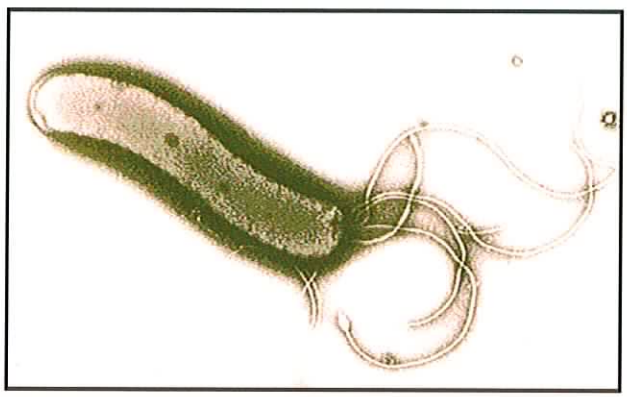

Fig. 1.5: *Helicobacter pylori.*

Source: http://www.shef.ac.uk/mbb/academic/staff/djk010.gif

(access date January 2007)

H. pylori was first identified in 1983 when two Australian researchers Robin Warren and Barry Marshall discovered a spiral shaped bacteria in the stomach (Marshall and Warren, 1984). This was followed in 1984 by a second article suggesting that the bacteria were the underlying cause of gastritis and peptic ulcers (Marshall *et al.*, 1985).

1.2.2 Prevalence of *H. pylori* Infection

H. pylori infects half the world's population and the prevalence varies widely in different parts of the world. Infection is highest in developing countries and increases rapidly during the first two decades of life, such that 80-90% of the population may be infected by early adulthood. In most developed countries, the prevalence of infection is substantially lower at all ages (Karaca *et al.*, 2004).

The prevalence of the bacterial infection worldwide is illustrated in Fig. 1.6; the rate of infection is clearly higher in the developing parts of the world. *H. pylori* infection rates on average are about 30% in Western populations; of these only 0.1-1% of patients, with induced gastritis, will develop distal gastric cancer. Infection rates in Asian countries (China, Japan, Thailand and Indonesia) are higher and range at 60-80%; distal adenocarcinoma is even more prevalent in these countries (Prinz *et al.* 2006).

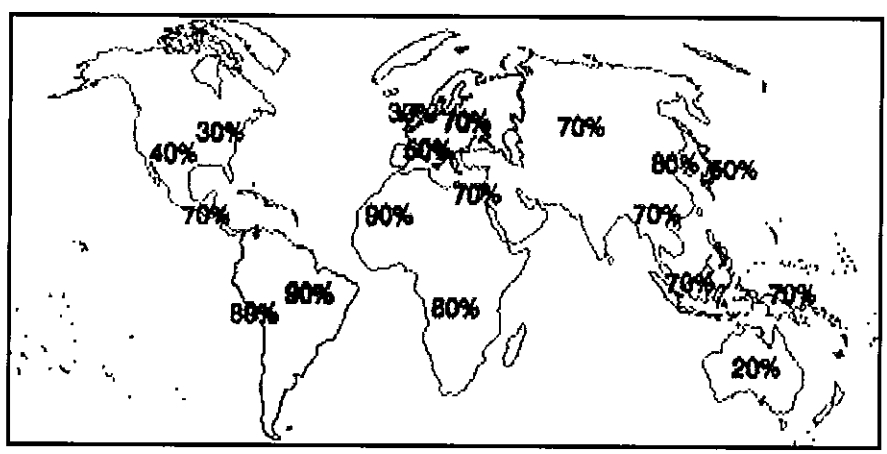

Fig. 1.6: Worldwide prevalence of *H. pylori* infection.

H. pylori has developed the ability to survive in the ecological niche of the human stomach, with the aid of several virulence factors.

An underlying factor critical to the survival of *H. pylori* in the gastric mucosa is acid resistance, which allows the organism to grow and proliferate within the acidic environment of the gastric mucosa. Initially, this was believed to be due to the presence of the urease enzyme, resulting in the neutralisation of the stomach acid by the production of ammonia. However in recent years, a urease negative strain of *H. pylori* which was capable of both colonisation and inducing the formation of gastric ulcers has been isolated (Mine *et al.*, 2005) suggesting that other mechanisms are also involved in acid resistance. Bijlsma *et al.* (2000) identified several proteins important in adaptation

to acid growth conditions. This group suggested that HpAKR may play a significant role in growth at acid pH and therefore contribute to the virulence of *H. pylori* strains. When *H. pylori* enters the stomach, it migrates from the acidic lumen and buries itself into the mucus layer of the stomach, where the pH is thought to vary between 4.0 and 6.5 and where the occasional acid shock as low as pH 2 can occur (Bijlsma *et al.*, 2002).

1.2.3 Clinical Manifestation of *H. pylori* Infection

The typical course of infection commences with superficial gastritis, which can, if left untreated, lead to gastric adenocarcinoma (Fig. 1.7). Infection with *H. pylori* is associated with an increased development of gastric carcinoma by up to 90-fold (Hardin and Wright, 2002). A selection of host factors have been associated with this increased risk of developing gastric cancer including the proinflammatory cyclooxygenase (COX)-2. This enzyme catalyses reactions, which promote the formation of inflammatory prostaglandins (Menaker *et al.* 2004). Overexpression of COX-2 in patients with both *H. pylori cagA*$^+$ (cag positive strain) infection and gastric cancer has been demonstrated (Menaker *et al.*, 2004). Host genetics also play an important role in determining the outcome of a *H. pylori* infection. For example, polymorphisms of the IL-1 cytokine are associated with a greater risk of gastric cancer (Crowe *et al.*, 2005). Potentially, the combination of host and bacterial genotyping may yield clues to the identification of patients with a high risk of developing gastric cancer.

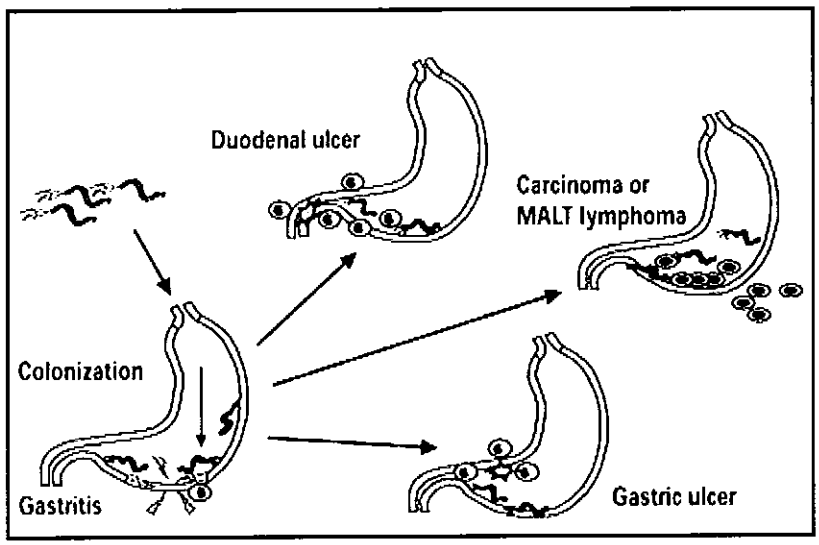

Fig. 1.7: Pathogenesis of *Helicobacter pylori*-associated gastroduodenal diseases. MALT, mucosa-associated lymphoid tissue (Nirag *et al.*, 2003)

1.2.4 Treatment for *H. pylori* Infection

Treatment of *H. pylori* infection is usually by a combination of antibiotic therapy to eliminate the organism, anti-inflammatory treatment to reduce the gastric inflammation and inhibition of acid secretion to speed the healing of damaged tissue.

Table 1.4 outlines the antibiotic agents and proton pump inhibitors recommended for the treatment of *Helicobacter pylori* infection. Proton pump inhibitors are prescribed as they suppress acid production in the stomach. Thus, the proton pump inhibitors provide an opportunity for ulcers to heal and heartburn or reflux symptoms to subside. However, it is worth noting that data on the issue of acid secretion are conflicting with both up and down regulation of the gastric acid output demonstrated in response to infection (Jacobson *et al.*, 2001 and Shimatani *et al.*, 2005).

The medication generally used in the treatment may have severe side effects (Hardin and Wright, 2002). Moreover, the emergence of antibiotic resistant *H. pylori* strains suggests that this type of therapy will be compromised in future years. Figure 1.8

outlines the diagnostic and therapeutic procedures used for *H. pylori* infected individuals.

Proton Pump Inhibitors	Antibiotic Agents
Lansoprazole 30mg	Amoxicillin 1g
Omeprazole 20mg	Clarithromycin 500mg
Pantoprazole 40mg	Metronidazole 500mg
Rabeprazole 20mg	Tetracycline 500mg

Table 1.4: Antibiotics and proton pump inhibitors used for treatment of *H. pylori* infection.

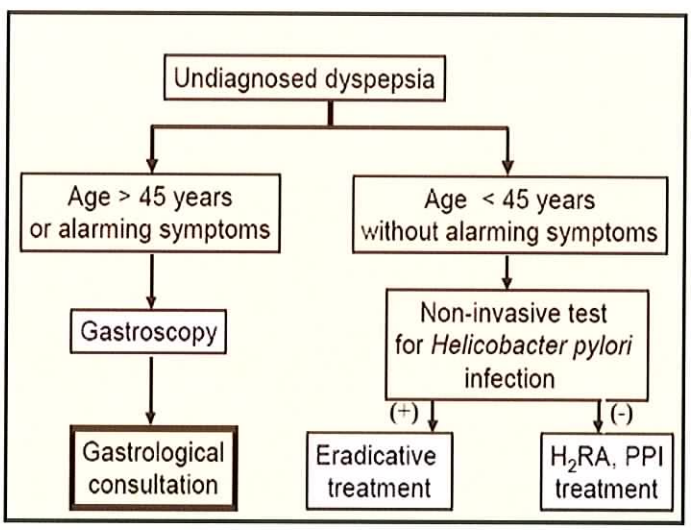

Fig. 1.8: Diagnostic and therapeutic procedures used for *H. pylori* infected individuals (Dzieniszewski *et al.*, 2006).

H_2RA: H2 receptor. PPI: protein pump inhibitor.

Although antibiotics are a useful treatment for *H. pylori* infection, they are not a practical solution for the treatment of the whole population especially in developing countries. Therefore, some workers have suggested immunisation maybe more appropriate (Hardin and Wright, 2002).

The development of a vaccine for *H. pylori* in mice has been successful, however, it is still not known whether this will be effective in humans. A major question that is still unanswered: why is vaccination effective when the natural immune response is not? The answer may lie in the observation that *H. pylori* infection is believed to induce an interferon-γ (Th1)-mediated pro-inflammatory response, which may not be able to eliminate the bacteria. However, it is also possible that vaccination triggers a Th2 immune response, which is capable of mediating protection (Hardin & Wright, 2002). It is now generally accepted that a balanced Th1/Th2 immune response is benefited in clearing the infection.

Reports in countries such as the USA and Germany, show that the prevalence of *H. pylori* is decreasing. As little as 10% of children are infected with the bacterium making the development of a vaccine of less interest in these areas (Prinz *et al.*, 2006).

1.2.5 Virulence Factors

A number of virulence factors for *H. pylori* associated infection have been characterised. These include:

(i) Vaculating cytotoxin (VacA)

(ii) Cytotoxin associated proteins (CagA)

(iii) Urease enzyme.

(i.) Vacuolating cytotoxin (VacA)

Initially discovered by Leunk *et al.* (1988), elucidation of the exact role, played by the vacuolating cytotoxin VacA, in the pathogenesis of *H. pylori* continues. It is now widely accepted that VacA has the capacity to induce the formation of vacuoles in the cytoplasm of cells exposed to the toxin. However the addition of purified VacA alone to gastric cells is not sufficient to produce vacuoles. As Li *et al.* (2004) discovered weak bases such as ammonium chloride are required in the medium. These workers also reported a clustering and redistribution of the markers for late endocytic compartments (Rab7, Lamp-1 and cathepsin D) in the presence of ammonium chloride and VacA. Interestingly, subsequent vacuoles formed in the VacA treated cells arose as expansions of these endosomal clusters. Therefore it was hypothesized that this clustering effect of the late endocytic compartments was a prerequisite for vacuole formation, where the concentrated source of vesicles provides membrane material for vacuole formation.

(ii.) Cytotoxin associated proteins (CagA)

The cag pathogenicity island (*cag* PAI) of *H. pylori* encodes proteins with homologies to structural and functional components of type IV secretion systems of other bacteria. These systems are membrane transport systems dedicated to the secretion or translocation of high-molecular-mass biomolecules such as protein, into the environment or into a recipient cell (Andrzejewska *et al.*, 2006). The CagA protein is found in approx 50-60% of *H. pylori* strains isolated in western countries and in over 90% of *H. pylori* isolated from Japan. More interestingly, epidemiological studies have shown that gastric cancer and peptic ulcers are more prominent in patients who are infected with *cag* PAI-positive *H. pylori* strains than those who are infected with *cag*-PAI negative strains (Busler *et al.*, 2006).

Upon entering the host cell, it has been reported that the CagA protein undergoes tyrosine phosphorylation leading to the rearrangement of the host cell actin cytoskeleton (Selbach *et al.*, 2002). This results in altered cell morphology and thus may enhance the attachment and survival of *H. pylori* cells, which are in close proximity (Garza-Gonzalez *et al.*, 2004).

However, the pathogenicity island also contains genes capable of inducing interleukin (IL)-8 production by epithelial cells. The IL-8 production attracts neutrophils, which localize between the epithelial cells. The localization of the neutrophils between the epithelial cells followed by the release of their digestive products (protease, reactive oxygen species etc.) is linked to ulcer formation (Marshall, 2002). Wang *et al.* (2004) cloned and sequenced a *CagA* gene fragment from *H. pylori* in a coccoid form. *H. pylori* cells grow *in vitro* in a curved rod form. After prolonged incubation they evolve into coccoid cells, which are nonculturable (Willen *et al.*, 2000). While the pathogenicity of the coccoid form is unclear, coccoid cells have been observed in regions of the gastric mucosa where cells are damaged (Janas *et al.*, 1995). Wang *et al.* (2004) succeeded in demonstrating that the coccoid form is both virulent and in possession of a complete *CagA* gene.

(iii.) Urease Enzyme

Urease is an enzyme that catalyzes the hydrolysis of urea into carbon dioxide and ammonia. The reaction is as follows:

$$(NH_2)_2CO + H_2O \rightarrow CO_2 + 2NH_3$$

It is thought that the high amounts of this enzyme present in the outer membrane of *H. pylori* are responsible for its resistance to acid. Thus, production of ammonia is thought to neutralise acid in the immediate environment of the *H. pylori* cell (Athmann *et al.*, 2000).

Several genes present in a cluster control the expression of urease: *ure*A and *ure*B encode the structural subunits of the protein while *ure* E, F, G and H are required for assembly of the protein and Ni^{2+} insertion, which is required for activation of the protein (Athmann *et al.*, 2000). Gobert *et al.* (2002) also identified the ability of urease to stimulate up-regulation of the inducible NO synthase (iNOS). It is possible that urease may contribute to mucosal damage in addition to conferring acid resistance to the bacterium. Previous studies identified urease as essential for colonisation (Tsuda *et al.*, 1994).

However, more recently Mine *et al.* (2005) infected Mongolian gerbils with a urease negative *H. pylori* strain and demonstrated that the bacterium was capable of both colonisation and inducing the formation of gastric ulcers. Therefore, the mechanism of acid resistance clearly involves factors other than urease.

The discovery of a pathogenic urease negative *H. pylori* strain has had serious implications, since this enzyme is utilised for diagnosis of infection. For example the urea breath test is routinely used to diagnose infection as it is quick, non-invasive and cost effective (Shirin *et al.*, 2005), however it clearly would fail to detect a urease negative *H. pylori* genotype infection.

Additional Virulence Factors

Several additional factors, which are believed to contribute to the virulence of *H. pylori* in addition to VacA, CagA and urease are listed in Table 1.8.

Factor	Predicted Role
Flagellar protein	Motility
HP-NAP	Neutrophil activation and a possible adhesion to mucin
BabA	Adhesion for Le^b blood group antigen on cells.
LPS	Stimulates the production of NF-κB and IL-8. Poor activator to initiate a immune response so unlikely to represent a major pathogenic factor
Lewis ^{xy} antigens	Molecular mimicry
OipA	Reported to assist in IL-8 induction, but this association is not universal
SabA	Binds to sialyl-Le^x and Le^a antigens and is involved in the activation of neutrophils.
IceA	Homologs of Nla III restriction endonuclease

Table 1.5: Virulence factors associated with *H. pylori* (Kusters *et al.*, 2006 and Covacci *et. al.*, 1999)

1.2.6 Role of HpAKR in *H. pylori* Acid Adaption

Ancillary genes required for growth at acid pH values have been identified using a random insertional mutagenesis technique (Biljsma *et al.*, 2000). Interestingly, these workers suggested that these genes were required when exposure to acid conditions was chronic, not simply for adaptation to acid shock. Several of these genes coded for proteins of unknown function. Of those proteins with a known function, some seemed

to be involved in signalling external pH to the cell while others were involved in energy generation.

Perhaps the most intriguing aspect of this study was the suggestion that certain enzymes might be directly involved in the adaptation to acidic environments by the capture or release of protons. These enzymes included the aldo keto reductase and an NADPH flavin oxidoreducatse. Direct disruption of the flavin oxidoreductase gene was accomplished and its role in acid adaptation was confirmed. The role of the aldo keto reductase was less clear. Disruption of the *H. pylori* genome upstream of the opening reading frame for the *H. pylori* aldo keto reductase (HpAKR) gave rise to an acid sensitive phenotype. Thus, it was suggested that this enzyme was involved in acid adaptation since it was located immediately 5' to the insertion point (Biljsma *et al.*, 2000). Direct disruption of the *HpAKR* gene, however, was not shown so these findings remained spectulative.

Despite the potential importance of HpAKR to acid adaptation in *H. pylori*, no further studies of this protein have been reported. Its role in acid adaptation has not been probed by direct gene disruption and the protein has not been characterised.

1.3 Aims of Research

The overall aims of this research group have been to characterise the oxidoreductases of *H. pylori* with a view to understanding their role in aldehyde detoxification. Previous studies in this laboratory showed that a cinnamyl alcohol dehydrogenase (HpCAD) in the cytosol of *H. pylori* was capable of reducing a range of aldehyde substrates with a preference for aromatic aldehydes. The *H. pylori* genome encodes two other enzymes likely to be capable of aldehyde reduction; an aldo keto reductase (HpAKR) and short chain alcohol dehydrogenase (HpSCADH) but their specificities were not known. In view of the importance of these enzymes for aldehyde detoxification, and, in the case of HpAKR, the suggestions that it was required for acid adaptation, these were cloned, overexpressed and their biochemical properties were evaluated and to study their role in *H. pylori* by gene ablation studies.

The roles played by HpAKR and HpCAD in acid adaptation were also evaluated.

This thesis presents:

(i). Cloning, expression and characterisation of HpAKR.

(ii). Kinetic and substrate specificity studies of HpAKR.

(iii). Generation of an isogenic HpAKR mutant and its characterisation under acid growth conditions.

(iv). Characterisation of previously constructed HpCAD mutant in terms of growth under acid conditions.

(v). Preliminary studies of the cloning, expression and purification of *H. pylori* short chain alcohol dehydrogenase (HpSCADH).

CHAPTER 2

Materials and Methods

2.0 Materials and Methods

2.1 Reagents

Bovine serum albumin, acrylamide:bisacrylamide (29:1), ammonium persulphate, Nonidet- P40, leupeptin, PMSF, β-mercpatoethanol, EDTA, ampicillin, kanamycin, chloramphenicol, sodium chloride, sodium hydroxide, magnesium chloride, potassium chloride, Tris(hydroxylmethyl)aminomethane (Tris), glycine, TEMED, Tween-20, dimethyl sulfoxide, Luria-Bertani Medium, Agar Select, sodium dodecyl sulphate, iminodiacetic acid-Sepharose 6B, DTT (Dithio-DL-threitol), NADH, NADPH, alcohol, aldehyde, sugar and steroid substrates and IPTG were obtained from Sigma Aldrich (Poole, Dorset, U.K. and St. Louis, M.O., U.S.A). Electrophoresis grade agarose, Brain Heart Infusion medium, were obtained from GIBCO BRL (Life Technologies, Scotland). Ethanol, methanol, glacial acetic acid, orthophosphoric acid, hydrochloric acid, acetone, glycerol and chloroform were obtained from BDH Ltd. (Poole, Dorset, U.K.). Sterile Horse Serum and *H. pylori* selective DENT supplement (SR-0147) were from Oxoid (Basingstoke, Hampshire, U.K.) Defibrinated horse blood was from Biological Laboratories Europe Ltd. DEAE-52 and CM-52 chromatography media were obtained from Whatmann Ltd. (Maidstone, U.K.). All buffer reagents for SDS-PAGE were prepared in deionised water (Elga Prima reverse osmosis). Restriction enzymes were from New England Biolabs (Herts, England). Taq-High Fidelity DNA polymerase was from Roche (Basel, Switzerland). T4 DNA ligase was from Invitrogen (Breda, the Netherlands).

2.2 Antibodies

Penta-His Antibody BSA-free (Cat. No. 34660) was from Qiagen, Hilden, Germany. Polyclonal anti-mouse (Cat. No. P0260) and anti-rabbit (Cat. No. P0217) antibodies were purchased from Dako (Glostrup, Denmark). A polycolonal antibody was produced in a New Zealand White rabbit using subcutaneous immunisation with purified recombinant AKR by Harlan (www.harlaneurope.com). The antibody was affinity purified as described by Harlow and Lane (1998); 200 µl of recombinant HpAKR (100 µl HpAKR (1mg/ml) + 100 µl sample buffer) were loaded onto the standard stacking gel (flat no wells); the proteins were separated by electrophoresis and transferred to a polyvinylidene fluoride PVDF membrane. A strip of HpAKR was removed and blocked by incubating with marvel/PBS (on orbital shaker) at RT for 1 h. The strip was then incubated with a 1:3 dilution of rabbit serum in 4 ml PBS at 4° C for 1 h. The serum was removed (retained) then washed with 0.1% PBS-Tween solution for 5 mim. The antibody was eluted from the blot with approximately 2 ml 0.1 M glycine (pH 3.0). Elution was carried out on an orbital shaker and the glycine was neutralised with the addition of 20 µl 1 M Tris (pH 8.0) (elution and neutralisation repeated 3 times).

2.3 Determination of Protein Concentration

The protein concentration of various cellular extracts and purified enzyme were determined primarily by the method of Bradford (1976) using Bio-Rad Protein Assay Concentrate (code 500-0006, Bio-Rad, U.K.). Assay concentrate was prepared freshly by diluting 1:5 with distilled water and mixed well prior to assay. A BSA standard curve was constructed by serially diluting the standard 1:2 to yield the following concentrations 20, 10, 5, 2.5, 1.25, 0.625 0.312 and 0 µg/ml of protein. The absorbance of protein standards and samples were measured at 595 nm in triplicate using the Tecan

Spectra Fluor Plus spectrophotometer. Excel was used to average readings, construct a standard curve and calculate the individual protein concentrations with reference to the standard curve automatically. In some instances, unknown samples were spiked with a BSA standard of known concentration (2mg/ml) to monitor accuracy and reproducibility of the Bradford method.

2.4 Protein Electrophoresis Analysis and Immunoblotting

2.4.1 SDS polyacrylamide gel electrophoresis

2.4.1.1 Sample and Molecular Weight Standard Preparation

Following protein estimation, samples were generally precipitated and resuspended to yield 50 μg of protein. For concentrating protein, this volume was diluted 1:5 with ice-cold acetone and incubated at –20°C for at least 2 h. The tubes were then centrifuged at 15,000 g for 4 min and the supernatant was aspirated and discarded. Any remaining acetone was allowed to evaporate at room temperature for approximately 1 h. Precipitated protein (50 μg) was resuspended in 25 μl 1X reducing or non-reducing sample buffer (diluted from 5 X stock) as required [see Appendix A]. Protein samples and appropriate molecular weight standards were boiled at 100°C for 5 min and centrifuged briefly (30 s) to remove insoluble solids.

2.4.1.2 SDS-PAGE

An ATTO system was used for all SDS-PAGE gels (ATTO Corporation, Japan) and protein samples were analysed using a Consort electrophoresis power supply unit. Proteins were separated on reducing gels prepared using a discontinuous buffer system as described by Laemmli (1970) and adapted by Sambrook *et al.* (1989). Resolving and stacking acrylamide gels were prepared to the required percentage acrylamide as

indicated in Tables 2.1 and 2.2. APS and TEMED were added last with gentle swirling of the mixture. Electrophoresis was carried out at 25 mA per gel for approximately 1.5 h until the dye front had reached a point just above the gel base, at which stage electrophoresis was terminated.

Component	10%	12.5%	15%	20%
Acryl/Bis	6.66ml	8.32ml	10ml	13.32ml
Tris 1.5M	5.00ml	5.00ml	5.00ml	5.00ml
Distilled H_20	8.32ml	6.56ml	4.89ml	2.78ml
Ammonium persulphate	100µl	100µl	100µl	100µl
TEMED	10µl	10µl	10µl	10µl

Table 2.1: Composition of reagents required for resolving gel in SDS-PAGE

Component	Volume
Acryl/Bis	1.33ml
Tris 1M (pH 6.8)	3.05ml
Distilled H_20	5.55ml
Ammonium persulphate	50µl
TEMED	10µl

Table 2.2: Composition of stacking gel reagents for SDS-PAGE

2.4.1.3 Two-dimensional Gel Electrophoresis (2-D GE)

First dimension run, *i.e.* isoelectric focusing, was performed using the IPGphor™ isoelectric focusing system (Amersham Pharmacia, U.K). Protein extracts were separated on 13 cm long immobiline drystrips (pH 3-10). Depending on the experiment, 50 to 150 μg of protein was solubilised in a rehydration solution [see Appendix 1] and applied to the strips. Proteins were focused to equilibrium using the IPGphor™ Isoelectric Focusing System (Amersham Pharmacia Biotech). Second-dimension runs, *i.e.* separation of proteins according to molecular weight, were performed by SDS-PAGE (Section 2.4.1.2). IEF was performed as recommended by the manufacturer, Amersham. Isoelectric focusing was then carried out under the following conditions: rehydration at 60 V overnight for 14 h, followed by focusing at 500 V for 1 h, 1000 V for 1 h and finally 8000 V for 2.5 h.

For second dimension electrophoresis, strips were equilibrated in approximately 10 ml of SDS Equilibration buffer [see Appendix A] for 10 to 15 min with shaking. Care was taken to ensure that the gel side of the strip was facing upwards during the equilibration step. Strips were washed once briefly with 1 x Running buffer [see Appendix A] and placed carefully onto pre-prepared SDS-PAGE gels (plastic backing of IPG strip flush with glass plate of the polyacrylamide gel). Second dimension gels were ran at 350 V, 50 mA for approximately 1.5 h.

2.4.2 Western Immunoblotting

Western immunoblotting was carried out using the semi-dry method for the transfer of electrophoresed proteins to immobilising membranes as described by Towbin (1979) and was performed using an ATTO semi-dry transfer system (ATTO Medical Supplies, Japan). During SDS-PAGE, polyvinylidene fluoride (PVDF) transfer membrane (0.45 μ Pall Life Sciences) of dimensions 6.5 x 9 cm was saturated with methanol for 30 s and then equilibrated briefly in transfer buffer prior to semi-dry transfer. Whatmann 3 MM filter paper cut to 6.5 x 9 cm was also saturated in transfer buffer prior to semi-dry blot sandwich construction, which was assembled in the order of cathode, filter paper, PVDF, acrylamide gel, filter paper and finally anode. Electrophoretic transfer was performed at 100 mA per gel for 60 min. Following semi-dry transfer; PVDF membrane was removed and processed for immunoblotting. The lane containing the molecular weight markers were stained with Coomassie Blue R-250 followed by destaining in 50% (v/v) methanol.

2.4.2.1 Immunoblot Detection and Development

Non-specific sites on the membrane following semi-dry transfer were blocked by incubation with freshly prepared PBS buffer containing 5% (w/v) non-fat skimmed milk (Blocking solution) [see Appendix A] for 1 h with gentle agitation on an orbital shaker (Stuart Scientific, U.K.) at room temperature. Blots were then washed twice with PBS and then incubated overnight at 4°C with 20 ml of primary antibody, diluted 1:3000 in Primary and Secondary Antibody Diluent Solution [see Appendix A]. Following incubation with primary antibody, blots were washed 5 times for 5 min each with PBS-Tween (0.1%) Washing Solution [see Appendix A]. Blots were then incubated with the relevant horse radish peroxidase-conjugated secondary antibody in

Primary and Secondary Antibody Diluent Solution for 2 h with shaking in a sealed plastic bag at room temperature. Following incubation with secondary antibody, blots were finally washed 5 times for 5 min with PBS-Tween (0.1%) Washing Solution. Prior to development, blots were placed in PBS. Blots were stored in PBS at 4°C if development could not be undertaken immediately.

Development of immunblots was performed using the enhanced chemiluminescence (ECL) method. Membranes were incubated for 1 min in a solution of iodophenol (400 μM), luminol (1.25 mM), and hydrogen peroxide (0.1% (v/v)) in 0.1 M Tris-HCl (pH 8.8) [see Appendix A]. The membrane was removed after 1 min and placed between acetate sheets, which were then exposed to Kodak X-OMAT S film for the appropriate time period (range 30 s to 30 min). Exposed films were developed using an automatic developer (CURIX 60, AGFA, Type 9462/100/140, Agfa-Gevaert AG, Munich, Germany).

2.5 Immunoprecipitation

Cell lysates were prepared by centrifuging 10 ml cell culture at 3200rpm for 30 mins. The cell pellet was resuspended in 1 ml 50 mM KH_2PO_4 and sonicated on ice for 2 min. The sonicate was spun at maximum speed (15000 rpm) for 5 min. The cytosol (supernatant) was removed and the Bradford protein assay (section 2.3) was preformed to ensure the protein concentration was between 1-10 mg/ml.

Protein extract (200 μl) was incubated, in eppendorf tubes, on a rotator with 30μl of primary antibody for 2 h at room temperature or overnight at 4°C. Tubes were spun at 15000 rpm for 1 min. Then 20 μl of protein A or protein G beads were added and the mixture was rotated for 1 h at room temperature. Beads were removed by centrifugation at 15000 rpm for 1 min and the supernatant was carefully removed (retain). The beads

were washed in 1 ml 50 mM KH_2PO_4 (pH 7.5) and centrifuged at 15000 rpm for 1 min. The resulting supernatant was carefully removed so as not to disturb the beads. The beads were resuspended in 30 µl of 1X sample buffer, boiled for 5 min at 100°C and then centrifuged briefly (10 s). The final supernatant was loaded onto a 12.5% SDS-PAGE. Parameters used for electrophoresis are outlined in section 2.4.1.2.

2.6 DNA Manipulations

2.6.1 Plasmid Preparation

Plasmids were purified using the QIAprep miniprep kit (Qiagen, Hilden, Germany) following the directions specified by manufacturer.

2.6.2 Restriction Digests

Restriction enzymes used were obtained from New England Biolabs (U.K). All digests were carried out at 37 °C for 3 h after which the restriction enzyme was inactivated either by freezing or heating to 65°C for 20 min. BamH I digests were supplemented with 100 µg/ml BSA.

2.6.3 Ethanol Precipitation of Treated DNA

Ethanol precipitation of digested (or blunt ended) DNA facilitated recovery of the treated sample in a concentrated form. A 1/5 volume of 3 M sodium acetate was added to the reaction mixture followed by the addition of 56 µl of ice-cold 96% ethanol (stored at -20°C). The mixture was then kept at -80 °C for 2 h and afterwards centrifuged at 1400 rpm, 4°C, 30 min. The supernatant was drained off and the resultant pellet washed with 60 µl of 80% ice-cold ethanol (stored at -20°C). It was allowed to stand for 5-10 min and then centrifuged as before. The supernatant was drained off and

the pellet resuspended in the buffer of choice (in the case of a sequential digest, a buffer compatible with the 2nd restriction enzyme)

2.6.4 PCR Amplification

Polymerase Chain Reactions were performed in a Perkin-Elmer 2400 thermal cycler (Perkin-Elmer, U.K.) with *Taq* DNA Polymerase (Boerhinger Mannheim, Germany). Primers were from Sigma-Genosys (U.K.). For standard amplifications, typically, in each reaction approximately 100 ng of template DNA was mixed with 5 pmol of each specific primer in a reaction volume of 25 µl. Reactions were performed by denaturing DNA at 94°C for 2 min 15 s, annealing at 45°C for 30 s and extension at 72°C for 45 s. A total of 30 cycles were performed.

2.6.5 Blunt Ending with T4 DNA Polymerase

T4 DNA polymerase (NEB, Herts, England) is compatible with all buffers. The *Xcm* I digest was stopped after 3 h at 37°C by heat inactivation of the restriction enzyme (65°C for 20 min). The reaction mixture was cooled (below 37°C) and supplemented with 1 µl of T4 DNA polymerase and 50 µM dNTPs. After 1 h at room temperature, the reaction was stopped by ethanol precipitation.

2.7 *E. coli* Manipulations

2.7.1 Preparation of Competent *E. coli* Cells for Transformation

An overnight culture of the appropriate *E. coli* strain (DH5α / BL21) was grown in LB liquid medium at 37°C. The overnight culture (1 ml) was used to inoculate 100 ml of fresh LB (in a 1L flask). The culture was shaken at 200 rpm at 37°C until cells reached a mid-log phase (OD at 600 nm of approximately 0.4-0.5). The cells were placed on ice

for 1 h, decanted into 2 x 50 ml falcon tubes and centrifuged at 2000 rpm for 15 min at 4°C. Each pellet was resuspended in 7.5 ml of 100 mM $MgCl_2$ (sterile & ice cold) and centrifuged at 2000 rpm for 5 min at 4°C. Each pellet was then resuspended in 25 ml of 100 mM $CaCl_2$ (sterile & ice cold) and centrifuged at 2000 rpm for 5 min at 4°C. Each pellet was then resuspended in 5.25 ml of 100 mM $CaCl_2$ and 750 µl of sterile ice-cold 80% glycerol was added gradually in a swirling motion (to give a final concentration of glycerol of 10%). The cells were aliquoted (0.5 ml), snap frozen using liquid nitrogen and stored at -80°C.

2.7.2 Transformation of Competent *E. coli* Cells

Competent cells were thawed on ice and 10-20 ng of plasmid DNA was added. The cells were then incubated on ice for 30 min, heat shocked at 42°C for 2 min and cooled on ice for 2 min. SOC medium (1 ml) was then added to the cells and they were incubated at 37°C for 1 hour (120-150rpm).

2.7.3 Screening of *E. coli* Cells (Transformants)

Screening was carried out according to the Sekar method (Sekar *et. al* 1987). 8 µl of lysis solution (Solution II; 90 µl 6X gel loading buffer [see Appendix A], 110 µl dH_2O & 400 µl Solution II was added to the bottom of a 1.5 ml autoclaved Eppendorf tube, any material collected at the side of the tube was removed by centrifuging for ≈10-20 sec. The material from a selected colony growing in an antibiotic plate was resuspended in lysis solution (sterile tips were used to collect colony material, a replica of each colony was produced by touching a replica plate before resuspending cells in lysis solution). The material was resuspended by repeated pipetting (should become stringy) and the addition of 1.5 µl of solution III [See appendix A] to the side of the eppendorf.

Centrifuge at 14800 rpm, for 5 min at 4°C. The final supernatant was loaded onto an agarose gel.

2.8 Molecular Mass Determination

The relative molecular mass of the purified enzyme was determined using a Superdex 75-HR gel filtration column equilibrated with 50 mM potassium phosphate buffer (pH 7.5) using an AKTA FPLC system (Amersham Pharmacia, UK). A standard curve was constructed using ovalbumin (molecular weight: 43 kDa), chymotrypsinogen A (molecular weight: 25 kDa) and ribonuclease A (molecular weight: 13.7 kDa) (Amersham Pharmacia, UK). AKR samples (0.8 mg) were applied and eluted at a flow rate of 1 ml/min.

2.9 Cloning and Expression of Recombinant HpAKR

2.9.1 Bacterial Strains and Plasmids

Escherichia coli DH5α (Invitrogen, Breda, Netherlands) was used for cloning procedures. *Escherichia coli* BL21(DE3)*pLysS* was used for expression of the target Aldo keto reductase (HpAKR) and Short Chain Alcohol Dehydrogenase (HpSCADH) proteins (Novagen, Darmstadt, Germany). Genomic DNA from *Helicobacter pylori* (strains 1061 and 26695) was used to amplify the *HpAKR* and *HpSCADH* genes by PCR (see also 2.6.4). The pET 16b vector (Novagen) was used to clone and overexpress the HpAKR and HpSCADH in *E. coli* BL21(DE3)*pLysS*. *E. coli* was grown at 37°C in LB medium supplemented with ampicillin (100 μg/ml) and chloroamphenicol (34 μg/ml) to select for the desired constructs.

2.9.2 Cloning Methods Used for the Amplification of *HpAKR/HpSCADH* genes

All DNA manipulations were performed under standard conditions as described by Sambrook *et al.* (1989). The *HpAKR* gene was amplified by PCR using genomic DNA from *H. pylori* 26695 and 1061 as templates and the oligonucleotides 5'-CGC CAT ATG CAA CAG CGT CATT-3'and 5'-CGC GGA TCC TTG ATT CAC CAT TTC AT-3', as the forward and reverse primers, respectively. The *HpSCADH* gene was also amplified by PCR using genomic DNA from *H. pylori* 26695 and 1061 as templates and the oligonucleotides 5'-CGC CAT ATG GCG CAC ATT-3' and 5'- CGC GGA TCC AGG GTT TTT ATG GGT G-3', as the forward and reverse primers, respectively. These primers were designed to introduce an NdeI site at the 5' end and a *Bam*H1 site at the 3' end. The PCR conditions used were those recommended by the manufactures (Roche) for *Taq* High Fidelity polymerase.

The amplified PCR product, containing the *HpAKR/HpSCADH* gene was cloned into the pET 16b vector (Novagen; all pET vectors are derived from the plasmid pBR322). The resulting construct was named pET-HpAKR and pET-HpSCADH. The construct was sequenced in both directions (DNA sequencing facility, University of Cambridge, England).

2.9.3 Purification of HpAKR/HpSCADH proteins

Over production of the recombinant HpAKR was achieved in *E. coli* BL21(DE3)*pLysS*. Cells harbouring pET-HpAKR/pET-HpSCADH were grown to an OD at 600 nm of 0.6, in LB media containing ampicillin (100 μg/ml) and chloroamphenicol (34 μg/ml). Production of HpAKR/HpSCADH was initiated by addition of 1 mM isopropyl β-D-thiogalactoside (IPTG), followed by incubation at room temperature, to minimise inclusion body formation. After 14 h, cells were harvested by centrifugation at

5 000 × **g,** for 30 min at 4°C. For protein purification, the cells from a 1l culture were resuspended in 30 ml of binding buffer (5 mM imidazole, 0.5 M NaCl, 20 mM Tris-HCl, pH 7.9) and sonicated on ice for 3 × 5 min, (Soniprep 150, Sanyo). The resulting cell lysate was centrifuged at 5 000 × **g** for 1 h at 4°C, and the supernatant filtered (0.45 μm) prior to loading onto a nickel charged iminodiacetic acid column. Unbound material was eluted using 10 column volumes of binding buffer and 6 column volumes of wash buffer (60 mM imidazole, 0.5 M NaCl, 20 mM Tris-HCl, pH 7.9). The recombinant AKR/SCADH protein was then eluted over 7 column volumes with elution buffer (500 mM imidazole, 0.5 M NaCl, 20mM Tris-HCl, pH 7.9). The purified protein was dialysed against 50 mM potassium phosphate buffer (pH 7.5) containing 50μM EDTA. Protein concentrations were determined by the Bradford method (Bradford, 1976).

2.10 Enzyme Kinetics

The kinetic parameters for aldehyde reduction were estimated using a spectrophotometric assay at 37°C using an Agilent 8453 diode array spectrophotometer. The purified enzyme was assayed for the reduction of aldehydes. The activities towards different aldehydes were assayed in reaction mixtures (2 ml) containing 50 mM potassium phosphate buffer (pH 7.5) and 0.2 mM NADPH. The decrease in NADPH absorbance at 340 nm was followed to assess the enzymatic activity towards the aldehydes. The molar extinction coefficient (ε) used (pH 7.5) were: $\varepsilon_{340} = 6.22\ mM^{-1} \cdot cm^{-1}$ for NAD(P)H. Steady-state parameters were determined by fitting initial rates to the Michaelis-Menten equation using the ENZFITTER program (Elsevier Biosoft, Cambridge, UK) and data for inhibition by sodium valproate were analysed by non-linear regression using the program MacCurveFit (Kevin Raner Software, Mt. Waverly, Victoria, Australia).

2.11 *Helicobacter pylori* Growth and Manipulations

2.11.1 *H. pylori* Strains and Growth Conditions

Helicobacter pylori strains 26695 (ATCC 700392) (Marias *et al.*, 1999) and 1061 (Goodwin *et al.*, 1998) were provided by Dr. A. Van Vliet and Dr. J. Kusters (Dijkzigt Hospital, Rotterdam, The Netherlands). Strains were maintained on Columbia Blood Agar plates (5% lysed horse blood) supplemented with DENT selective supplement (SR-0147) (Oxoid, Basingstoke, U.K.) and supplemented with kanamycin (20 μg/ml). Plates were incubated in a microaerophilic-humidified atmosphere generated using a MART Microbiology Anoxomat system (Lichtenvoorde, the Netherlands) or alternatively using a Gas Generating Kits (BR-0038) (Oxoid, Basingstoke, Hampshire, U.K.) For liquid culture, strains were grown in Brain Heart Infusion Medium (GIBCOBRL, Life Technologies, Scotland) supplemented with 5% FCS. Cultures were grown in 25 cm^2 cell culture flasks (Nunclon, Roskilde, Denmark), which had been equilibrated in a CO_2 atmosphere prior to flask sealing and incubation with constant shaking (120 rpm) at 37°C in an orbital incubator (S1 50, Stuart Scientific, U.K.).

An acidic environment was created using Brucella broth which was adjusted to the desired pH using HCl after the addition of foetal calf serum and DENT supplement and subsequently filter sterilised.

2.11.2 Preparation of *H. pylori* Genomic DNA

H. pylori genomic DNA was purified using the Puregene DNA Isolation kit (Gentra systems, Minneapolis, MN). Eppendorf tubes were labelled as appropriate and 300 μl of lysis solution was added to each. An inoculation loop of bacterial culture was resuspended in the solution. The tubes were incubated at 80°C for 5 min, cooled and 1.5 μl of protein kinase added. The tubes were inverted 25-30 times and incubated at 37°C

for 60 min. They were then cooled to room temperature and 100 µl of protein precipitation solution was added to each. The tubes were mixed (15-20 times and the solution should turn cloudy) and placed on ice for 15 min prior to centrifuging at 680 x **g** for 5 min. The supernatant was removed and 300 µl of 100% isopropanol was added. While mixing the tubes, the solution turned stringy. It was centrifuged at 680 x **g** for 10 min and the supernatant poured off. The pellet was resuspended in 300 µl of 70% ethanol and the tubes were inverted several times to wash the pellet. The suspension was centrifuged at 680 x **g** for 5 min and the supernatant was aspirated off. The pellet was allowed to air dry for 15 min and then resuspended in 50 µl of hydration solution (10mM Tris, 1mM EDTA pH 7-8).

2.11.3 *H. pylori* Cytosolic Extract Preparation

H. pylori was harvested in ice-cold 50 mM potassium phosphate buffer (pH 7.5) from 3-4 day old Columbia Blood Agar plates. Cells were washed three times in ice-cold buffer and pelleted by centrifugation (8000 x g, 10 min, 4°C) on each occasion. Pellets were then stored at –20°C until required. For total lysate preparation, frozen pellets were thawed on ice and were resuspended in the appropriate ice-cold buffer by vortexing. The resuspended material was then lysed by sonication (4 x 120 sec pulses, the sample was kept on ice water during sonication, 120 sec sonicating followed by 120 sec on ice) using a Soni-prep 150, Sanyo sonicator. The lysate was then centrifuged at 14,000 rpm for 25 min at 4°C. The supernatant was filter sterilised using a 0.45 µ low-protein binding filter (Acrodisc, Pall, U.K.) and stored at –20°C prior to protein estimation.

2.12 Insertional mutagenesis

2.12.1 Construction of *H. pylori* Aldo Keto Reductase Isogenic Mutant by Insertional Mutagenesis

The HpAKR was inactivated in the *H. pylori* clinical isolate strain 1061 by gene disruption as described below.

The purified PCR-amplified *AKR* gene was ligated into the cloning vector pGEM-T Easy (Promega, UK). The resultant plasmid, pGEM::HpAKR construct, was cleaved at the unique *X*cm I site within the *HpAKR* gene and the sticky ends were blunted with using T4 DNA polymerase. The primers used to amplify the *HpAKR* gene were 5' - ATG CAA CAG CGT CAT T-3' as the forward primer and 5'– TTA TTG ATT CAC CAT TTC AT –3' as the reverse primer. A 1.5-kb PCR product from plasmid pJMK30 containing a gene encoding resistance to kanamycin was amplified using the universal sequencing primers M13 and cloned into the unique Xcm I site within the AKR gene to yield the pGEM:HpAKR::*aphA-3* construct. This construct was digested with *Psi* I (generating two fragments) to determine the orientation of the *aphA-3* cassette. PCR and DNA sequencing were used to confirm the disruption of the gene. *H. pylori* genomic DNA was purified as outlined in section 2.11.2 and PCR was used to confirm the presence of the disrupted copy of the genomic *AKR* gene prior to DNA sequencing confirmation.

2.12.2 Natural Transformation of *H. pylori*

Natural transformation of *H. pylori* was performed essentially as described by Smeets *et al.* (2000). Briefly, transformation of *H. pylori* was achieved by the addition of 5 μg of plasmid DNA to a patch of freshly grown *H. pylori* on Columbia Blood Agar plates. After incubation for 15 hours at 37°C under microaerobic conditions, the bacteria were

transferred to selective Columbia Blood Agar plates containing kanamycin (20 μg/ml) and grown under microaerobic conditions for a further 5-7 days.

2.12.3 Electroporation of *H. pylori*

Since the natural transformation of *H. pylori* 26695 was unsuccessful on several occasions, insertion of the mutant construct was carried out using electroporation. Electroporation was performed essentially as described by Ferrero *et al.* (1992). *H. pylori* cells were harvested after 2-3 days growth on Columbia Blood Agar plates, in 1 ml of 15% glycerol/9% sucrose solution. The cells were centrifuged at 8000 rpm for 2 min, supernatant removed and the pellet resuspended in 50 μl of 15% glycerol/9% sucrose solution. DNA (1μg) was added and cells were placed on ice for 60 s. Electroporation was carried out at 25 μF, 2.5 kV, and 200 Ω for a time range of 4-5 ms. The cells were resuspended in 100 μl of Brucella broth and spread onto Columbia Blood Agar plates and incubated for 2 days in an microaerophillic environment. The plates were harvested and the bacteria were resuspended in 500 μl of Brucella broth. The culture was divided up into 5 x 100 μl and spread onto Columbia Blood agar plates supplemented with kanamycin (20 μg/ml) to select for the desired mutant and incubated in a microaerobic environment at 37°C for 4-5 days. However this protocol was unsuccessful in the course of this work.

Chapter 3

Cloning, Expression, Purification & Characterisation of *H. pylori* Aldo-Keto Reductase

3.0 Cloning, Expression, Purification & Characterisation of an Aldo Keto Reductase

3.1 Introduction

The sequenced genome of *H. pylori* 26695 identified a single putative *aldo keto reductase* (HpAKR) gene, designated in the TIGR database (www.TIGR.org) as Hp1193.

To gain a better understanding of the role played by the HpAKR in the bacterium, the gene was cloned and the gene product was expressed and purified in a recombinant form. This allowed for sufficient quantity of protein to be purified in order for biochemical and kinetic characterisation studies to be performed and was an initial step in the gene ablation studies.

3.2 Sequence Analysis of HpAKR

3.2.1 Classification of HpAKR

The *HpAKR* gene encodes a protein of 329 amino acids with an apparent molecular mass of 37 kDa. The sequence was submitted to the AKR superfamily website (http://www.med.upenn.edu/akr) (submitted on April 2006) for nomenclature assignment and was classified as AKR13C1. There are only two other members in this family, AKR13A1, the *YacK* protein from *Schizosaccaromyces pombe*, (Morita *et al.*, 2002) and the AKR13B1, a phenylacetaldehyde dehydrogenase enzyme from *Xylella fastidiosa* (Rosselli *et al.*, 2006).

3.2.2 BLAST analysis

A BLAST analysis was carried out (June 2005) using the amino acid sequence for HpAKR, which was compared to the amino acid sequences of a wide variety of

organisms. BLAST analysis can be used to infer functional and evolutionary relationships between sequences as well as to help identify members of gene families. The protein BLAST analysis revealed that the *HpAKR* gene had the highest sequence similarity with other putative aldo keto reductase and oxidoreductases from several different bacterial families. A sequence alignment was constructed using the sequences with the highest identity. Greatest identity to the HpAKR was observed in *Yersinia frederiksenii* ATCC 33641 (53% identity), *Thermotoga maritime* MSB8 (51% identity), *Yersinia pestis* KIM (51% identity), *Azotobacter vinelandii* (50% identity) and *Escherichia coli* CFT073 (50% identity). To the best of our knowledge, none of the proteins obtained from the BLAST analysis has been characterised. Therefore comparison to these proteins based on substrate specificity was not possible. The alignment (Fig. 3.1) constructed includes the other members of the AKR13C family so that their amino acid sequence could also be compared to these putative oxidoreductases.

3.3 Cloning of the HpAKR

3.3.1 Primer Design, PCR and cloning of *HpAKR* gene

Oligonucleotides used for the amplification of the Hp*AKR* gene were designed using the putative aldo-keto reductase gene sequence from *H. pylori* 26695, available at www.TIGR.org. The primers (Table 3.1) were designed to introduce Nde I and BamH I restriction enzyme cleavage sites at the N-terminus and C-terminus, respectively (Fig 3.2).

These restriction sites were also present in the multiple cloning site of the plasmid pET16(b) and therefore allow for directional cloning. Following sequential restriction

digests with *Nde* I and *BamH* I, the amplified HpAKR was directionally ligated into the cloning pET 16(b) plasmid.

During the course of this research, an update was made to the TIGR database and the HpAKR nucleotide sequence was modified to include a stop codon (TAA). The HpAKR reverse primer used in these studies did not contain a TAA stop codon; however a duplicate codon was present in the pET16(b) plasmid (Fig. 3.3).

PCR amplification of the gene encoding HpAKR from *H. pylori* strains 26695 and 1061 showed the presence of the *HpAKR* gene in both strains. The PCR products generated, using the primers in Table 3.1, can be seen in Fig. 3.4. All PCR products were the expected size of 990 bp as predicted from the sequence in the TIGR database.

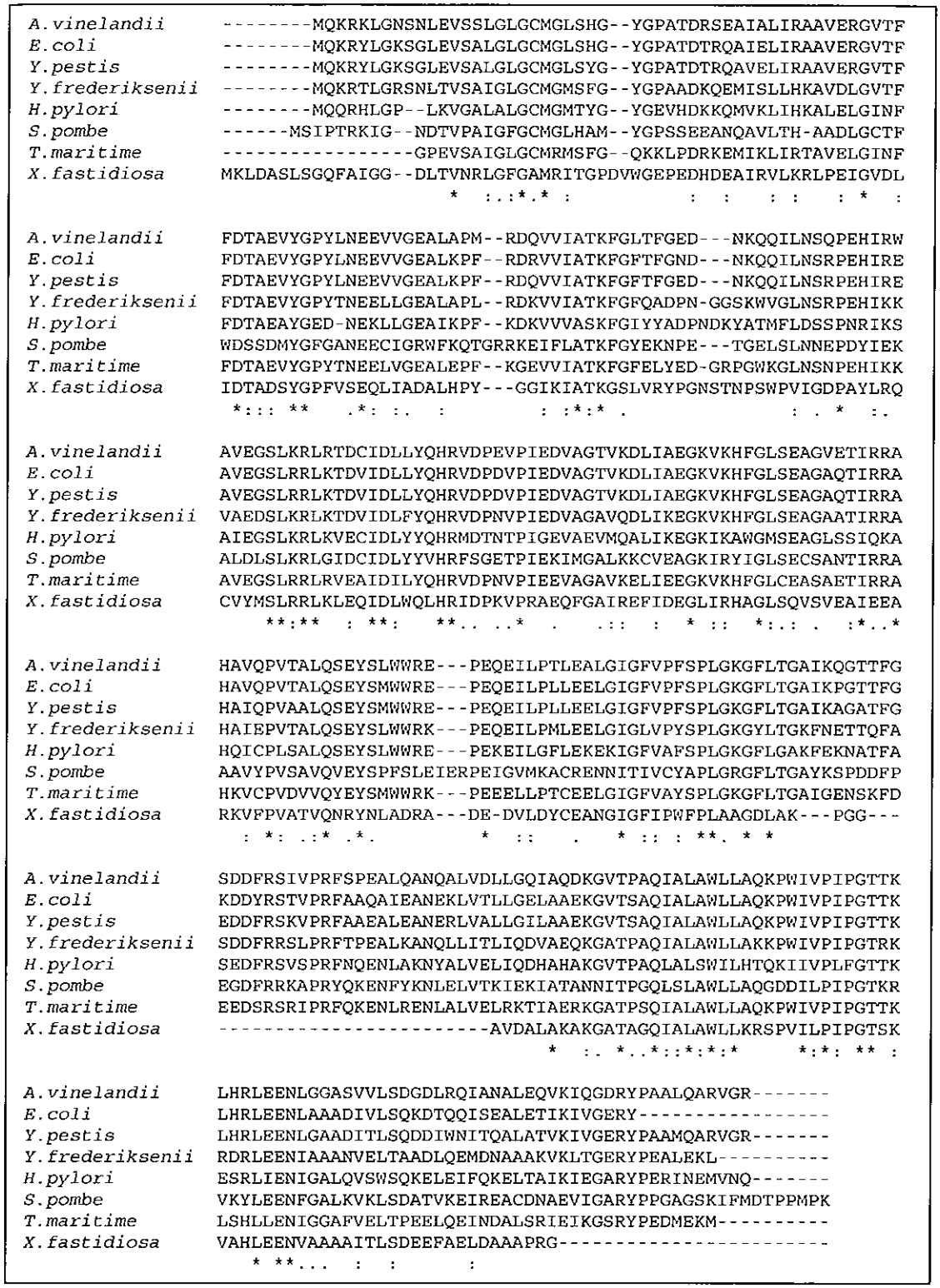

Figure 3.1: ClustalW sequence alignment of proteins with greatest homology to HpAKR. The alignment includes the sequence for the *YakC* protein (AKR13A1) from *S. pombe* and phenylacetaldehyde dehydrogenase from *X. fastidiosa* (AKR13B1), the other two members of the AKR13 family. Sequence similarity is indicated by (*) exact matches, (:) strong similarity, (.) weak similarity.

Primer direction	Primer sequence
Forward	5'-CGC-CAT-ATG CAA CAG CGT CATT-3' **Nde I**
Reverse	5'-CGC-GGA-TCC- TTG ATT CAC CAT TTC AT-3' **BamH I**

Table 3.1: Oligonucleotide primers designed for the amplification of the *HpAKR* gene from *H. pylori* 26695 and 1061.

CGCCATATGCAACAGCGTCATTTAGGCCCTTTAAAAGTGGGTGCATTAGCTCTAGGGTG
CATGGGCATGACTTATGGGTATGGGGAAGTCCATGATAAAAAGCAGATGGTTAAACTTA
TCCATAAGGCTTTGGAATTGGGTATTAACTTTTTTGACACTGCAGAGGCTTATGGGGAAG
ATAATGAAAAGCTTTTAGGCGAAGCGATCAAGCCTTTTAAAGACAAGGTTGTGGTAGCG
AGCAAGTTTGGGATTTACTACGCAGATCCTAATGACAAATACGCAACCATGTTTTTAGAC
TCCAGTCCTAACCGCATTAAGAGCGCCATTGAAGGGAGTTTGAAACGCTTAAAAGTAGA
ATGCATTGATTTATACTACCAACACCGCATGGATACTAACACGCCCATAGGAGAAGTGG
CAGAAGTTATGCAGCTTCTTATTAAAGAAGGAAAAATTAAAGCTTGGGGGATGAGTGAG
GCAGGGTTATCTAGCATCCAAAAAGCCCATCAAATTTGCCCTTTAAGCGCGTTGCAGAG
CGAATATTCCTTGTGGTGGCGCGAACCTGAAAAAGAGATTTTAGGTTTTTTAGAAAAAGA
AAAAATTGGATTTGTCGCTTTTTCGCCTTTGGGTAAGGGGTTTTTAGGCGCGAAATTTGA
AAAAAATGCCACTTTCGCTAGTGAGGATTTTAGAAGCGTTTCTCCTAGGTTTAATCAAGA
AAATCTAGCCAAAAATTACGCCTTGGTGGAATTAATCCAAGATCATGCACACGCTAAAGG
CGTTACACCAGCCCAACTGGCTCTCTCATGGATTTTGCACACGCAAAAAATCATTGTCCC
TCTCTTTGGCACCACCAAAGAATCTAGGCTCATAGAAAATATAGGGGCTTTGCAGGTTTC
TTGGAGTCAAAAAGAATTGGAGATTTTCCAAAAAGAATTGACTGCAATCAAAATAGAAGG
GGCCCGCTACCCTGAAAGAATCAATGAAATGGTGAATCAACCTGGATAA

Figure 3.2: Gene Sequence for HpAKR. Primers used for the amplification of the gene are underlined. The inserted Nde I restriction enzyme cleavage site is highlighted in yellow. The inserted BamHI restriction enzyme cleavage site is highlighted in red.

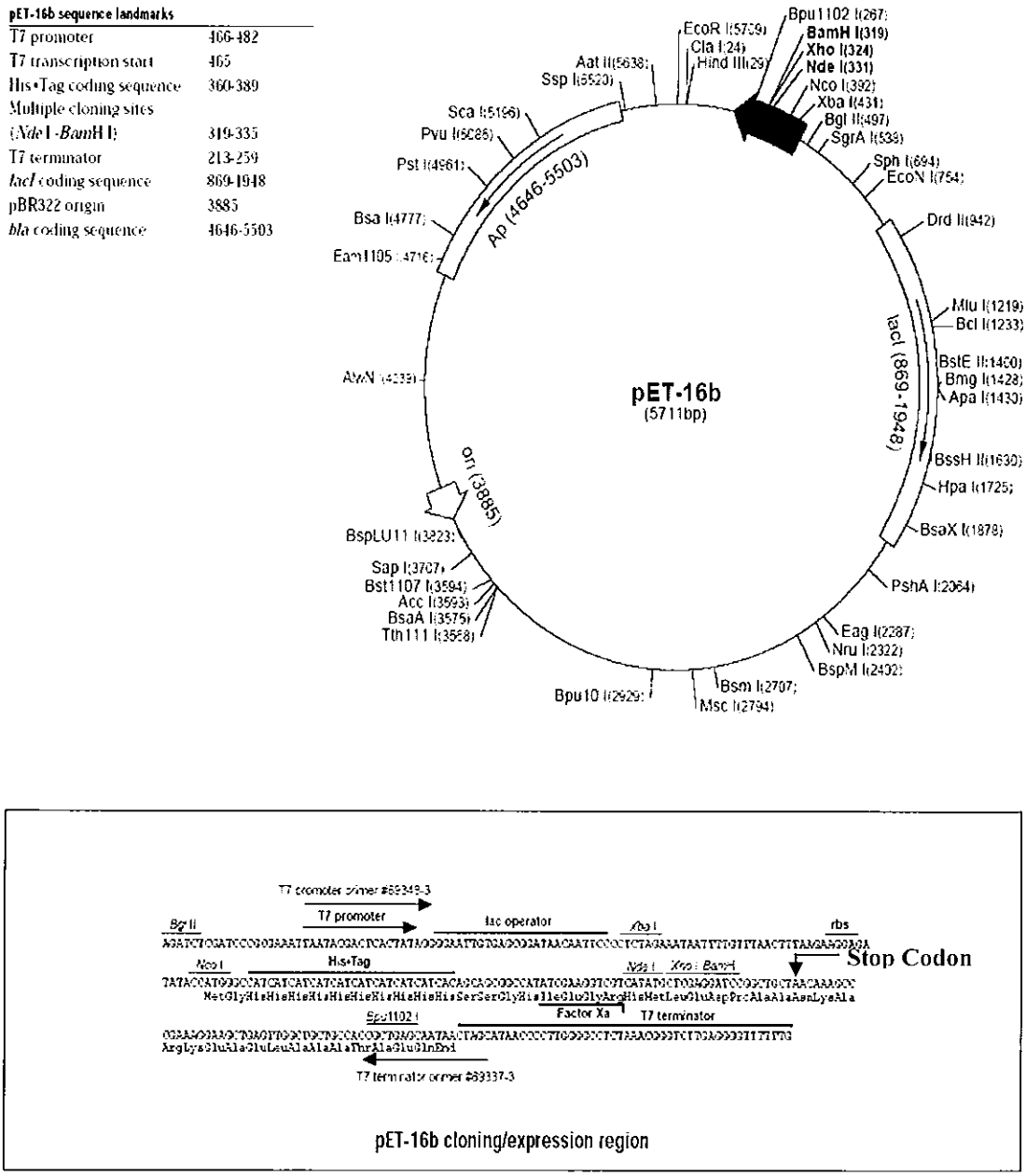

Fig. 3.3: Figure illustrating the pET16(b) vector. The TAA stop codon is indicated in the nucleotide sequence inset.

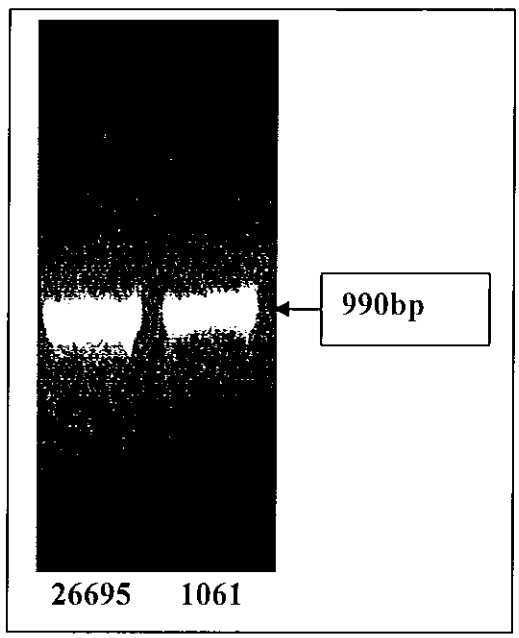

Fig. 3.4: Agarose (1 %) gel electrophoresis of the PCR products obtained by amplification of the *HpAKR* gene from *H. pylori* strains 26695 (Lane 1) and 1061 (Lane 2) using High Fidelity *Taq* polymerase (Roche, UK). Amplification was carried out as described in Materials and Methods, section 2.6.4.

3.3.2 Generation of pET-HpAKR Construct

For the generation of the pET-HpAKR construct, DNA from *H. pylori* 26695 was used. Essentially, cloning involved the digestion of the PCR amplicon and the pET16(b) vector using *BamH* I and *Nde* I restriction enzymes. Due to the overhangs generated from the digest, the subsequent ligation of the vector and insert was directional. The resulting plasmid, pET-HpAKR was transformed into *E. coli* DH5α. Transformed colonies were selected by their resistance to the antibiotic ampicillin conferred by the pET16(b) vector. *E. coli* DH5α colonies screened containing the pET16(b) plasmid with an inserted *AKR* gene were identified by a 990 bp increase in the size of the pET16(b) vector (Fig. 3.5).

A total of 6 transformants exhibited a 990 bp increase in size. The constructs were sequenced and found to have inserts corresponding to the sequence for the *HpAKR* gene. However, sequence analysis of the *HpAKR* gene cloned in this study revealed the presence of an alanine residue at position 153 (highlighted in light grey) (Fig. 3.6), rather than the leucine residue indicated in the TIGR sequence. The cloning of the *HpAKR* gene was repeated in triplicate and the same sequence was obtained. To ensure this residue was not present on a conserved region, such as the active site tetrad (highlighted in dark grey), the *HpAKR* gene sequence was aligned with the rat liver *3α-hydroxysteroid dehydrogenase* (3α-HSD) gene since this is a common AKR standard used for numbering purposes. The sequence alignment was performed using the Tcoffee programme (www.igs.cnrs-mrs.fr/Tcoffee/tcoffee_cgi/index.cgi) (Fig. 3.6) and the alignment indicated that the alanine residue is not adjacent to the active site tetrad.

3.4 Overexpression and Purification of *HpAKR* gene product

3.4.1 Transformation and screening of *E. coli* BL21(DE3)*pLysS* colonies

The sequenced pET-HpAKR construct, containing the inserted *HpAKR* gene, was transformed into *E. coli* BL21(DE3) *pLysS* for overexpression. The expression host, *E. coli* BL21(DE3) *pLysS*, has a T7 promoter driven system containing a *pLys* plasmid, which encodes T7 lysosyme, a natural inhibitor of T7 RNA polymerase transcription. The ability of T7 RNA polymerase to transcribe target genes is reduced in uninduced cells (*i.e.* cells that are not exposed to IPTG). T7 lysozyme expression induces rapid lysis of *E. coli* cells after freeze thawing. The *pLysS* plasmid confers resistance to the antibiotic chloroamphenicol.

Transformed colonies were selected on the basis of dual ampicillin and chloroamphenicol resistance. These colonies were screened for the presence of the plasmid pET-HpAKR (Fig. 3.7). All of the transformants screened showed a 990 bp increase in size indicating the presence of the inserted *HpAKR* gene. A smaller band for the *pLysS* plasmid, was also evident in each lane.

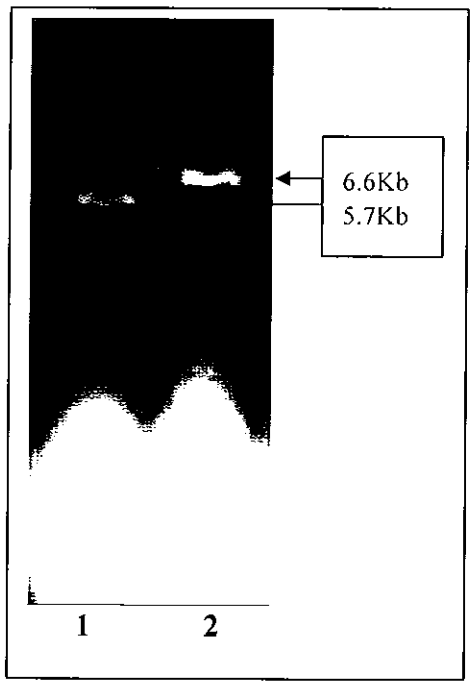

Fig. 3.5: Agarose (1 %) gel electrophoresis screening of plasmids isolated from transformed *E. coli* DH5α colonies, for insertion of the amplified HpAKR product into the pET16(b) plasmid. Lane 1 contains the pET16(b) vector with no insert as a control at a size of 5.7 Kb. Lane 2 contains a pET16(b) vector with the inserted *HpAKR* gene (990bp). The size of this plasmid is 6.6 Kb. Screening was carried out as described in Materials and Methods, section 2.7.3.

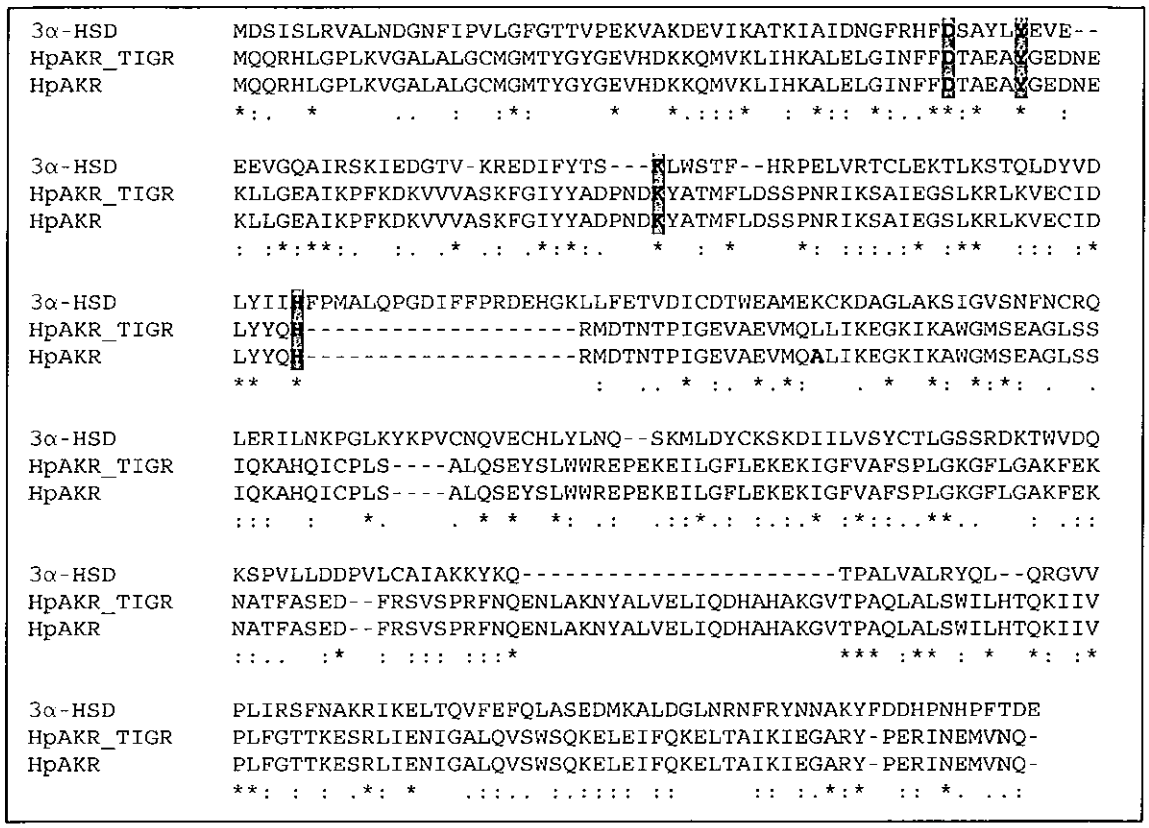

Figure 3.6: T-coffee Sequence alignment of cloned HpAKR against TIGR database AKR sequence and *3 α-hydroxysteroid dehydrogenase* gene. The amino acid highlighted in light grey indicates the position of the alanine residue identified in the cloned HpAKR described in this study. The amino acid residues highlighted in dark grey are the conserved active site amino acid residues characteristic of the AKR family (Jez *et al.*, 1997). Sequence similarity is indicated by (*) exact matches, (:) strong similarity, (.) weak similarity.

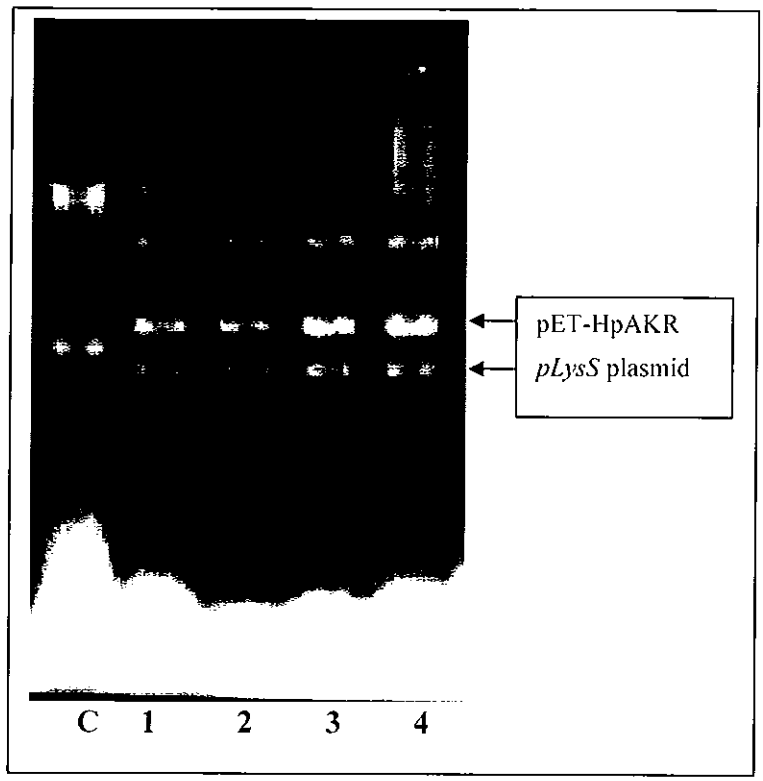

Fig. 3.7: Agarose (1 %) gel electrophoresis screening of plasmids isolated from transformed *E. coli* BL21(DE3)*pLysS* colonies. Lane C is the control: *E. coli* BL21(DE3)*pLysS* cells transformed with unrestricted pET 16(b) plasmid. Lanes 1 –4 shows plasmids isolated from the transformed cells. The screening process is outlined in Materials and Methods: Section 2.7.3

3.4.2 Induction of HpAKR protein

The *E. coli* BL21(DE3)*pLysS* cells, which harboured the pET-HpAKR construct, were induced by the addition of 1 mM IPTG to a liquid culture (at an OD_{600nm} of 0.4-0.6). The cells were induced at 37°C for 4 h followed by reduction of the temperature to 20°C for a further 14-16 h.

3.4.3 Purification of HpAKR protein

In general, a 1 l culture of pET-HpAKR transformed *E. coli* BL21(DE3)*pLysS* was used for isolation of the recombinant protein. The His-tag present on the N-terminus of the expressed HpAKR protein facilitated one-step affinity purification on a nickel-charged iminodiacetic acid column. The purity of fractions collected was assessed using SDS-PAGE analysis. The gels were stained with Coomassie brilliant blue and showed a single band with a molecular mass of approx 39 kDa (Fig. 3.8). Thus, 1 l of culture yielded between 0.6-0.8 mg of purified HpAKR.

3.4.4 Dialysis of HpAKR

The purified fractions, as seen on SDS-PAGE, from the nickel affinity chromatography column were pooled and dialysed. It became apparent that the enzyme bound non-specifically to the dialysis tubing. In order to minimise loss, the dialysis conditions were optimised using various buffers. The buffers are outlined in Table 3.2.

Purified fractions of HpAKR were pooled and split into 4 equal volumes. Dialysis with the four different buffers was performed simultaneously. The HpAKR was dialysed against 1 l of each buffer for 4 h with 2 buffer changes at 4°C.

The Bradford (Bradford., 1976) assay was used to determine protein concentration after dialysis (Table 3.3).

From Table 3.3, it was evident that the 50 mM potassium phosphate buffer (pH 7.5) containing 50 μM EDTA yielded the most protein after dialysis. Therefore this buffer was used for all subsequent experiments.

For a typical preparation from 1 l of culture, a total of 8 x 1 ml fractions were dialysed. The fractions chosen were based on their purity and their protein concentration, which was assessed visually by SDS-PAGE.

After dialysis was completed, the protein was concentrated using ultra-centricon tubes so that the final concentration of purified HpAKR was approximately 3-fold that after dialysis. The tubes were centrifuged at 400 x **g** for 45 min at 4°C. The Bradford assay was used to quantify the final protein concentration.

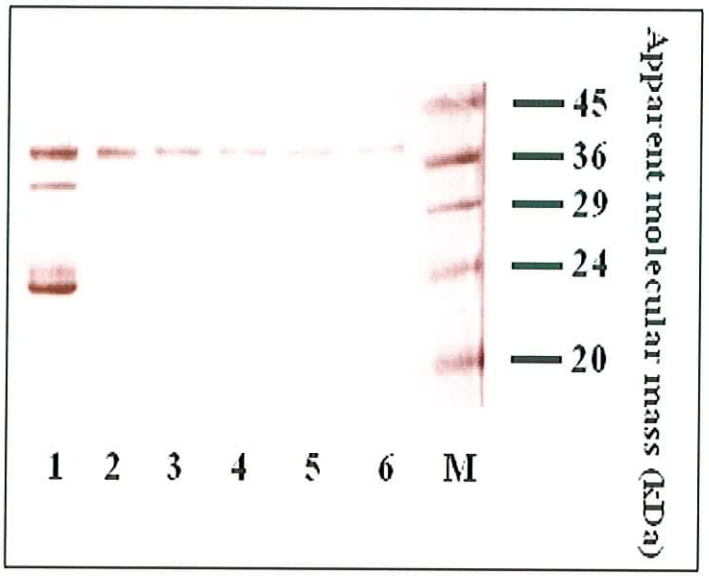

Fig. 3.8: 15% SDS-PAGE indicating the protein purity of recombinant HpAKR eluted from the nickel-charged iminodiacetic acid column. Lane 1 contains the nickel column wash. Lanes 2-6 contains fractions collected from the nickel column showing the presence of a single band for the HpAKR protein with an approximate molecular mass of 39 kDa after staining with Coomassie brilliant blue. Lane M contains molecular weight markers

Buffer	Components
MES	25 mM MES, 0.3 M NaCl, 50 μM EDTA (pH 7.5)
Phosphate buffered saline	8 mM $Na_2HPO_4.2H_2O$,1.5 mM KH_2PO4, 137 mM NaCl, 2.7 mM KCl (pH 7.5)
Potassium phosphate buffer	50 mM KH_2PO_4 (pH 7.5)
Potassium phosphate & EDTA buffer	50 mM KH_2PO_4, 50 μM EDTA (pH 7.5)

Table 3.2: Buffers used for the optimisation of the dialysis process

Buffer	Protein Concentration	
	Before Dialysis	After Dialysis
MES (pH 7.5)	0.114mg/ml	0.074mg/ml
Phosphate buffer saline (pH7.5)	0.167mg/ml	0.099mg/ml
Potassium phosphate buffer (pH 7.5)	0.165mg/ml	0.137mg/ml
Potassium phosphate & EDTA (pH 7.5)	0.150mg/ml	0.145mg/ml

Table 3.3: Optimisation of dialysis of purified HpAKR: Protein concentration was quantified before and after dialysis for various buffers. Table 3.4 outlines the reagents used for the preparation of these buffers. The Bradford assay was used to quantify the protein concentration. The Bradford protein assay is outlined in Materials and Methods; Section 2.3.

3.5 Gel Filtration Analysis of HpAKR

To determine the molecular weight of purified HpAKR under native conditions, gel filtration analysis was carried out using a Superdex 75-HR column. A standard curve was constructed using ovalbumin (43 kDa), chymotypsinogen A (25 kDa) and ribonuclease A (13.7 kDa). The standard curve was generated by plotting the Log of the protein standard molecular mass as a function of their corresponding Kav values. The Kav values were calculated using the equation

Kav = (Vr – Vo) / (Vc – Vo);

Where;

Vr = Retention volume (specific for each standard),

Vo = Void Volume (8.15 ml),

Vc = Bed volume of 24 ml.

The void volume was defined as the volume of mobile phase required to carry an un-retained component through the column. The void volume was determined using the standard, blue dextran. The elution profile for the standards can be seen in Fig. 3.9.
The standard curve was constructed using the Kav values calculated for the protein standards (Fig. 3.10).

Purified HpAKR (0.8 mg/ml) was applied to the Superdex75 HR column (Fig. 3.11) for estimation of the molecular mass under native conditions.

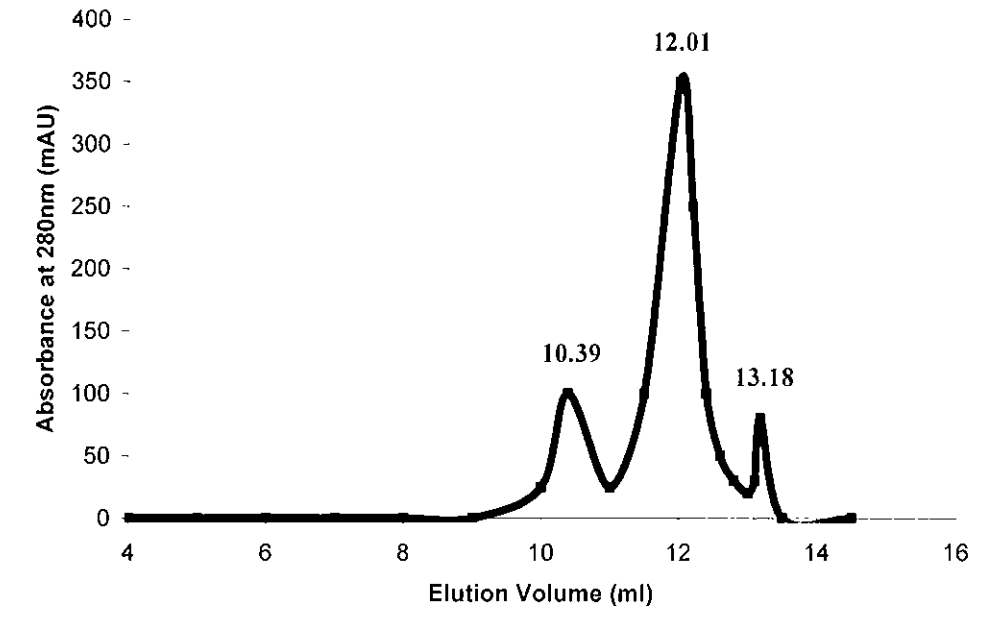

Fig. 3.9: Gel filtration of protein standards on Superdex75 column. Elution profile of the protein standards used for the construction of a standard curve; ribonuclease A 13.18 min, chymotrypsinogen A 12.01 min and ovalbumin 10.39 min. Gel Filtration method outlined in Materials and Methods; section 2.8.

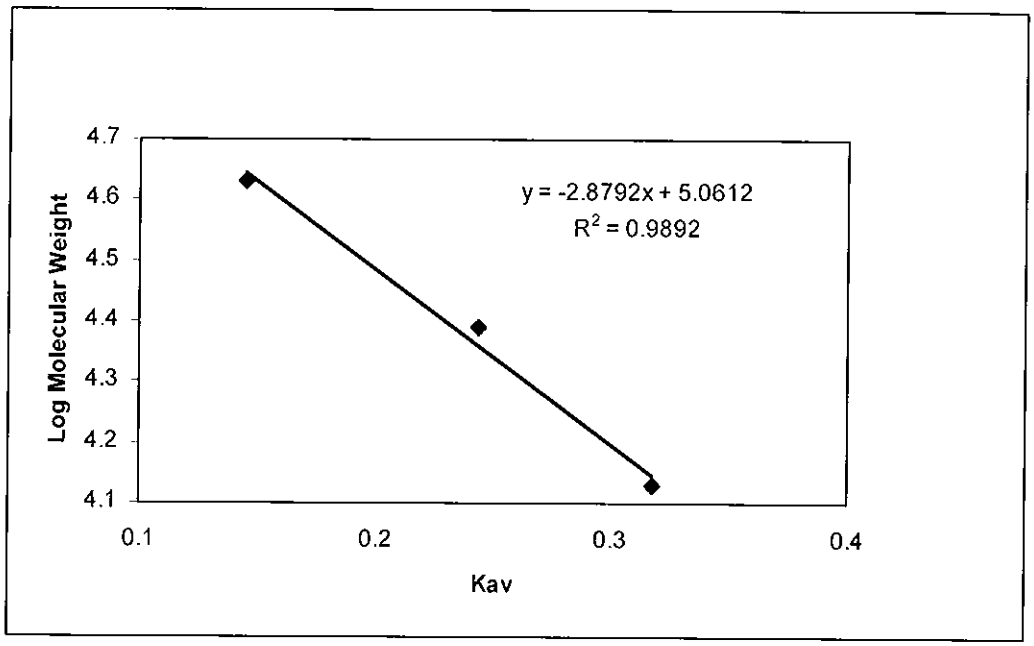

Fig. 3.10: Standard curve for protein molecular weight. Standard curve constructed using standard Kav calculated from protein elution volumes as shown in Fig. 3.9. The gel filtration method is described in Materials and Methods; Section 2.8.

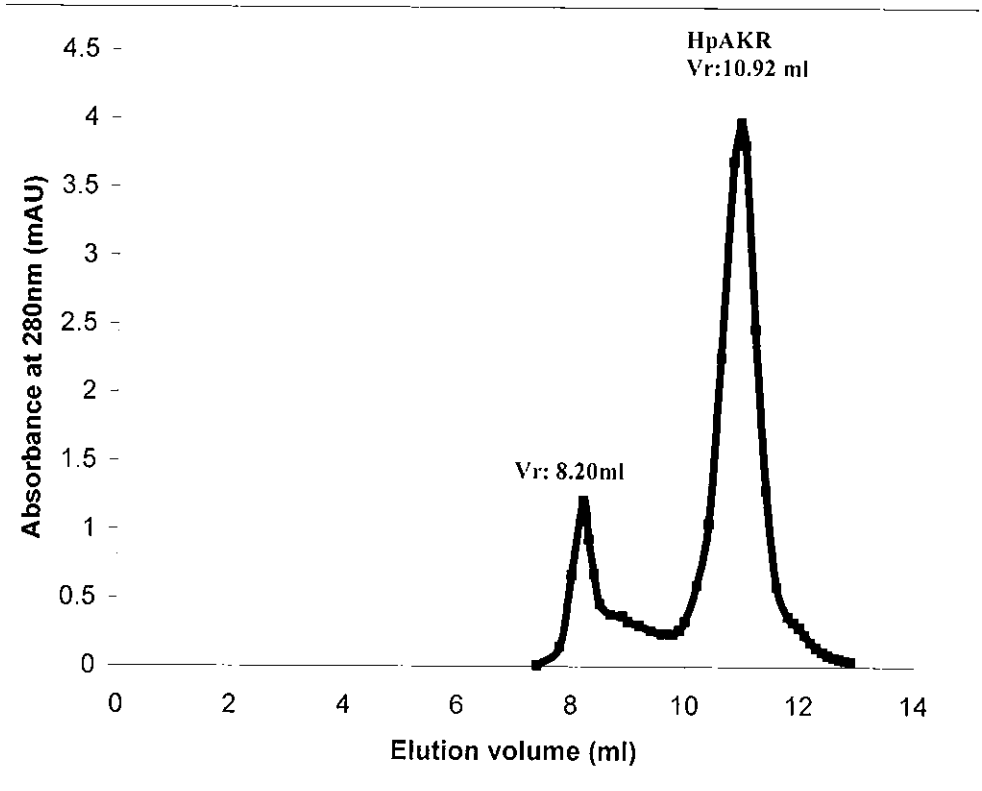

Fig. 3.11: Elution profile for HpAKR. The elution volume for HpAKR peak was 10.92 ml. The presence of a second peak with an elution volume of 8.20ml was evident.

Using this elution volume, HpAKR was estimated to have a molecular mass of approximately 49 kDa.

The second peak present in Fig. 3.11 (retention volume 8.20 ml) was thought to be a dimeric form of HpAKR, which may have been formed by reaction of thiol groups to form disulphide bridges. However, when the purified preparation was incubated with DTT (50 mM), no change in the gel filtration profile was observed.

Moreover, the molecular mass using the elution volume for the second peak showed the size of the contaminants to be approximately 56 kDa. Therefore, the size of these unknown protein species was too small to represent a dimeric form of HpAKR.

To analyse this contaminant peak further, fractions were collected from the gel filtration column and subjected to SDS-PAGE gel (Fig. 3.12).

This analysis revealed that the purified fraction of recombinant HpAKR (lane 6) also contained some higher molecular weight proteins, which only became apparent after protein concentration.

Since these high molecular weight proteins may have affected enzyme assays, fractions were collected from the Superdex75 gel filtration column and assayed for aldehyde reducing activity as described in materials and methods using pyridine-2-aldehyde as a substrate at a concentration of 2 mM. No aldehyde reducing activity was associated with fractions 1 and 2 and therefore they did not act as a source of interference in the enzyme kinetic studies (data not shown). Fractions 3 and 4 demonstrated aldehyde reductase activity towards pyridine-2-aldehyde.

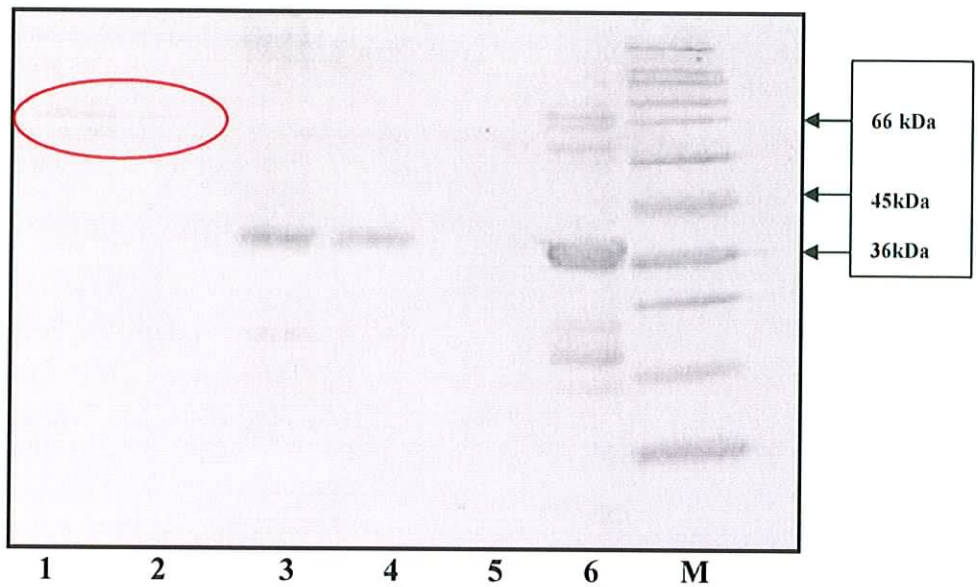

Fig. 3.12: 15% polyacrylamide gel electrophoresis of fractions collected from the superdex75 FPLC column. Lanes 1-2 contains samples of the 56 kDa peak. Lanes 3-4 contains samples of the 49 kDa peak (HpAKR protein). Lane 5 is empty. Lane 6 contains purified HpAKR. Lane M contains the molecular weight marker.

3.6 Discussion

This chapter details the cloning, expression and purification of an aldo keto reductase from *Helicobacter pylori.*

On submission of the HpAKR sequence to the AKR superfamily website, (http://www.med.upenn.edu/akr), the enzyme was designated as a new member of the AKR13 family and assigned the name AKR13C1.

However, AKR13 is a little characterised branch of the family consisting of only two other members, the AKR13A1, *YacK* protein from *Schizosaccaromyces pombe,* (Morita *et al.*, 2002) and the AKR13B1, phenylacetaldehyde dehydrogenase enzyme from *Xylella fastidiosa* (Rosselli *et al.*, 2006). The *YacK* protein was found to catalyse the reduction of 2-nitrobenzaldehyde and pyridine-2-aldehyde while the phenylacetaldehyde dehydrogenase enzyme was found to reduce 2-nitrobenzaldehyde and glyceraldehyde.

A protein BLAST analysis of HpAKR, revealed that it had significant identity to several other putative bacterial aldo keto reductases. The most significant candidates were: *Yersinia frederiksenii* ATCC 33641 (53% identity), *Thermotoga maritime* MSB8 (51% identity), *Yersinia pestis* KIM (51% identity), *Azotobacter vinelandii* (50% identity) and *Escherichia coli* CFT073 (50% identity). However, none of these proteins have been characterised in terms of their substrate specificity.

Sequence analysis revealed that the HpAKR amino acid sequence is more similar to the other putative prokaryotic AKRs from the BLAST search, with up to 53% identity, in comparison to the amino acid sequences for the other AKR13 family members.

The *HpAKR* gene of this study was cloned from *H. pylori* strain 26695. DNA sequencing of the PCR product revealed the presence of an alanine residue at position

153 in contrast to the leucine identified in the TIGR database (www.TIGR.org). The PCR and cloning were repeated three times and in each case the sequence of the PCR product was identical. It is therefore unlikely that the amino acid difference is due to a PCR artefact. To ensure that this residue was not present in any conserved region, the amino acid sequence was aligned against the *3α-hydroxysteroid dehydrogenase* gene, for numbering purposes. Figure 3.5 illustrates this alignment and indicates that this alanine-leucine difference is not present near the active site tetrad, Asp-50, Tyr-55, Lys-84 and His-117 (Jez *et al.*, 1997).

The exact effect of this alanine residue on the enzyme's activity is unknown. However, this substitution is conservative and the residue is unlikely to be directly involved in catalysis. To assess this, the alanine residue on the HpAKR amino acid sequence would need to be replaced with a leucine residue and differences in enzymatic activity assessed. It is most likely that the difference in amino acid sequences for the HpAKR sequence is due to a sequencing error on the TIGR database.

The pET-HpAKR construct was transformed into the *E. coli* BL21(DE3)*pLysS* cells for overexpression of the *HpAKR* gene product. In general a 1 l culture yielded 6-8 mg of purified HpAKR. The presence of the His-Tag on the N-terminus allowed for a 1-step affinity purification. The purity of the fractions collected from the column was assessed by SDS-PAGE, which showed a single band with a molecular weight of 39 kDa. This compares favourably with the molecular mass calculated from the amino acid sequence on the TIGR database (37 kDa). The slight increase in molecular weight is primarily due to the presence of the His-Tag.

Pure fractions of HpAKR, were pooled and dialysed against 50 mM potassium phosphate containing 50 μM EDTA (pH 7.5) since this buffer minimised adherence of

the protein to the dialysis tubing. Prior to use, the recombinant protein was concentrated using centrifugal concentrators.

Gel filtration analysis was carried out on a Superdex75 column, to assess the protein's molecular mass under native conditions. The purified HpAKR migrated as a monomer with a molecular weight of 49 kDa. A second minor peak with an approximate size of 56 kDa was also evident from this analysis. It was possible that this 56 kDa peak may be a dimeric form of the HpAKR formed as a result of disulphide bridge formation within the protein. However after incubating purified HpAKR with 50 mM DTT, no change in elution profile was observed. Fractions were collected from the Superdex75 column and analysed by SDS-PAGE. High molecular weight proteins were observed (Fig. 3.12) in the purified fractions of the 56 kDa peak. There was no aldehyde reductase activity associated with these minor contaminants when tested for AKR activity spectrophotometrically. Fractions of purified HpAKR from the Superdex75 column demonstrated aldehyde reductase activity towards pyridine-2-aldehyde thus confirming that the purified HpAKR is an active aldehyde reductase.

In summary, this chapter presents a robust system for the expression and purification of recombinant HpAKR in high yield. It further confirms that this protein is indeed an aldo keto reductase as indicated by its putative designation in the TIGR database.

Chapter 4

Kinetic Analysis of Purified HpAKR

4.0 Kinetic Analysis of Purified HpAKR

4.1 Introduction

Aldo keto reductases (AKR) are a class of enzymes that reversibly reduce toxic aldehydes and ketones to their corresponding alcohol product. The AKRs are generally approximately 35 kDa in size and utilise a nicotinamide co-factor (Jez *et al.*, 1997).

These proteins break down a diverse range of substrates including aliphatic and aromatic aldehydes, monosaccharides, steroids, prostaglandins, polycyclic aromatic hydrocarbons and isoflavinoids (Jez *et al.*, 1997 and Hyndman *et al.*, 2003). Even though these enzymes can reduce a wide range of aldehyde compounds, their affinity for individual aldehydes may differ greatly.

Aldo keto reductases are found in all living organisms however, they often play a different role in different tissues as well as in different organisms. The microbial AKR span 10 families in the AKR superfamily (Ellis., 2002).

In this chapter, the purified recombinant HpAKR is characterised in terms of its substrate preference, inihibiton studies and stability. The inhibition of HpAKR by sodium valproate, results in non-compliance to Michaelis-Menten kinetics. This is only the second time this type of kinetic behaviour has been reported for this class of enzyme. The first observation was reported in for an aldehyde reductase isolated from sheep liver (De Jongh *et al.*, 1987).

Assay conditions are described in materials and methods section 2.10. All assays were carried out at pH 7.5, 37°C unless otherwise specified.

Steady-state parameters were determined by fitting the initial rates to the Michaelis-Menten equation using the ENZFITTER program. However the kinetic data are displayed as Lineweaver-Burke plots, a linear form of the Michaelis-Menten equation for illustrative purposes (Fig. 4.1).

Lineweaver-Burk Plot

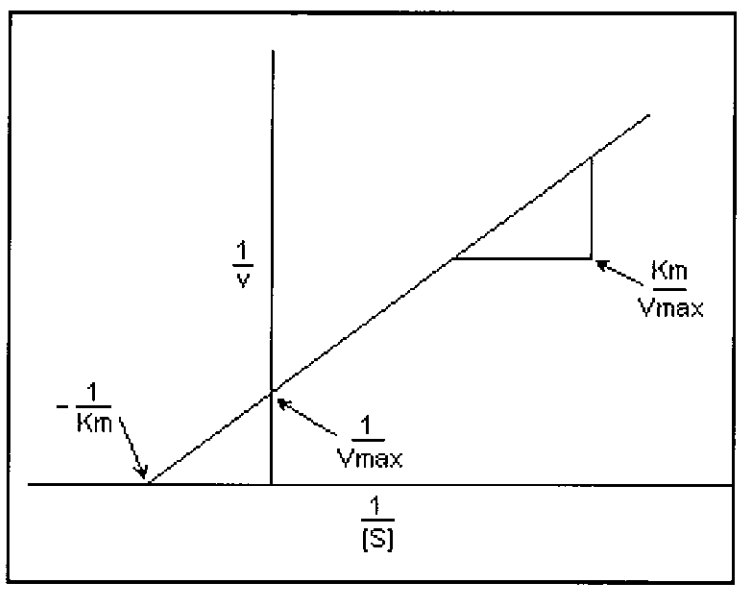

Fig. 4.1: Illustration of Lineweaver-Burke plot: where **v** = initial velocity, **s** = substrate concentration, V_{max} = the maximum rate of reaction for a given concentration of enzyme and K_m = is the concentration of substrate at half the V_{max}.

4.2 Plot of Initial Rates as a Function of the Amount of HpAKR

A plot of amount of enzyme versus initial velocity was constructed to examine the linear range for the HpAKR assay (Fig. 4.2). The initial rates measured were linearly dependant on HpAKR concentration. The concentration of HpAKR employed was varied between 0.05-0.3 μg/ml. The 3-nitrobenzaldehyde substrate concentration was kept constant at 6.4 mM and NADPH at 0.2 mM for this plot.

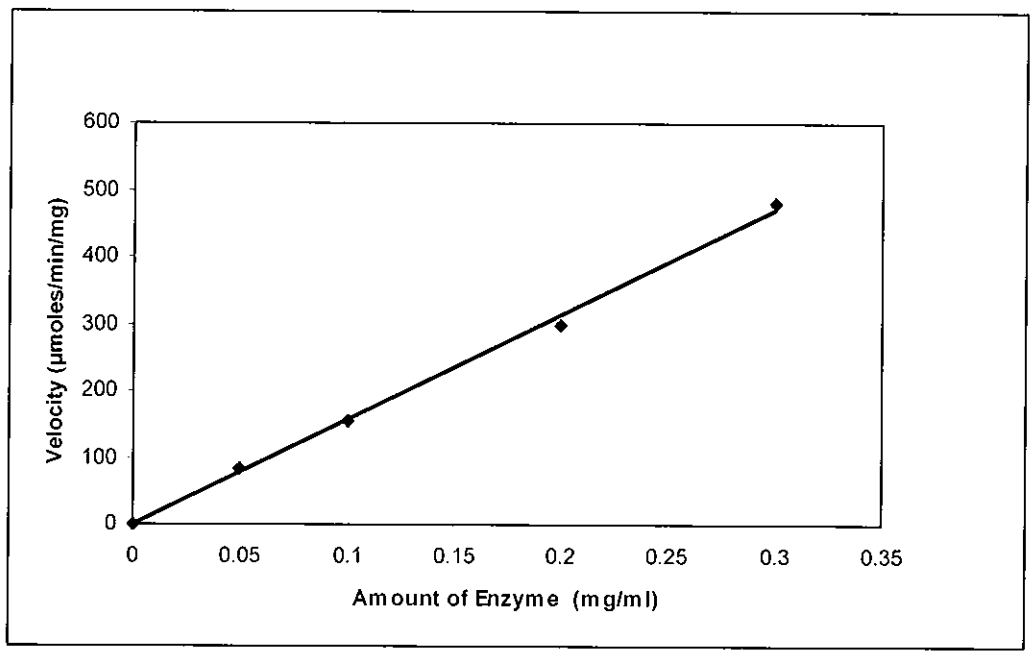

Fig. 4.2: Plot of enzyme amount versus initial velocity calculated using different amounts of HpAKR (0.05-0.3 μg) with a fixed concentration of 3-Nitrobenzaldehyde (6.4 mM) and NADPH (0.2 mM).

4.3 Kinetic Constants for Co-factors NADPH/ NADH and Aldehyde Substrates.

4.3.1 NADPH

Determination of Michaelis constants for the oxidation of NADPH by HpAKR (Fig. 4.3)

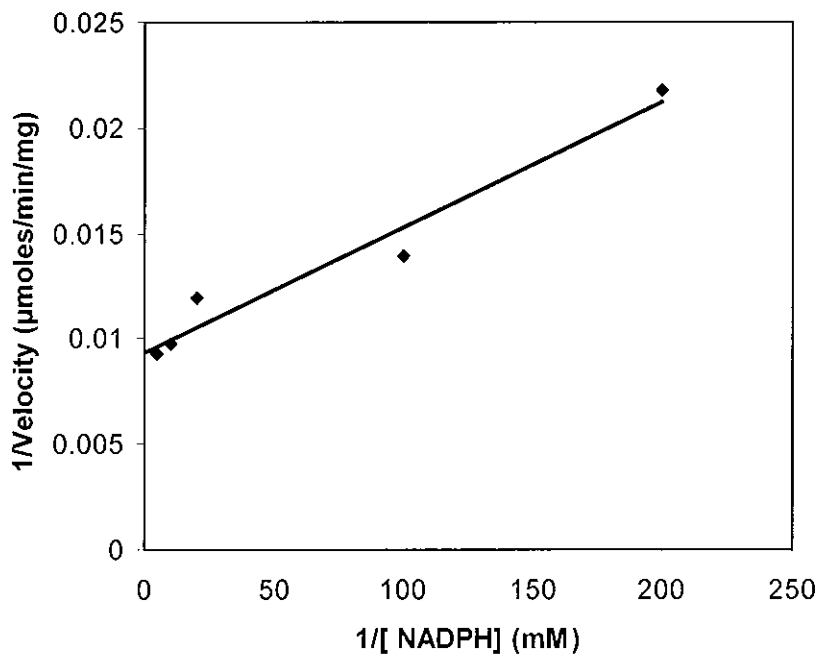

Fig. 4.3: Lineweaver Burke plot for the oxidation of NADPH by purified HpAKR over a concentration range of 0.005-0.3 mM. Benzaldehyde was used as a co-substrate and was present at a fixed concentration of 7 mM

A K_m value of 6 µM was estimated for NADPH. Subsequent K_m values for aldehyde substrates were estimated using a fixed NADPH concentration of 0.2 mM. This ensures saturation with co-factor at all times. Kinetic constants for all substrates are summarised in Table 4.1.

4.3.2 NADH

Unlike many AKRs, HpAKR was found to utilise both NADPH and NADH as co-factors. Determination of Michaelis constants for the oxidation of NADH by HpAKR is shown in Fig. 4.4.

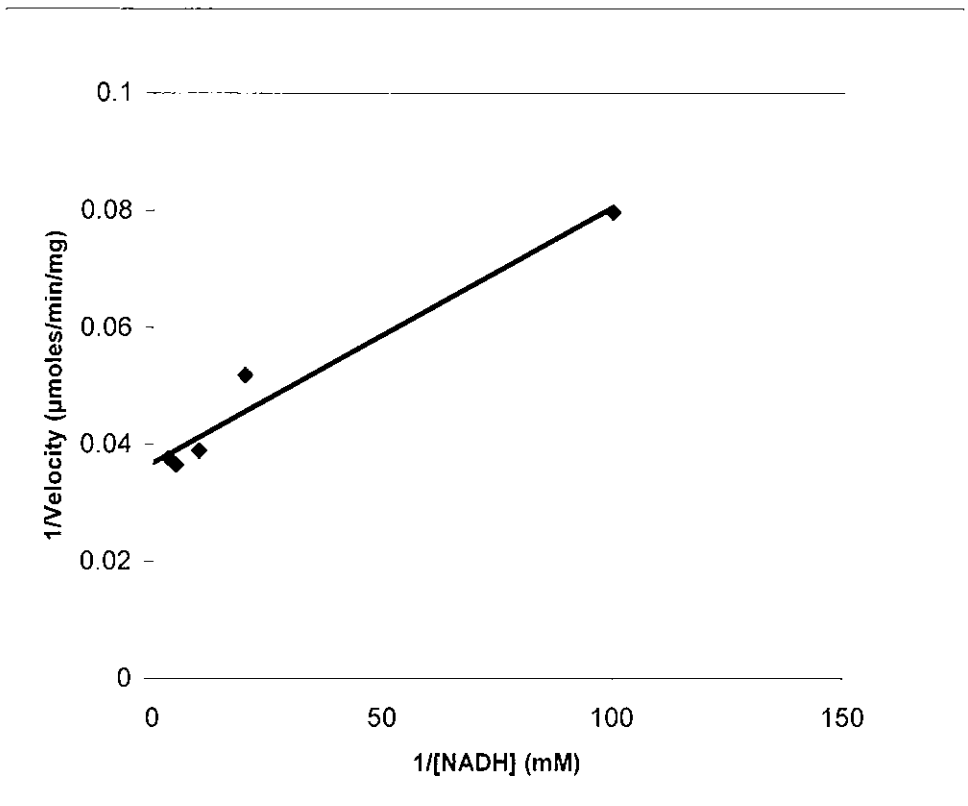

Fig. 4.4: Lineweaver Burke plot of the reduction of NADH by purified HpAKR over a concentration range of 0.01-0.3 mM. Benzaldehyde was used as a co-substrate and was fixed at 7 mM

A K_m of 0.01 mM was estimated for NADH. Kinetic constants for all substrates are summarised in Table 4.1 (page 102).

4.3.3 Benzaldehyde

Determination of Michaelis constants for the reduction of benzaldehyde in the concentration range of 0.2-20 mM by HpAKR (Fig. 4.5).

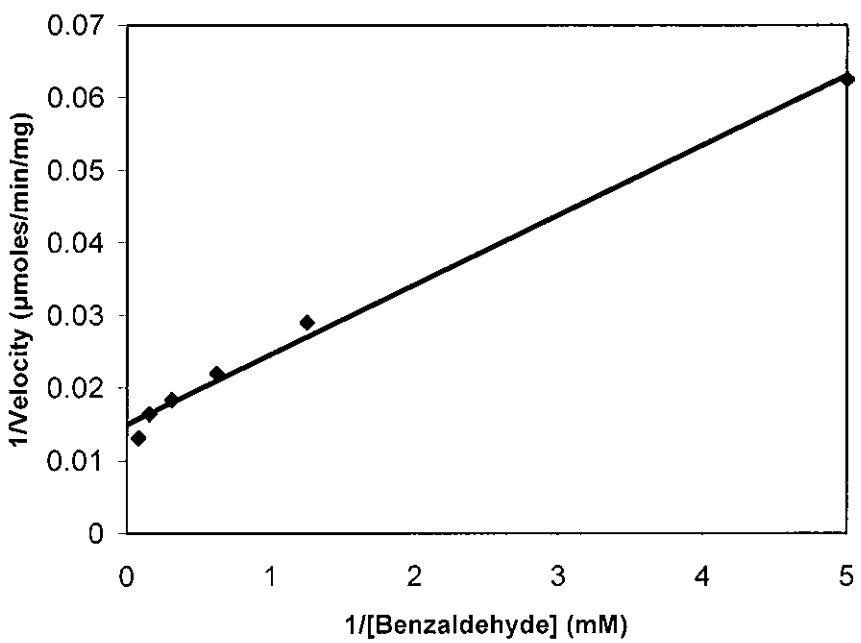

Fig. 4.5: Lineweaver Burke plot of the reduction of benzaldehyde by purified HpAKR over a benzaldehyde concentration range of 0.2-20 mM. The NADPH concentration was fixed at 0.2 mM

A K_m of 1.9 ± 0.7 mM was estimated for benzaldehyde. Kinetic constants for all substrates are summarised in Table 4.1 (page 102).

4.3.4 3-Nitrobenzaldehyde

Determination of Michaelis constants for the reduction of 3-nitrobenzaldehyde in the concentration range of 0.2-6.4 mM by HpAKR (Fig. 4.6).

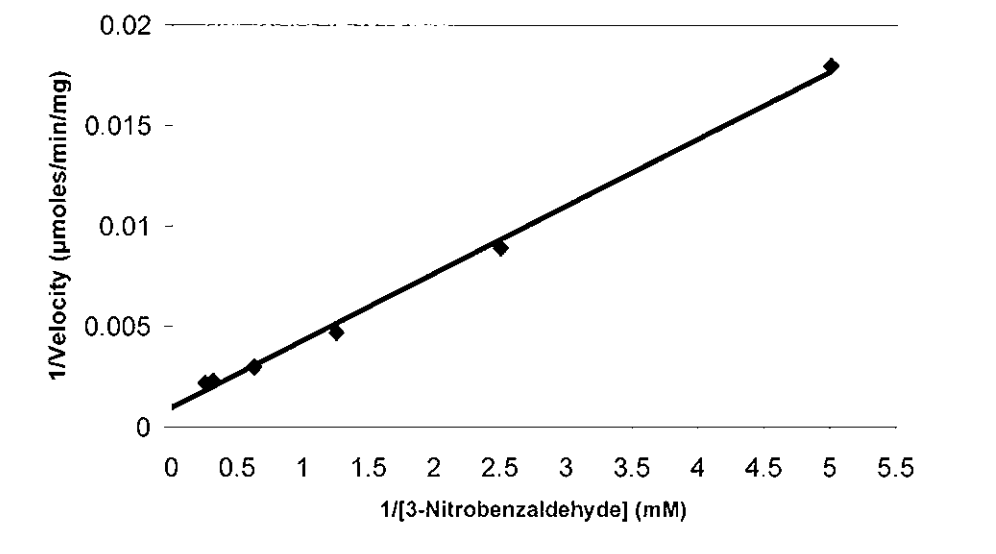

Fig. 4.6: Lineweaver Burke plot of the reduction of 3-nitrobenzaldehyde by purified HpAKR over a 3-nitrobenzaldehyde concentration range of 0.2-6.4 mM. The NADPH concentration was fixed at 0.2 mM

A K_m of 1.7 ± 0.18 mM was estimated for 3-nitrobenaldehyde. Kinetic constants for all substrates are summarised in Table 4.1 (page 102).

4.3.5 4-Nitrobenzaldehyde

Determination of Michaelis constants for the reduction of 4-nitrobenzaldehyde in the concentration range of 0.2-4 mM by HpAKR (Fig. 4.7).

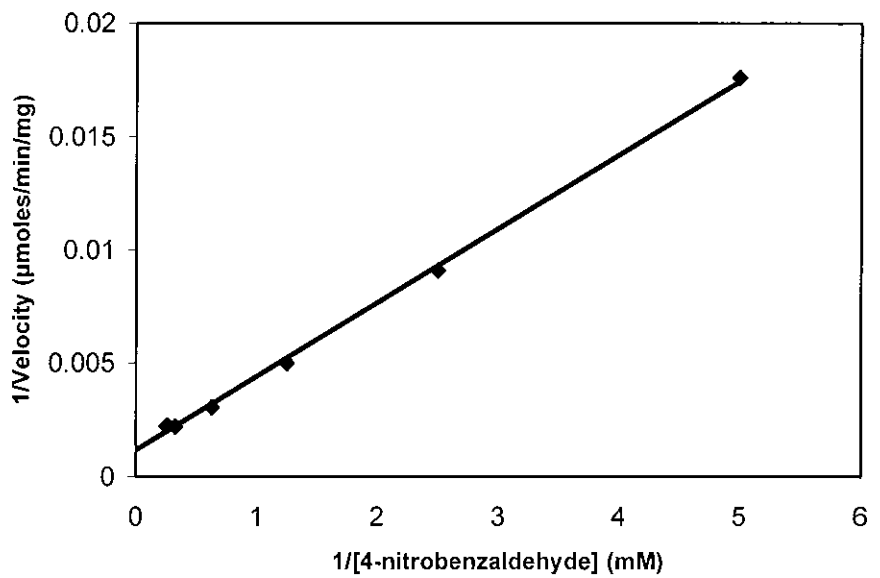

Fig. 4.7: Lineweaver Burke plot of the reduction of 4-nitrobenzaldehyde by purified HpAKR over a 4-nitrobenzaldehyde concentration range of 0.2-4 mM. The NADPH concentration was fixed at 0.2 mM.

A K_m of 1.8 ± 0.25 mM was estimated for 4-nitrobenaldehyde. Kinetic constants for all substrates are summarised in Table 4.1 (page 102).

4.3.6 Pyridine-2-Aldehyde

Determination of Michaelis constants for the reduction of pyridine-2-aldehyde in the concentration range of 0.2-6.4 mM by HpAKR (Fig. 4.8).

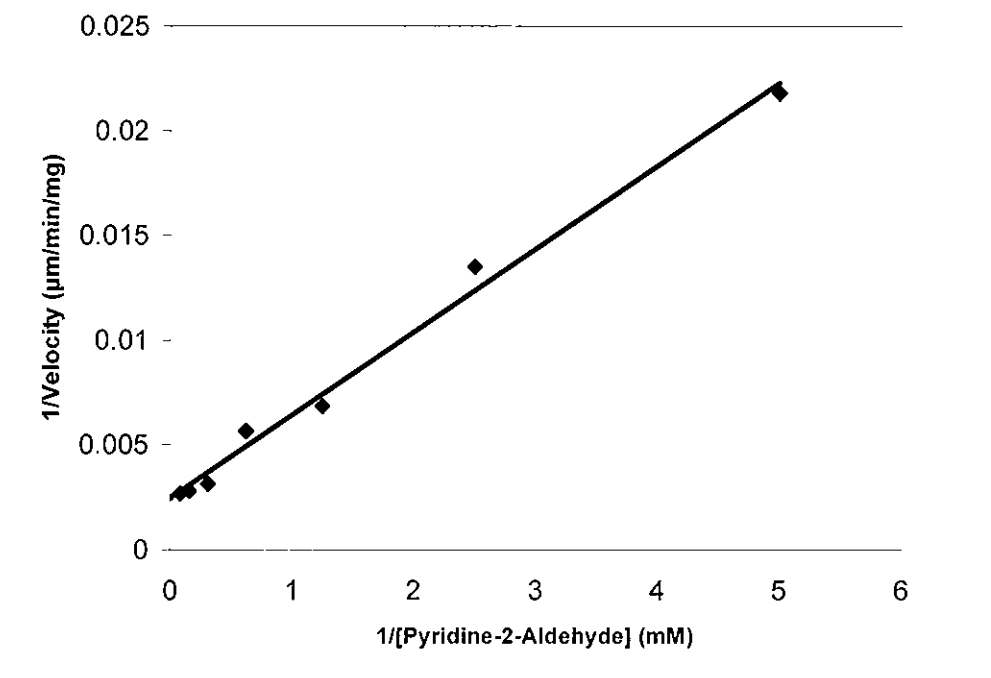

Fig. 4.8: Lineweaver Burke plot of the reduction of pyridine-2-aldehyde by purified HpAKR over a pyridine-2-aldehyde concentration range of 0.2 – 6.4 mM. The NADPH concentration was fixed at 0.2 mM.

A K_m of 1.7 ± 0.4 mM was estimated for pyridine-2-aldehyde. Kinetic constants for all substrates are summarised in Table 4.1 (page 102).

4.3.7 Pyridine-3-Aldehyde

Determination of Michaelis constants for the reduction of pyridine-3-aldehyde in the concentration range of 0.8-50 mM by HpAKR (Fig. 4.9).

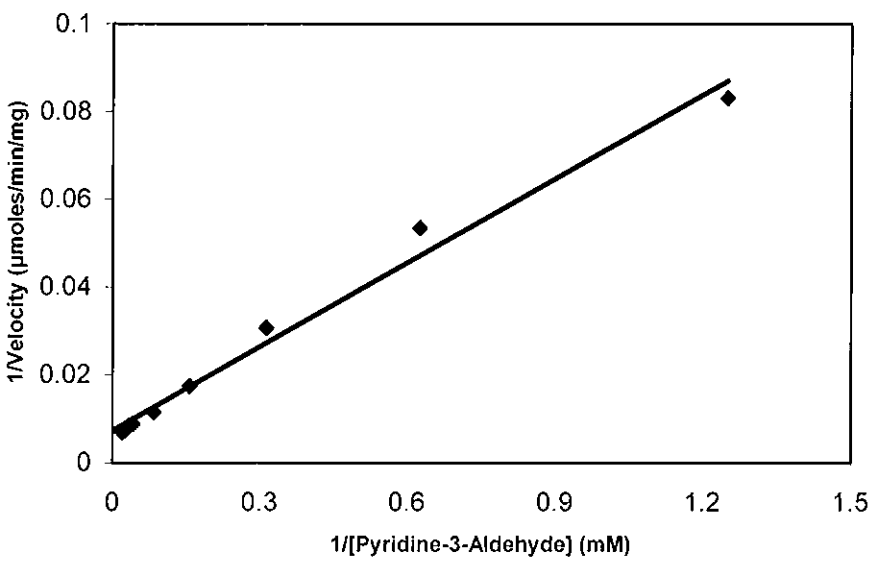

Fig. 4.9: Lineweaver Burke plot of the reduction of pyridine-3-aldehyde by purified HpAKR over a pyridine-3-aldehyde concentration range of 0.8 - 50 mM. The NADPH concentration was fixed at 0.2 mM.

A K_m of 13 ± 1.2 mM was estimated for pyridine-3-aldehyde. Kinetic constants for all substrates are summarised in Table 4.1 (page 102).

4.3.8 Pyridine-4-Aldehyde

Determination of Michaelis constants for the reduction of pyridine-4-aldehyde in the concentration range of 0.2-30 mM by HpAKR (Fig. 4.10).

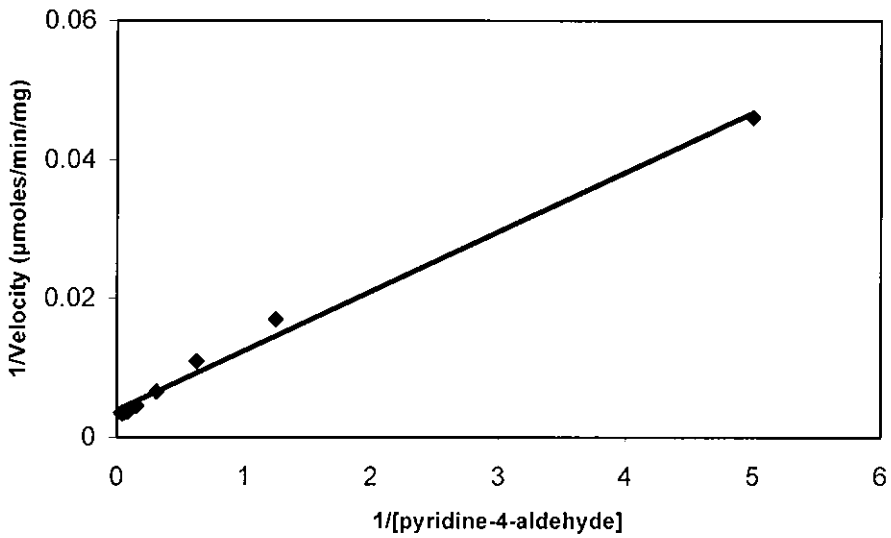

Fig. 4.10: Lineweaver Burke plot of the reduction of pyridine-4-aldehyde by purified HpAKR over a pyridine-4-aldehyde concentration range of 0.2 - 30 mM. The NADPH concentration was fixed at 0.2 mM.

A K_m of 3.6 ± 0.4 mM was estimated for pyridine-3-aldehyde. Kinetic constants for all substrates are summarised in Table 4.1 (page 102).

4.3.9 Succinic Semialdehyde

Determination of Michaelis constants for the reduction of succinic semialdehyde in the concentration range of 3.2-25 mM by HpAKR (Fig. 4.11).

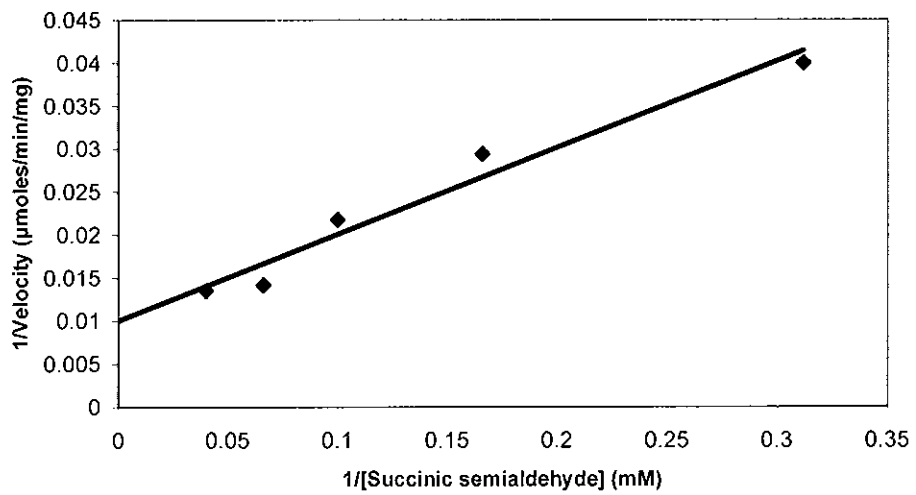

Fig. 4.11: Lineweaver Burke plot of the reduction of succinic semialdehyde by purified HpAKR over a succinic semialdehyde concentration range of 3.2 - 25 mM. The NADPH concentration was fixed at 0.2 mM.

A K_m of 10 ± 2.6 mM was estimated for succinic semialdehyde. Kinetic constants for all substrates are summarised in Table 4.1 (page 102).

4.3.10 2-Methylbutyraldehyde

Determination of Michaelis constants for the reduction of 2-methylbutyraldehyde in the concentration range of 0.8-40 mM by HpAKR (Fig. 4.12).

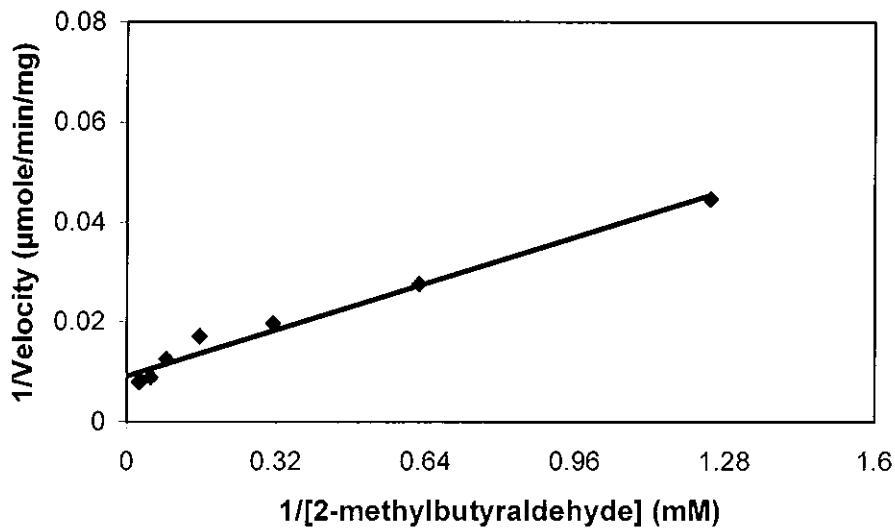

Fig. 4.12: Lineweaver Burke plot of the reduction of 2-methylbutyraldehyde by purified HpAKR over a 2-methylbutyraldehyde concentration range of 0.8 - 40 mM. The NADPH concentration was fixed at 0.2 mM.

A K_m of 7.4 ± 2.0 mM was estimated for 2-methylbutyraldehyde. Kinetic constants for all substrates are summarised in Table 4.1 (page 102).

4.3.11 Isatin

Determination of Michaelis constants for the reduction of isatin in the concentration range of 0.2-4 mM by HpAKR (Fig. 4.13).

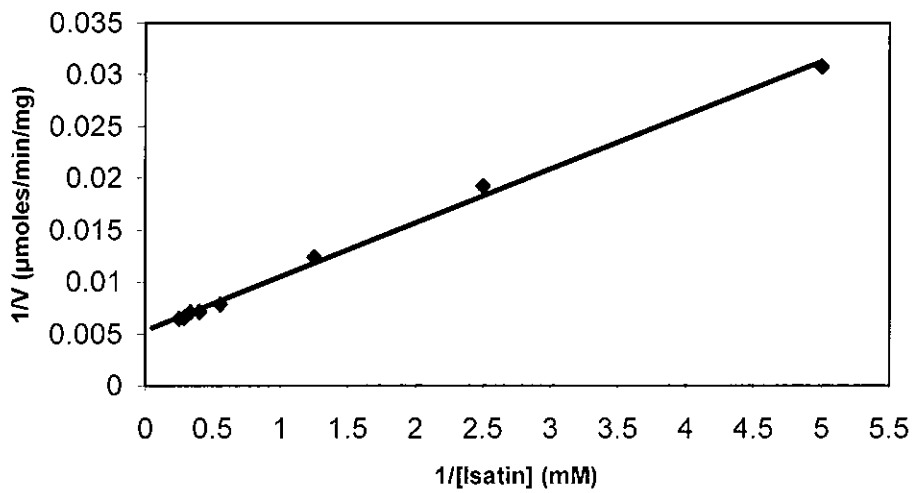

Fig. 4.13: Lineweaver Burke plot of the reduction of Isatin by purified HpAKR over a Isatin concentration range of 0.2 - 4 mM. The NADPH concentration was fixed at 0.2 mM.

A K_m of 2.8 ± 0.07 mM was estimated for isatin. Kinetic constants for all substrates are summarised in Table 4.1 (page 102).

4.3.12 Methylglyoxal

Determination of Michaelis constants for the reduction of methylglyoxal in the concentration range of 1.6-70 mM by HpAKR (Fig. 4.14).

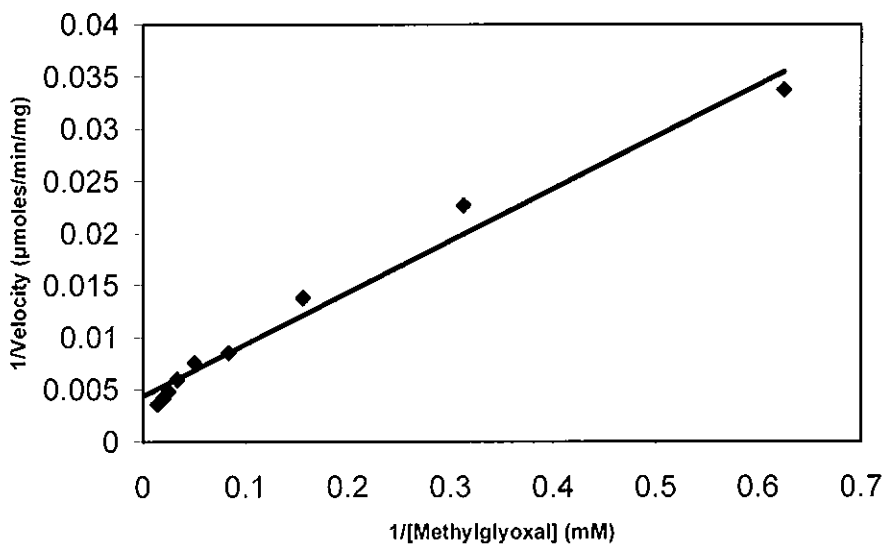

Fig. 4.14: Lineweaver Burke plot of the reduction of Methylglyoxal by purified HpAKR over a methylglyoxal concentration range of 1.6 - 70 mM. The NADPH concentration was fixed at 0.2 mM.

A K_m of 38 ± 9.4 mM was estimated for methylglyoxal. Kinetic constants for all substrates are summarised in Table 4.1 (page 102).

4.3.13 Phenylglyoxal

Determination of Michaelis constants for the reduction of phenylglyoxal in the concentration range of 0.2-6.5 mM by HpAKR (Fig. 4.15).

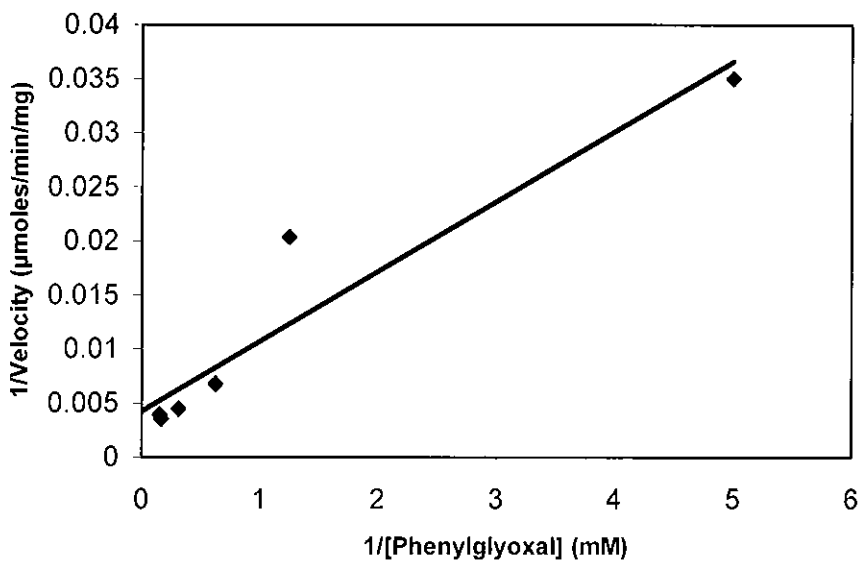

Fig. 4.15: Lineweaver Burke plot of the reduction of Phenylglyoxal by purified HpAKR over a phenylglyoxal concentration range of 0.2 – 6.5 mM. The NADPH concentration was fixed at 0.2 mM.

A K_m of 2.0 ± 0.6 mM was estimated for phenylglyoxal. Kinetic constants for all substrates are summarised in Table 4.1(page 102).

4.3.14 9, 10 Phenanthrenequinone

Determination of Michaelis constants for the reduction of 9,10 phenanthrenequinone within the concentration range of 0.2-6.4 mM by HpAKR (Fig. 4.16).

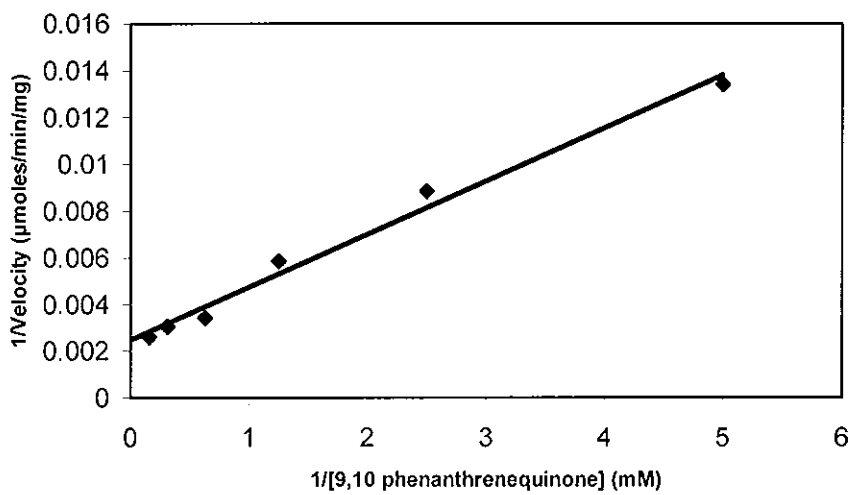

Fig. 4.16: Lineweaver Burke plot of the reduction of 9,10 phenanthrenequinone by purified HpAKR over a 9,10 phenanthrenequinone concentration range of 0.2 – 6.4 mM. The NADPH concentration was fixed at 0.2 mM.

A K_m of 1.0 ± 0.1 mM was estimated for 9,10 phenanthrenequinone. Kinetic constants for all substrates are summarised in Table 4.1 (page 102).

4.4 Overview of Substrate Specificity Analysis

The HpAKR of *Helicobacter pylori* 26695 is active as an aldo keto reductase. The substrate specificity of the pure enzyme was examined for several aldehyde substrates. The values of the steady-state parameters are summarised in Table 4.1. HpAKR has a high turnover towards these aldehydes when compared to other characterised aldo keto reductases.

Substrate	Km (mM)	Kcat (S^{-1})	Kcat/Km ($mM^{-1}.S^{-1}$)	Structure
Benzaldehyde	1.9 ± 0.7	58.5 ± 6	30.8 ± 12	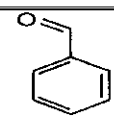
3-Nitrobenzaldehyde	1.7 ± 0.19	399.3 ± 19	234.9 ± 11	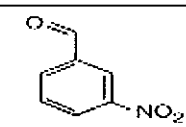
4-Nitrobenzaldehyde	1.8 ± 0.25	416.9 ± 24	231.6 ± 35	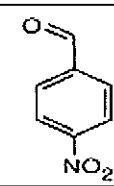
Pyridine-2-Aldehyde	1.7± 0.4	273.0 ± 3.4	160.6 ± 4.0	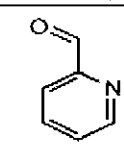
Pyridine-3-Aldehyde	13 ± 1.2	111.3 ± 18	8.6 ± 2.0	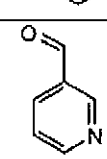
Pyridine-4-Aldehyde	3.6 ± 0.4	205.6 ± 7.1	205.1 ± 7.1	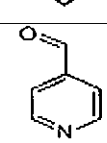
Succinic Semialdehyde	10 ± 2.6	63.8 ± 6.0	6.4 ± 1.7	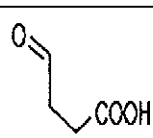
2-Methylbutyraldehyde	7.4 ± 1.8	90.7 ± 7.1	12.3 ± 3.1	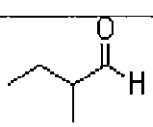
Isatin	2.8 ± 0.07	122 ± 24	44 ± 9.0	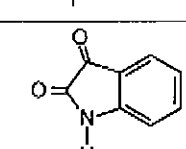

Table 4.1 continued...

Substrate	Km (mM)	Kcat (s-1)	Kcat/Km ($mM^{-1}.S^{-1}$)	Structure
Methylglyoxal	38 ± 9	261.5 ± 15	6.9 ± 1.7	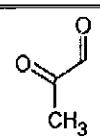
Phenylglyoxal	2.00 ± 0.6	226 ± 30	113 ± 35	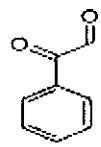
9,10 phenanthrenequinone	1 ± 0.11	274 ± 7.7	274 ± 31	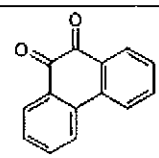

Table 4.1: Kinetic parameters of HpAKR. Enzymatic activities were measured in 50 mM potassium phosphate buffer (pH 7.5) with 0.2 mM NADPH. All parameters were determined at 37°C. Assays were carried out as described in Materials and Methods; Section 2.10.

4.5 Substrate Specificity Analysis for Sugar/Steroid Substrates

Various sugar substrates were assayed against the purified HpAKR to assess if the enzyme possessed aldose reductase activity. These substrates included; glyceraldehydes (0.2- 6.4 mM), xylose (0.2- 6.4 mM), glucose (0.2- 6.4 mM) and arabinose (0.2- 6.4 mM). The enzyme exhibited no measurable activity towards any of these sugar substrates. This lack of activity precludes HpAKR from membership of the aldose reductase subgroup and reduces the possible number of biochemical pathways in which the enzyme may participate in *H. pylori*.

The HpAKR also exhibited no measurable activity towards several steroid substrates. The steroids assayed were testosterone (0.2-16 mM), oestrogen (0.2-16 mM), cortisone (0.2-20 mM) and progesterone (0.2-16 mM). Since most hydroxysteroid dehydrogenases exhibit reductase activity against these substrates, membership of this subgroup can be discounted.

Since the HpAKR exhibited a pH optimum of 5.5, (section 4.8), these assays were repeated at pH 5.5 to check whether the enzyme was active with these substrates in an acidic environment. However, again no measurable activity was observed.

4.6 Oxidation of Alcohol Substrates

Many aldehyde-reducing oxidoreductases are capable of oxidising alcohols to their corresponding aldehyde product. HpAKR was assayed against various alcohol substrates. The alcohols used were; ethanol, propanol, and benzyl alcohol at a concentration up to 50 mM for each alcohol substrate.

No activity was observed using these alcohol substrates. It is not clear why this reaction is not readily reversible since there is no thermodynamic barrier to alcohol oxidation. However, similar findings have been reported for the aflatoxin aldehyde reductase from rat liver (Ellis *et al.*, 1995).

4.7 Stability of HpAKR

Freeze thaw assays were preformed using 3-nitrobenzaldehyde as the substrate and NADPH as the co-factor. The enzyme, 3-nitrobenzaldehyde (3.2 mM) and NADPH (0.2 mM) concentrations were kept constant. The HpAKR was found to be an extremely stable enzyme as it was able to withstand several freeze-thaw cycles, (freezing was carried out –20°C for 2 h), with little significant loss of activity. There was approximately an 8% loss in activity (Fig. 4.17) after 8 freeze-thaw cycles. The purified enzyme was stored at -20°C for up to 6 months without significant loss of activity.

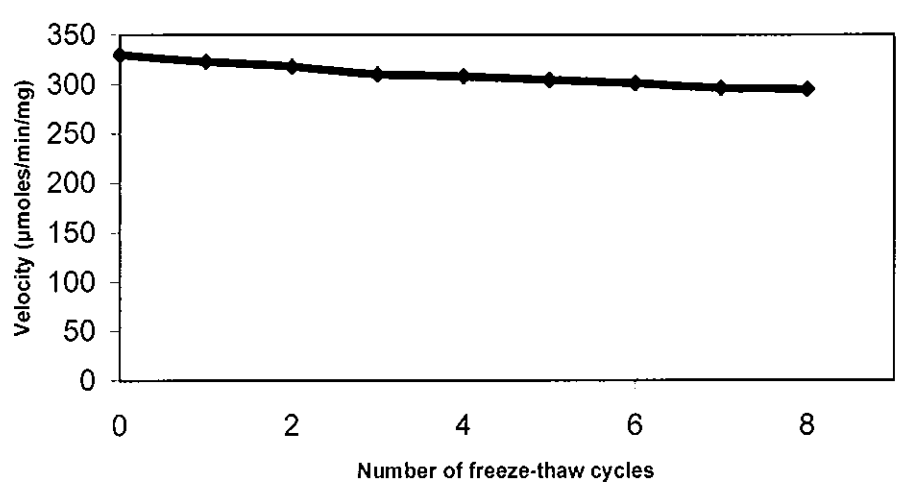

Fig. 4.17: Plot illustrating the loss of activity observed after several freeze-thaw cycles. The assays were performed using 3-nitrobenzaldehyde (3.2 mM) as a substrate and 0.2 mM NADPH.

4.8 Effect of pH on HpAKR Activity

To determine the optimum pH for aldehyde reduction, the enzyme was assayed in buffers of various pH ranging from pH 4-10. Optimum activity was observed at pH 5.5 using 3-nitrobenzaldehyde (3.2 mM) as the substrate and NADPH (0.2 mM) as the co-factor (Fig. 4.18). Media of different pH values were obtained using the following buffers: pH 4-5: 50 mM sodium citrate, pH 6-8: 50 mM potassium phosphate and pH 9-10 50 mM glycine. At pH 4, 50% activity remained whereas at pH 10 the activity was only 3% of that at pH 5.

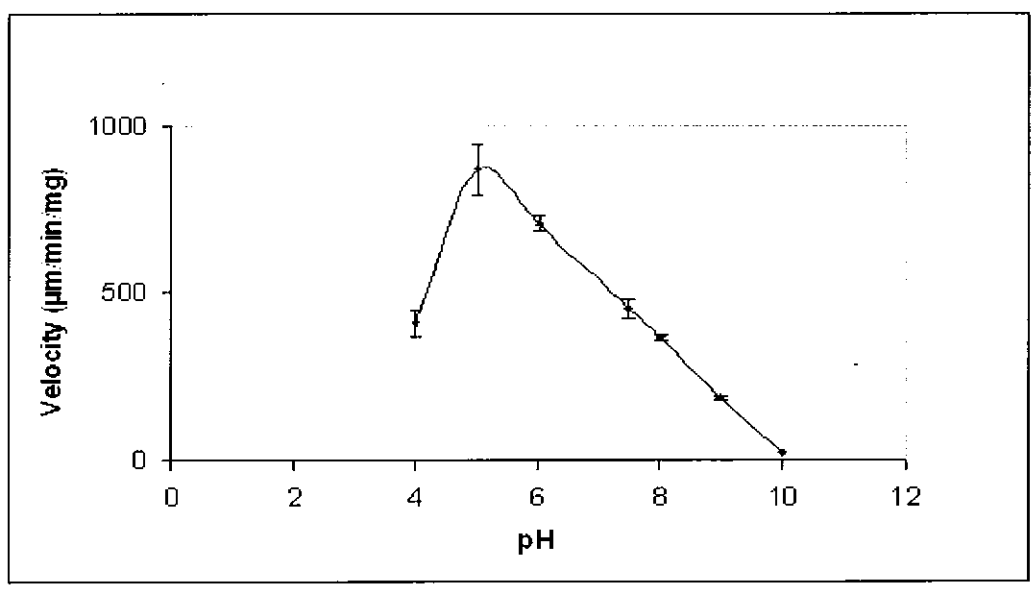

Fig. 4.18: Initial rates of 3-nitrobenzaldehyde reduction (3.2 mM) at the indicated pH values. The buffers used were as follows: pH 4-5: 50 mM sodium citrate, pH 6-8: 50 mM potassium phosphate and pH 9-10 50 mM glycine.

4.9 Inhibition Studies

4.9.1 EDTA Inhibition

EDTA is a chelating agent for divalent metal ions. The addition of EDTA to metalloenzymes may render the enzyme inactive. Since EDTA was used throughout the purification, it was important to assess the enzyme's susceptibility to this compound. EDTA inhibition assay was carried out using pyridine-2-aldehyde (2 mM) as the substrate and NADPH as the co-factor (0.2 mM). The concentration of both the substrate and co-factor were kept constant throughout the study. The EDTA concentration was varied between 0-40 mM. EDTA was found to have no effect on HpAKR activity up to a concentration of 40 mM (Fig. 4.19).

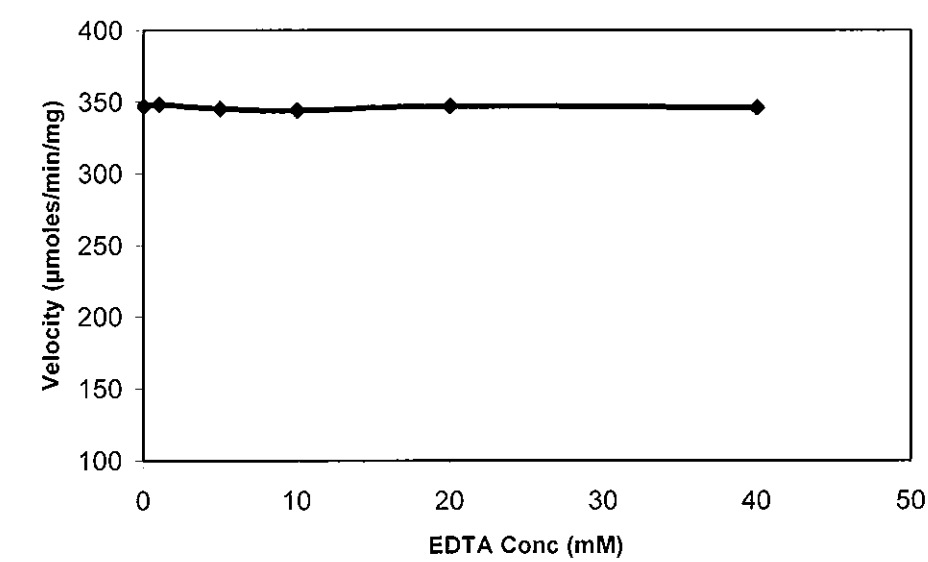

Fig. 4.19: Initial reaction rate for HpAKR in the presence of EDTA. EDTA concentration was varied between 0- 40 mM. The assay was performed at 37°C using 50 mM potassium phosphate buffer pH 7.5, pyridine-2-aldehyde (2mM) as the substrate and NADPH (0.2 mM) as the co-factor.

4.9.2 DTT Inhibition

Due to the presence of the three-cysteine residues in HpAKR, it was of interest to evaluate the effect of a reducing agent on HpAKR activity. For this, Dithiothreitol (DTT) was chosen as the reducing agent.

DTT is a reducing agent that is commonly used to maintain protein thiols in a reduced state. The addition of this reducing agent to proteins may be used to determine whether there are any disuphide bridges, which are essential for activity.

HpAKR was incubated with DTT for 30 min at room temperature. The activity of HpAKR in the presence and absence of DTT was the determined using pyridine-2-aldehyde (2 mM) as the substrate and NADPH as the co-factor (0.2 mM). The concentration of both the substrate and co-factor were kept constant throughout the study. The DTT concentrations used were between 0-20 mM.

DTT inhibited HpAKR activity in a concentration dependent manner with maximal inhibition of 79% being observed with 20 mM DTT (Fig. 4.20). However it is important to note that this concentration of DTT was high and might reflect binding of DTT to the enzyme in a non-specific manner rather than an effect on thiol reduction.

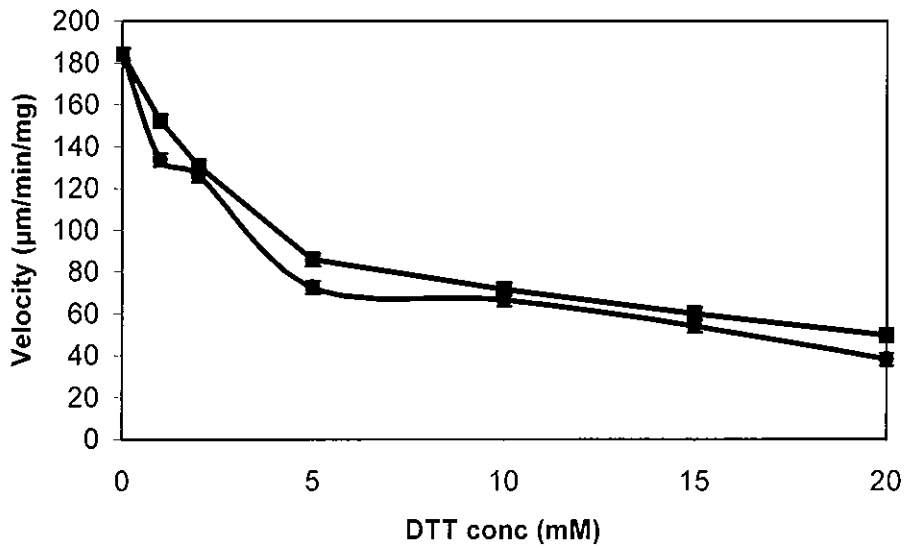

Fig. 4.20: Initial reaction rate calculated for HpAKR in the presence of DTT. The enzyme was pre-incubated in potassium phosphate buffer (pH 7.5) at 37°C with the indicated concentrations of DTT for 0 (■) and 30(•) mins before determination of the activity using pyridine-2-aldehyde (2 mM) and NADPH (0.2 mM). DTT concentrations were varied from 0-20 mM.

4.9.3 Sodium Valproate Inhibition

Sodium valproate is a potent inhibitor of most aldo-keto reductases (Ellis *et al.*, 1995, Hinshelwood *et al.*, 2002, Kuhn *et al.*, 1995 and Todaka *et al.*, 2000). Inhibition by sodium valproate has been used to distinguish aldehyde reductases from aldose reductase, although not all aldehyde reductases are sensitive to inhibition by this compound (Wermuth *et al.*, 1982).

Sodium valproate inhibition was carried out by measuring the level of inhibition observed in different concentrations of sodium valproate (0-1.6 mM). The sodium valporate concentration remained fixed whilst the substrate (pyridine-2-aldehyde) concentration was varied between 0- 6 mM.

Sodium valproate was found to be a reversible inhibitor of HpAKR. Kinetic analysis showed inhibition to be essentially of a mixed-type with respect to pyridine-2-aldehyde, since the apparent K_m and V_{max} values were altered in its presence. However, the standard equation for such inhibition:

$$v = \frac{V_{max}}{\frac{K_m}{[S]}(1 + \frac{[I]}{K_i}) + (1 + \frac{[I]}{K'_i})}$$

where [S] and [I] are the pyridine-2-aldehyde and sodium valproate concentrations, respectively, was not applicable in this case.

As shown in Fig. 4.21a, the curves at different sodium valproate concentrations demonstrate that both the K_m and V_{max} values are altered in the presence of the inhibitor.

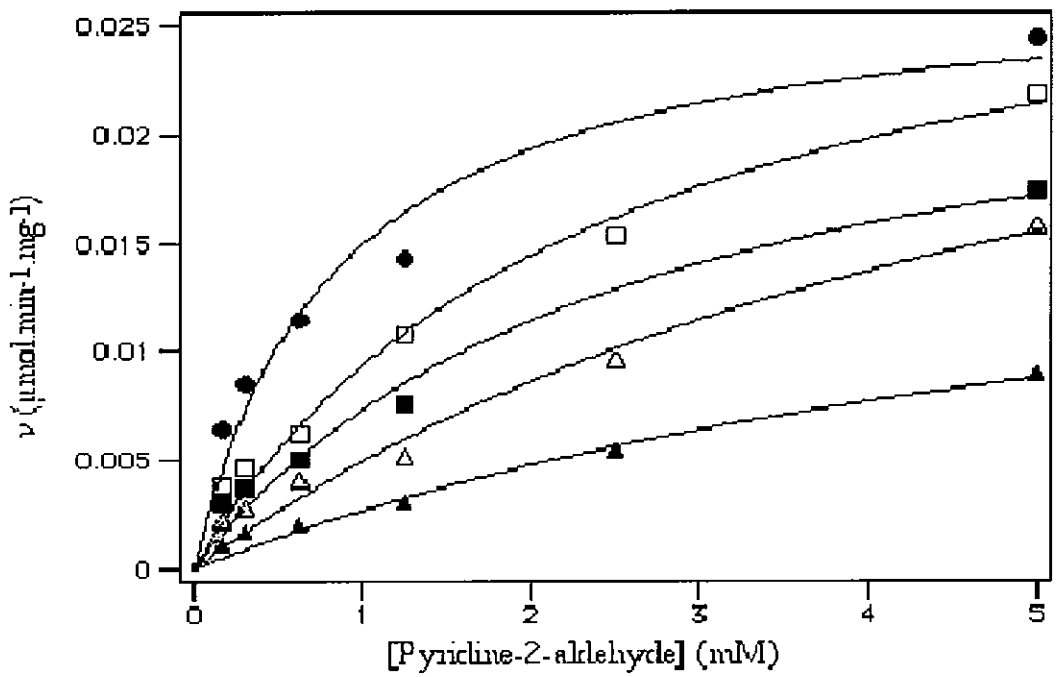

Fig. 4.21a: Inhibition of HpAKR by sodium valproate. The reductase activities towards a range of pyridine-2-aldehyde concentrations were determined at fixed sodium valproate concentrations. The concentrations of sodium valproate were ●, 0; □, 0.2; ■, 0.4; △, 0.8; and ▲, 1.6 mM. Points for individual lines were fitted to the Michaelis-Menten equation.

The replot of the reciprocal apparent $1/V_{max}$ values against the sodium valproate concentration was apparently linear (Fig. 4.21b) yielding a *Ki* value of 0.22 ± 0.03 mM for the competitive element (K'_I) of this inhibition. However, this value should only be regarded as being an approximation, since higher concentrations of sodium valproate appeared to cause the initial rate behaviour to depart from simple Michaelis-Menten kinetics.

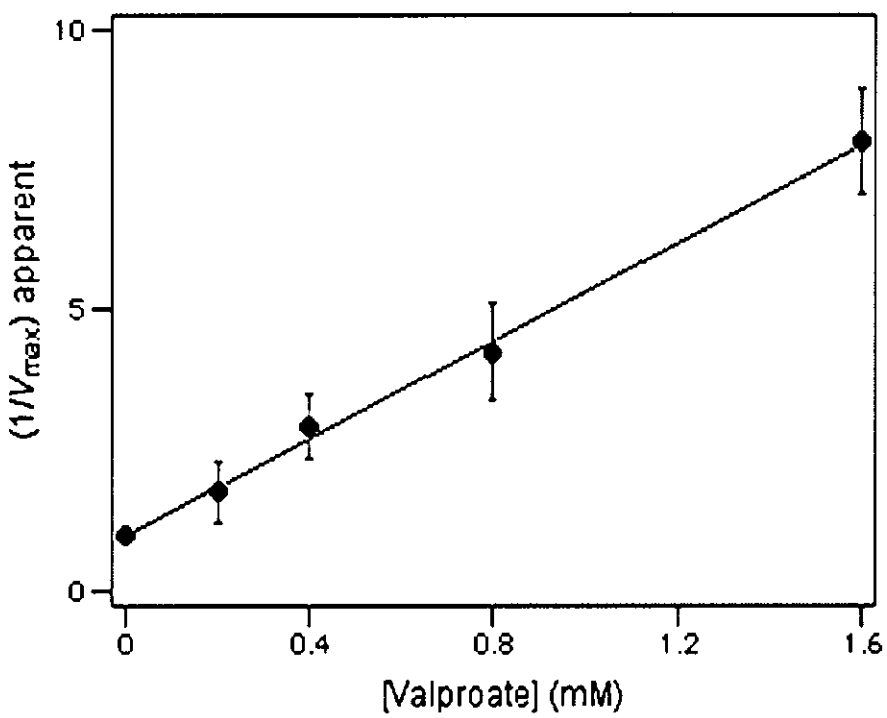

Fig. 4.21b: The dependence of the reciprocal apparent V_{max} values on the concentration of sodium valproate. Units for ($1/V_{max}$) apparent are $\mu moles^{-1}$ min^{-1} mg^{-1}.

The replot variation of the reciprocal apparent V_{max}/K_m values with the sodium valproate concentrations was clearly non-linear (Fig. 4.21c). Thus, an inhibitor constant for the uncompetitive element of the inhibition (K'_I) could not be determined.

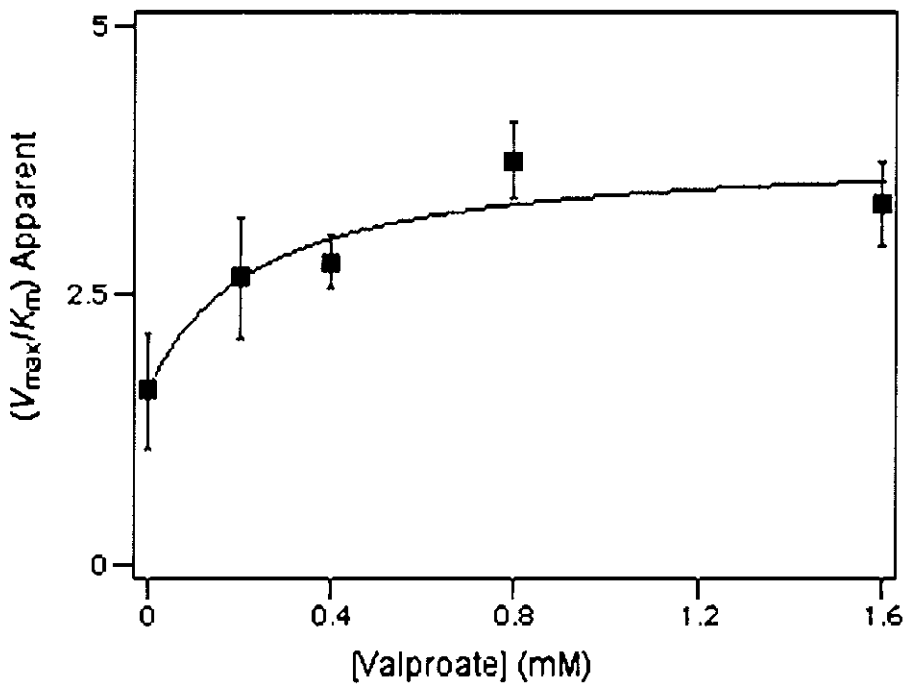

Fig. 4.21c: The dependence of the reciprocal apparent V_{max}/K_m values on the sodium valproate concentration. Units for $(1/V_{max})$ apparent are μmoles/min/mg.

The reason for this departure from Michalis-Menten kinetics is unknown and was not explored further in these studies.

4.10 Discussion

The kinetic and substrate preference analysis presented here confirms that the HpAKR is an active aldo keto reductase. The HpAKR exhibited broad substrate specificity for aldehyde substrates with a high turnover (Table 4.1) however the enzyme's affinity for various aldehyde substrates did vary appreciably. The enzyme was susceptible to inhibition by DTT and sodium valproate. The pH optimum was observed at pH 5.5.

Optimum enzyme activity was observed against aldehyde substrates such as 3-nitrobenzaldehyde, 4-nitrobenzaldehyde and pyridine-2-aldehyde. The nitrobenzaldehydes are considered typical substrates for microbial AKRs (Ellis *et al.*, 2002). The position of the nitro group did not seem to affect the efficiency of the nitrobenzaldehyde reduction activity since both the K_m and the K_{cat} calculated for both nitrobenzaldehyde substrates were very similar. However, the presence of the nitro group did dramatically increase the K_{cat} when compared to benzaldehyde.

One observation seen throughout the substrate specificity studies was that HpAKR had a high turnover towards the various aldehyde substrates assayed when compared to other characterised aldo keto reductases. This high turnover is clearly illustrated by taking 4-nitrobenzaldehyde as an example. HpAKR exhibited a K_{cat} value of 416.9 S^{-1} for 4-nitrobenzaldehyde. This value was compared to K_{cat} obtained for 4-nitrobenzaldehyde using other aldo keto reductases. The 2-methylbutyraldehyde reductase from *Saccharomyces cerevisiae* had a K_{cat} of 29.60 S^{-1} (Ford *et al.*, 2002), the *Saccharomyces cerevisae* AKR had a K_{cat} of 2.37 S^{-1} (Kuhn *et al.*, 1995), the human succinic semialdehyde reductase had a K_{cat} of 1.1 S^{-1} (Schaller *et al.*, 1999) and the

pyridoxal reductase from *Schizosaccharomyces pombe* had a K_{cat} of 11.76 S^{-1} (Nakano *et al.*, 1999).

The catalytic rate for the dicarbonyl 9, 10 phenanthrenequinone in this study was 60 fold higher than that observed for the 2-methylbutyraldehyde reductase (Ford *et al.*, 2002) and 100 fold higher than that observed for the human brain succinic semialdehyde reductase (Scheller *et al.*, 1999).

The K_m values were generally within the 1-10 mM range, with the exception of methylglyoxal (38 mM). The lowest K_m (1 mM) was obtained for the dicarbonyl 9,10 phenanthrenequinone. However, unlike the aldo keto reductase from *Digitalis purpurea* and xylose reductase from *Candida parapsilosis* (Gavidia *et al.*, 2002 and Lee *et al* 2003), HpAKR showed no significant activity towards sugar or steroid substrates. In this respect, the enzyme resembles AKR7A5 and AKR1C19 (Hinshelwood *et al.*, 2003 and Ishikura *et al.*, 2005).

As mentioned in Chapter 3, HpAKR was assigned membership of the 13th AKR family and was named AKR13C1. The other two family members, *YakC* protein from *S. pombe* (AKR13A1) and the AKR from *Xyella fastidiosa* (AKR13B1), have also been characterised. The AKR13A1 protein was found to reduce the following aldehydes: pyridine-2-aldehyde, 2-nitrobenzaldehyde and 2-phthalaldehyde (Morita *et al.*, 2002). The lowest K_m of 0.185 mM was obtained for 2-nitrobenzaldehyde. The highest catalytic efficiency (K_{cat}/K_m) of 238.0 $mM^{-1}.S^{-1}$ was also obtained for 2-nitrobenzaldehyde. Thus this enzyme seems to prefer aromatic aldehydes. AKR13B1 was capable of reducing glyceraldehyde and 2-nitrobenzaldehyde however the highest K_{cat}/K_m of 78 $mM^{-1}.S^{-1}$ was obtained for the latter. Table 4.2 summarises the substrate specificity of the AKR13 family members other than the HpAKR. Comparison of

HpAKR to AKR13A1 shows that the catalytic efficiency (K_{cat}/K_m) for pyridine-2-aldehyde by HpAKR was 6 fold higher than that for AKR13A1. Due to the limited substrate specificity data available for AKR13B1, comparison to HpAKR is difficult. However, it is noted that AKR13B1 is capable of reducing glyceraldehyde, a substrate in which neither AKR13A1 or HpAKR are capable of reducing.

Substrate	AKR13A1			AKR13B1		
	Km (mM)	Kcat (s^{-1})	Kcat/Km ($mM^{-1}.S^{-1}$)	Km (mM)	Kcat (s^{-1})	Kcat/Km ($mM^{-1}.S^{-1}$)
2-Nitrobenzaldehyde	0.185	44.03	238.0	0.15	11.74	78
2-phthalaldehyde	0.333	19.7	59.3	NMA	NMA	NMA
Pyridine-2-aldehyde	0.302	83.7	25.3	NMA	NMA	NMA
DL-Glyceraldehyde	NMA	NMA	NMA	0.012	2.08	0.312

Table 4.2: Summary of kinetic constants calculated for the other members of the AKR13 family.

The HpAKR was the second oxidoreductase in this laboratory to be characterised from *H. pylori.* The *Helicobacter pylori* cinnamyl alcohol dehydrogenase (HpCAD) has been previously characterised in terms of its biochemical properties (Mee *et al.*, 2005). The HpCAD enzyme exhibited similar properties with respect to the broad substrate specificity. However HpCAD had a particular affinity for cinnamyl alcohol as might be expected from its designation as a cinnamyl alcohol dehydrogenase. The HpCAD was susceptible to high substrate inhibition at concentrations as low as 250 μM. This property was not observed with the HpAKR. The HpAKR was assayed against several of the substrates employed in the HpCAD study including; cinnamylaldehyde, coniferylaldehyde, acetaldehyde, benzaldehyde and sinapyl aldehyde. However

substrate preference overlap between these two enzymes only occurred with benzaldehyde. These results suggest that the HpAKR and HpCAD are involved in separate biochemical pathways within the bacterium.

A rather unusual property associated with the HpAKR was its dual coenzyme specificity for NADH and NADPH, although it had a preference for NADPH. In this respect, it is similar to the AKR7A5, AKR1C19 and thermostable alcohol dehydrogenase from *E. coli* (Hinshelwood *et al.*, 2003, Ishikura *et al.*, 2005 and Machielsen *et al.*, 2006). In contrast, some yeast (Itoh *et al.*, 2004, Kuhn *et al.*, 1995 and Lee *et al.*, 2003) and plant AKRs (Colrat *et al.*, 1999 and Gavidia *et al.*, 2002) do not possess such dual co-enzyme specificity.

The optimum pH for HpAKR activity, using 3-nitrobenzaldehyde as substrate and NADPH as the co-factor, was pH 5.5 but it is apparent (Fig. 4.18) that the enzyme can function over a broad pH range (pH 4-9).

Some other members of the aldo keto reductase superfamily can function over a broad pH range. These include AKR7A5 and the AKR from *Saccharomyces cerevisiae* (Hinshelwood *et al.*, 2002, Hinshelwood *et al.*, 2003 and Kuhn *et al.*, 1995).

However, several other members of the aldo keto reductase family have been reported to function only over a narrow range from pH 6-8. These include xylose reductase from *Candida parapsilosis* (Lee *et al.*, 2003), AKR1C19 (Ishikura *et al.*, 2005), thermostable alcohol dehydrogenase from *E. coli* (Machielsen *et al.*, 2006), benzil reductase from *Bacillus cereus* (Maruyama *et al.*, 2002), pyridoxal reductase from *Schizosaccharomyces pombe* (Nakano *et al.*, 1999) and aldehyde reductase from pig liver (Kanazu *et al.*, 1991).

In the presence of the reducing agent, DTT, up to 79% inhibition of HpAKR activity was observed. It would seem that DTT is a concentration dependent inhibitor of HpAKR. However, this level of inhibition may not necessarily be due to the reduction of the disulphide bonds. It is possible that at least a proportion of the inhibition observed is due to DTT binding non-specifically to the active site of the HpAKR, especially at higher concentrations.

The enzyme was susceptible to inhibition by sodium valproate, which is a known potent AKR inhibitor (Ellis *et al.*, 1995, Hinshelwood *et al.*, 2002, Kuhn *et al.*, 1995 and Todaka *et al.*, 2000). The kinetic behaviour of HpAKR in the presence of sodium valproate was complex. Similar behaviour has been reported by De Jongh *et al* (1987) for the AKR from sheep liver, who ascribed it to the formation of Enzyme.Valproate and Enzyme.NADPH.Valproate complexes in the inhibitory process. Such behaviour precluded the determination of K_i values.

In conclusion, this study confirms the putative assignment of HpAKR as a functional aldo keto reductase. The enzyme has a high turnover for a wide range of aldehyde substrates with a preference for aromatic aldehydes. From the data available, HpAKR is biochemically distinct from the other two members of the AKR13 family since it is capable of reducing a wider range of aldehydes than the other family members. The HpAKR is an extremely stable enzyme since it can withstand several freeze-thaw cycles with little loss of activity and functions over a broad pH range.

The fact that this is the second aldehyde-reducing enzyme characterised in this strain of *H. pylori* illustrates aldehyde detoxification can be achieved efficiently in the bacterium, at least for aromatic aldehydes. Due to the high K_m values obtained for the various

aldehyde substrates assayed, this suggests that HpAKR can reduce a higher concentration of aldehydes without reaching saturation.

From the kinetic data, it is clear that HpCAD and HpAKR reduce different types of aldehydes thus facilitating the reduction of a wider range of aldehydes within *H. pylori*. The presence of these two aldehyde-reducing enzymes clearly shows that detoxification of a wide range of aromatic aldehydes by their reduction to alcohols is possible in *H. pylori*. It is therefore highly unlikely that such aldehydes could be exported from the cell to interact with the gastric mucosa leading to inflammation.

Chapter 5

Construction and Characterisation of Isogenic HpAKR-Negative Mutant of *H. pylori*

5.0 Construction and Characterisation of Isogenic HpAKR-Negative Mutant of *H. pylori*

5.1 Introduction

A key factor in the colonisation of the gastric mucosa is the ability of *H. pylori* to survive acidic environments. Initially, survival in such conditions was thought to be dependent on the presence of the urease enzyme however, a recent report described the isolation of a urease-negative strain suggesting other mechanisms are involved (Mine *et al.*, 2005).

A report in the literature has identified ancillary genes, which are required for growth at acid pH, using random insertional mutatgenesis (Bijlsma *et al.*, 2000). This report suggested that HpAKR may be involved in acid adaptation by the capture or release of protons. Bijlsma *et al.* (2000) showed that disruption of the *H. pylori* genome upstream of the ORF for the HpAKR gave rise to an acid sensitive phenotype. Thus, it was suggested that this enzyme was involved in acid adaptation since it was located immediately 5' to the insertion point (Bijlsma *et al.*, 2000). No reports characterising this potential virulence factor have subsequently appeared in the literature.

In view of the fact that this protein might represent a potential target for drug therapies, it was surprising that it had not received more attention. While Bijlsma *et al.* (2000) showed that disruption of the genome upstream of this protein gave rise to an acid sensitive phenotype, their experiments were not definitive since a direct disruption of the *HpAKR* gene was not accomplished.

Therefore to address this issue, a defined isogenic mutant was generated by insertion of a kanamycin antibiotic resistance cassette within the coding region of the HpAKR. This

strategy has been used by others to create isogenic mutants in other *H. pylori* genes (Martino *et al.*, 2001, Foyes *et al.*, 2000, Kuipers *et al.*, 1998, McGee *et al.*, 1999 and Ando *et al.*, 1999). The effects of exposure to acid environments on growth of the HpAKR mutant was assessed.

In collaboration with Dr. Blanaid Mee of this laboratory (Ph.D thesis, DIT, 2005, Characterisation of the Cinnamyl alcohol Dehydrogenase from *Helicobacter pylori*), a previously constructed HpCAD negative mutant was characterised in terms of its growth under acid conditions. A report in the literature suggested that HpCAD is upregulated in response to acid stress (Ang *et al.*, 2001) thus indicating that, in addition to HpAKR, it too may be involved in acid adaptation.

5.2 Generation of pGEM:HpAKR construct

5.2.1 Primer Design, PCR and Xcm I Restriction Digests

The cloning strategy used for the generation of the HpAKR isogenic mutant by insertion of a kanamycin antibiotic resistance cassette is summarised in Fig. 5.1.

All plasmids and bacterial strains used in the study are detailed in Table 5.1

The *HpAKR* (990bp) gene was amplified using the primers shown in Table 5.2. The *HpAKR* gene was amplified by PCR from the genomic DNA of *H. pylori* strains 26695 and 1061. The amplified PCR products were then cut with the restriction enzyme *Xcm*I to ascertain whether the predicted target restriction site was still present. The presence of a unique *Xcm*I restriction in the *HpAKR* gene, (Fig. 5.2) but absent in pGEM T-Easy vector, was required to facilitate insertion of a kanamycin resistance cassette (*aphA-3*) within the gene, in order both to disrupt it and to select for transformants. The restriction site was present in the HpAKR amplified from both *H. pylori* 1061 and 26695 (Fig. 5.3).

5.2.2 Insertion of amplified HpAKR into pGEM-T Easy

The *HpAKR* genes were amplified by PCR using a Taq polymerase without proofreading capacity to generate a product with A' overhangs. The overhangs facilitated the ligation of the amplified products into the pGEM-T Easy vector, which was provided with 3' terminal thymidines added to both ends of the insertion site (Fig. 5.4). An insert:vector ratio of 1:3 yielded ≈ 90 *E. coli* DH5α transformants (with a transformation efficiency 1.16 x 10^6 cfu/ μg DNA). The point of insertion of the PCR product into pGEM-T Easy was within the LacZ gene. This provided a simple blue/white colony-screening marker for the detection of inserted foreign DNA material. The resulting construct was called pGEM:HpAKR (Fig. 5.5).

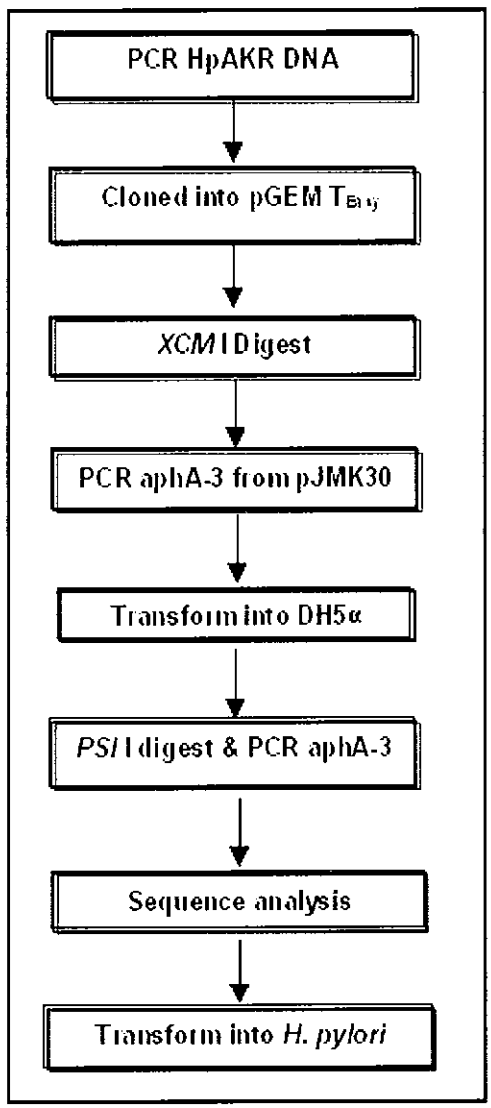

Fig. 5.1: Overview of the cloning strategy used for the generation of the *H. pylori* isogenic HpAKR negative mutant.

Strain/Plasmid	Genotype/Characteristics	Source/Reference
Strain		
E. coli DH5α	ø80dlacZΔM15, Δ(lacZYA-argF)U169 supE4 hsdR17 recA1 endA1 gyrA96 thi-1relA deoR	Promega
H. pylori 1061	Wild type	A. van Vliet[1]
H. pylori 1061: AKR::*aphA-3*	----------	This study
H. pylori 1061: CAD::*aphA-3*		This study
Plasmid		
pGEM-T Easy	Cloning vector	Promega
pJMK30	pUC19 containing *aphA-3* cassette (Amp^r)	A. van Vliet[1]
pGEM:HpAKR	pGEM T-Easy containing the inserted 990bp HpAKR.	This study
pGEM:HpAKR::*aphA-3*	pGEM:HpAKR with the *aphA-3* cassette inserted at the unique *Xcm* I site	This study
pGEM:HpCAD	pGEM T-Easy containing the inserted HpCAD.	This study
pGEM:HpCAD::*aphA-3*	pGEM:HpCAD with the *aphA-3* cassette inserted at the unique *Xcm* I site	This study

Table 5.1: Plasmids and strains used for the generation of the pGEM:HpAKR::*aphA-3* mutant. ([1]A. van Vliet , Dijkzigt Hospital, Rotterdam, The Netherlands (Goodwin *et al.*, 1998))

Gene	Primer direction	Primer sequence
HpAKR	Forward	5' – ATG CAA CAG CGT CAT T – 3'
HpAKR	Reverse	5'– TTA TTG ATT CAC CAT TTC AT –3'

Table 5.2: Primers used for the amplification of HpAKR from *H. pylori* strains 26695 and 1061. PCR was carried out as described in Chapter 2, section 2.6.4.

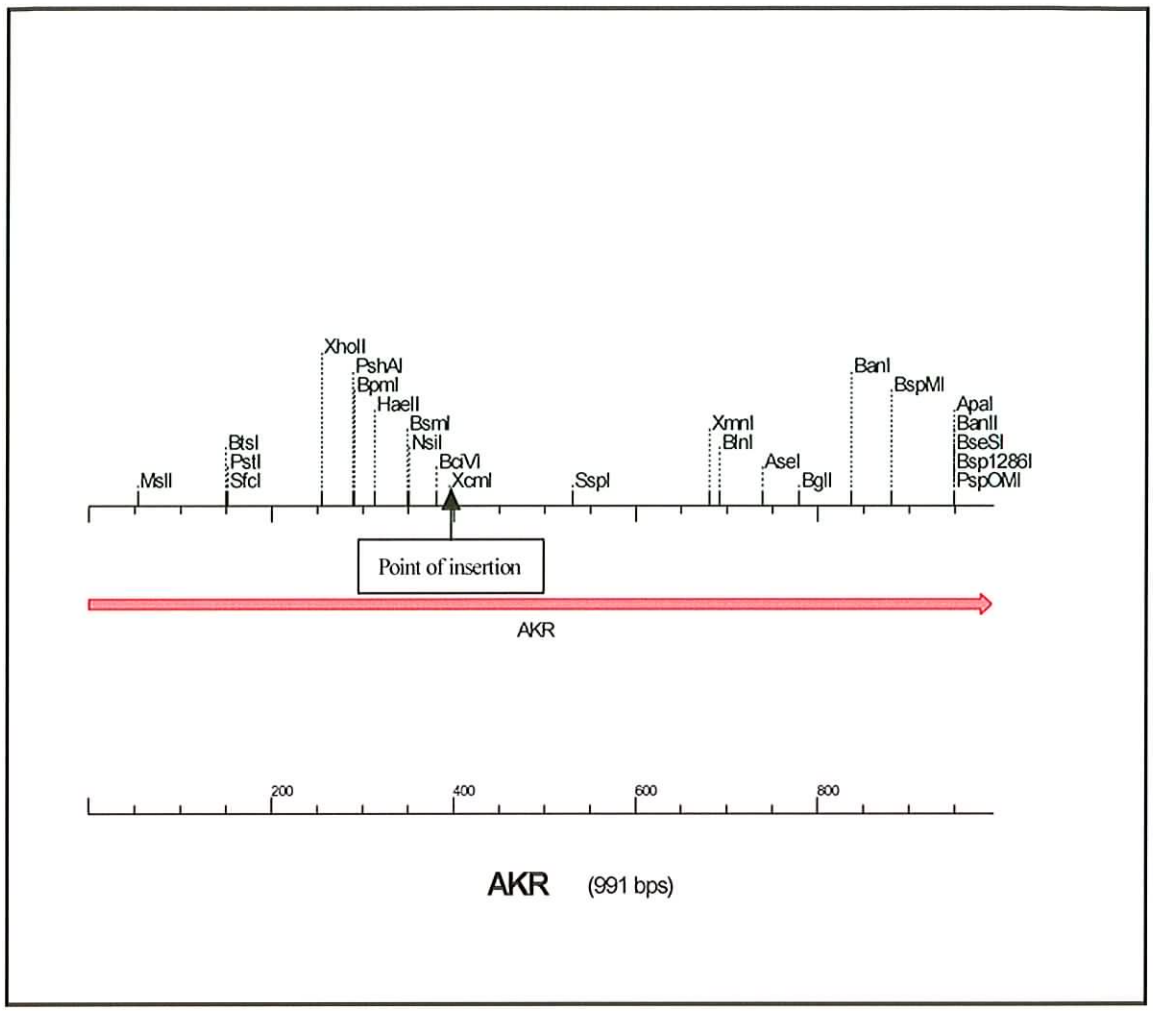

Fig. 5.2: Scientific Educational (www.scied.com) software was used to identify restriction sites on the *HpAKR* gene. The point of insertion for kanamycin resistance cassette (*aphA-3* cassette) after digestion with the restriction enzyme, *Xcm*I, is indicated.

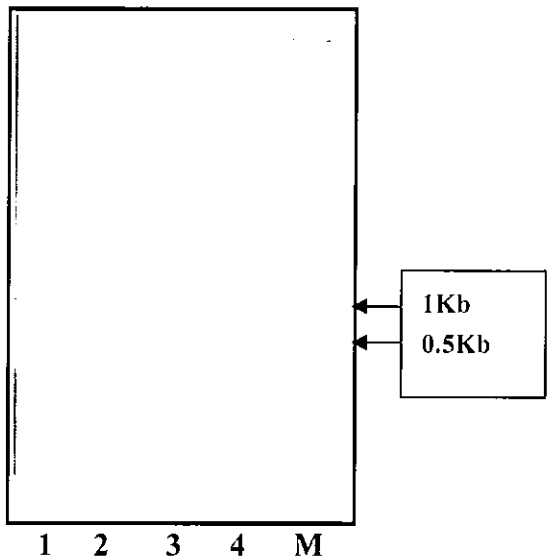

Fig. 5.3: Agarose (1%) gel electrophoresis of Xcm I restriction digests of PCR amplified HpAKR from *H. pylori* 26695 (1 & 2) and 1061 (3 & 4). Lanes 2 and 4 contain the untreated HpAKR.

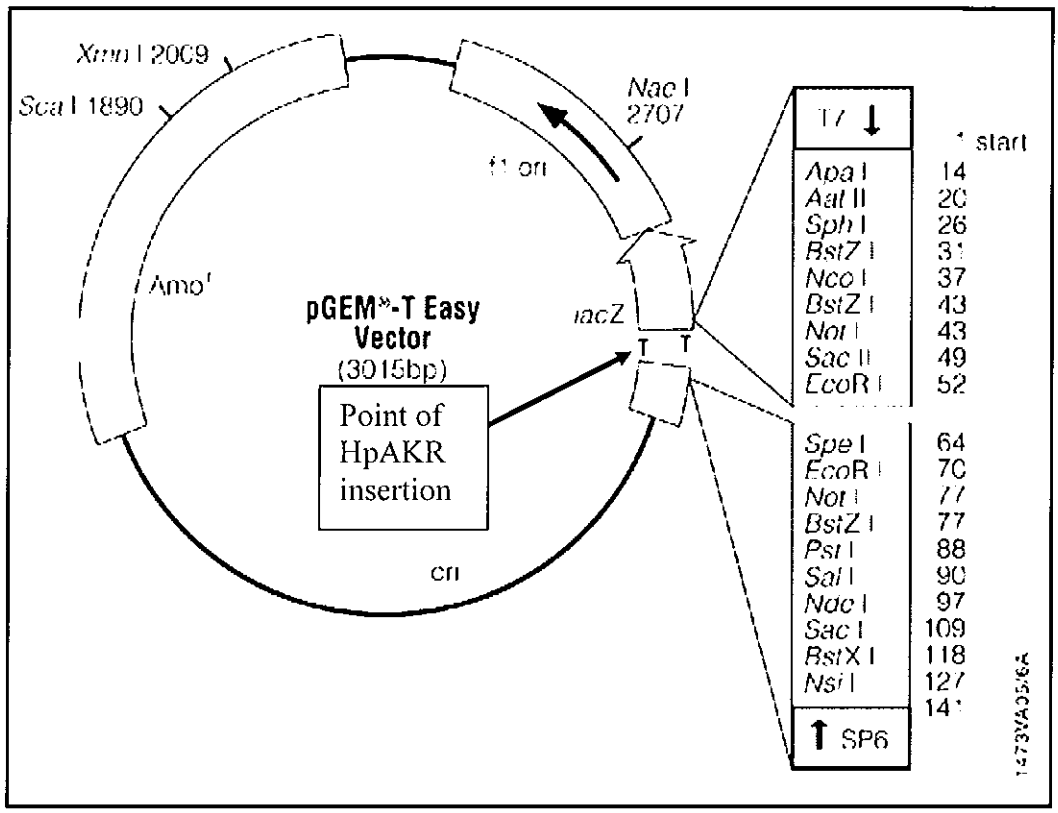

Fig. 5.4: The pGEM-T EASY vector used to generate pGEM:HpAKR construct from Promega.

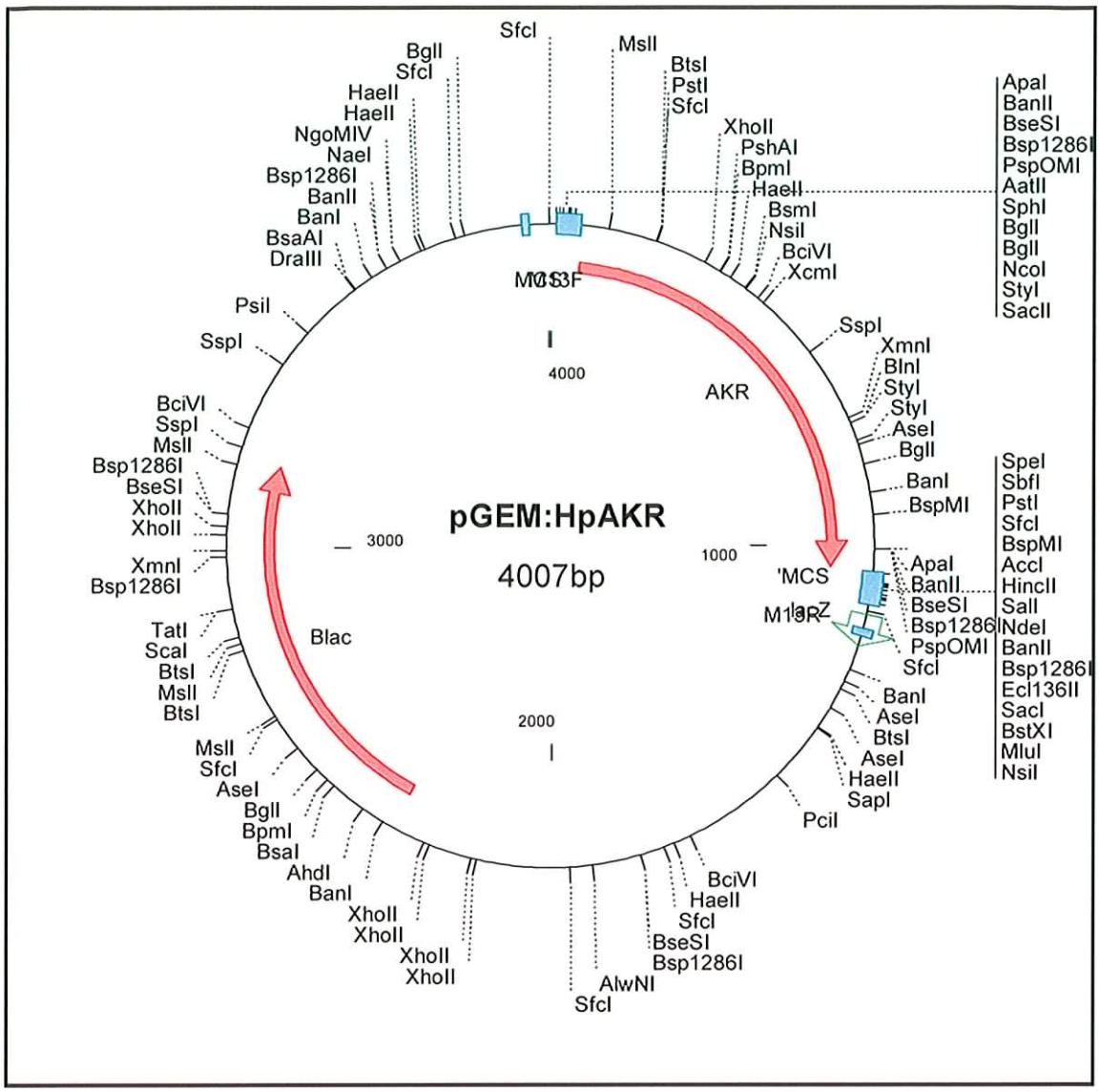

Fig. 5.5: Scientific Educational software simulation of pGEM:HpAKR construct. The diagram shows the presence of a disrupted LacZ gene due to the presence of the inserted *HpAKR* gene.

5.3 Generation of pGEM:HpAKR::*aphA-3* construct

5.3.1 Xcm I restriction digest of pGEM:HpAKR construct

The unique Xcm I restriction site (Fig. 5.2) was the target site for insertion of the kanamycin resistance cassette (*aphA-3*). Restriction with Xcm I produced a linearised pGEM:HpAKR construct, visualised by an increase in size of the construct on an agarose gel (Fig. 5.6).

The digest created DNA fragments with a single base 3' extension, as detailed below;

Xcm I restriction site –

5'.....C C A N^1 N^2 N^3 N^4 N^5 ▼ N^6 N^7 N^8 N^9 T G G.....3'
3'.....G G T N^9 N^8 N^7 N^6 ▲ N^5 N^4 N^3 N^2 N^1 A C C.....5'

5.3.2 Generation of pGEM:HpAKR::*aphA-3* construct

The kanamycin cassette (*aphA-3*) was obtained by amplification from the pJMK30 plasmid (Fig. 5.7) using high fidelity Taq polymerase, which allowed for the generation of a blunt ended amplified product.

The *aphA-3* cassette was amplified using standard M13 pUC primers, as detailed below (Table 5.3). The *aphA-3* cassette amplicons (Fig. 5.8) were purified using a Qiagen kit following the manufactuers guidelines.

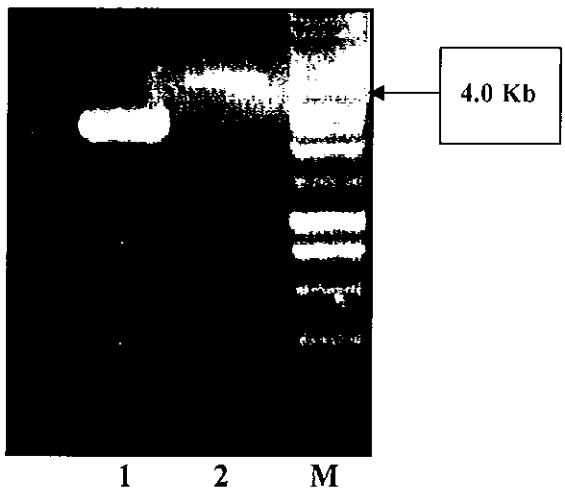

Fig. 5.6: Agarose (1 %) gel electrophoresis of *Xcm* I restriction digest of pGEM:HpAKR construct (lane 1). Lane 2 shows the uncut pGEM:HpAKR construct (used as a control). Lane M contains the DNA size ladder.

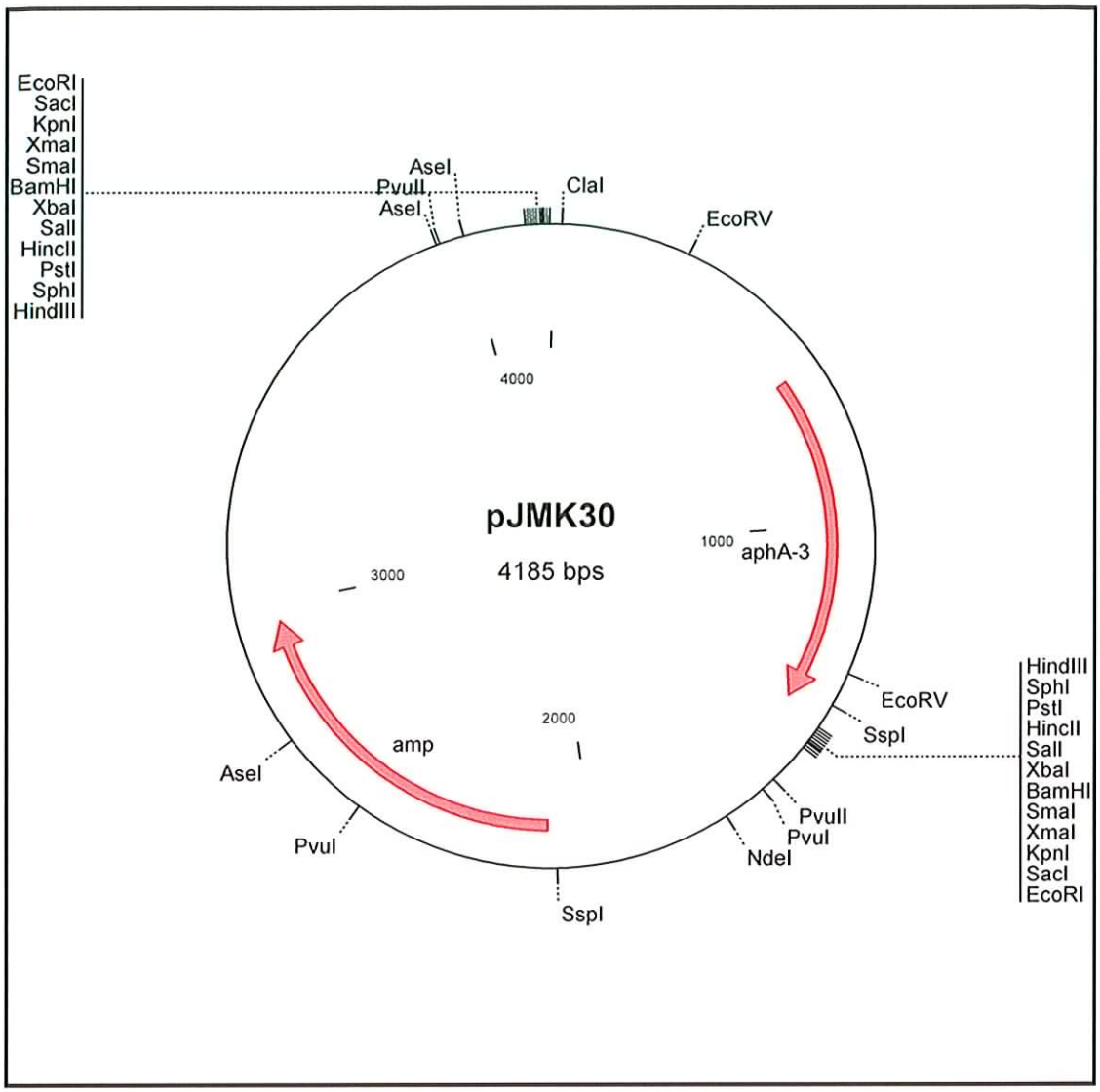

Fig. 5.7: Scientific Educational software simulation of the pJMK30 plasmid from which the *aphA-3* cassette was purified.

Gene	Primer direction	Primer sequence
S1211	Forward	5' – GTA AAA CGA CGG CCA GT -3'
S1210	Reverse	5' – AAC AGC TAT GAC CAT G – 3'

Table 5.3: Primers used for the cloning of the *aphA-3*, kanamycin resistance cassette from the pJMK30 plasmid.

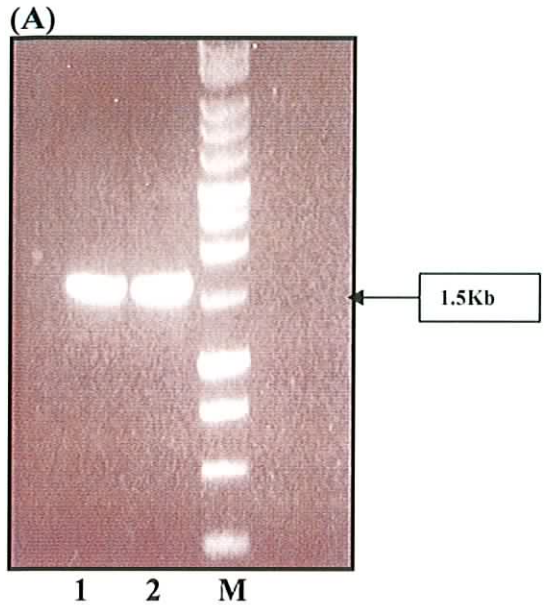

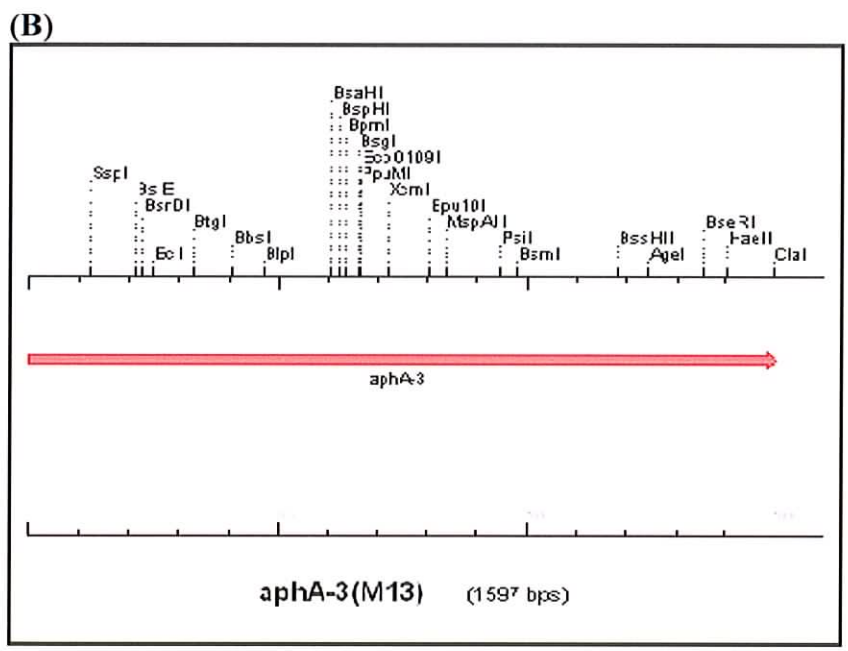

Fig. 5.8: (A) Agarose (0.8%) gel electrophoresis of the PCR amplified kanamycin cassette (*aphA-3*). The kanamycin cassette was amplified by PCR using the pJMK30 plasmid as template DNA and high fidelity Taq polymerase. Lanes 1 & 2 contains the PCR amplicons. The PCR products yielded were of the expected size (1597 bp). Lane M is the DNA size ladder. **(B)** Restriction map of the kanamycin cassette generated using Scientific Educational Software.

The pGEM:HpAKR construct was cleaved at the Xcm I site to allow for the insertion of the kanamycin cassette (*aphA-3*). Restriction with Xcm I produced a linearised pGEM:HpAKR construct. Prior to the insertion of the *aphA-3* into the linearised pGEM:HpAKR, the overhangs created by the Xcm I digest were removed using T4 DNA polymerase supplemented with dNTPs. An insertional ratio of 1:10 (insert: plasmid) yielded approximately 15 DH5α transformed colonies, which were selected on their basis of dual antibiotic resistance to ampicillin and kanamycin.

The presence of the inserted *aphA-3* cassette was visualised as a 1.5 Kb increase in size of the construct to a final molecular size of 5.6 Kb (Fig. 5.9).

5.3.3 Determination of *aphA-3* Orientation Within pGEM:HpAKR::*aphA-3* Construct

Since both the *aphA-3* insert and the pGEM:HpAKR were linearised and blunt ended, it was necessary to determine the orientation of the *aphA-3* cassette. This was determined by Psi I restriction digest, *aphA-3* PCR amplification and finally confirmed by DNA sequencing.

Digestion of the plasmids isolated from the transformation, using the Psi I restriction enzyme, determined the direction of insertion of the *aphA-3* cassette. After the restriction digest, forward insertion of the *aphA-3* cassette is expected to yield two fragments of the following sizes: 3655bp and 1948bp while reverse insertion of the *aphA-3* cassette should yield two fragments of: 3952bp and 1651bp.

A total of 5 plasmids generated two fragments of the expected size profile after restriction with Psi I. Four of these plasmids contained the HpAKR DNA amplified from *H. pylori* 26695. Of these four, three contained the *aphA-3* in the reverse direction

and one in the forward direction (Fig. 5.10a). The fifth plasmid contained the AKR amplified from *H. pylori* 1061 and it contained the *aphA-3* in the forward direction (Fig. 5.10b).

The constructs were subjected to PCR amplification of the *aphA-3* cassette, using the primers outlined in Table 5.3. Several bands were obtained due to sequence overlap in the pGEM T-Easy and the *aphA-3* cassette. Therefore, the primers also amplified part of the construct however a 1.5 Kb band for the *aphA-3* cassette was obtained (Fig. 5.11a & b).

The resulting pGEM:HpAKR constructs containing the inserted kanamycin cassette (*aphA-3*) in the forward orientation were named the HpAKR mutant. Scientific Educational software was used to simulate a graphical image of the HpAKR mutant construct (Fig. 5.12)

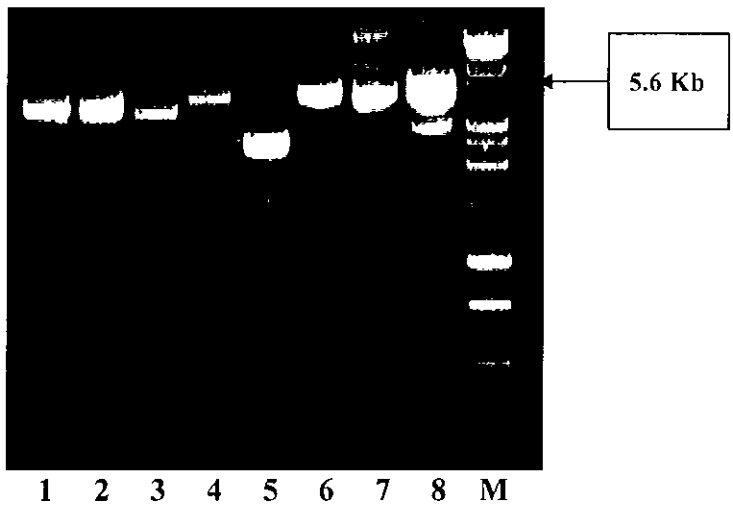

Fig. 5.9: Agarose (1%) gel electrophoresis of pGEM:HpAKR::*aphA-3* construct. Lanes 4 & 6 contain constructs of the expected size (5.6 Kb) and were used throughout the rest of the study. Lanes 1-3 and 5 contain constructs of the incorrect size and therefore were not used in the study. Lanes 7-8 contain multiple bands and were not used in the study. Lane M contains the DNA ladder.

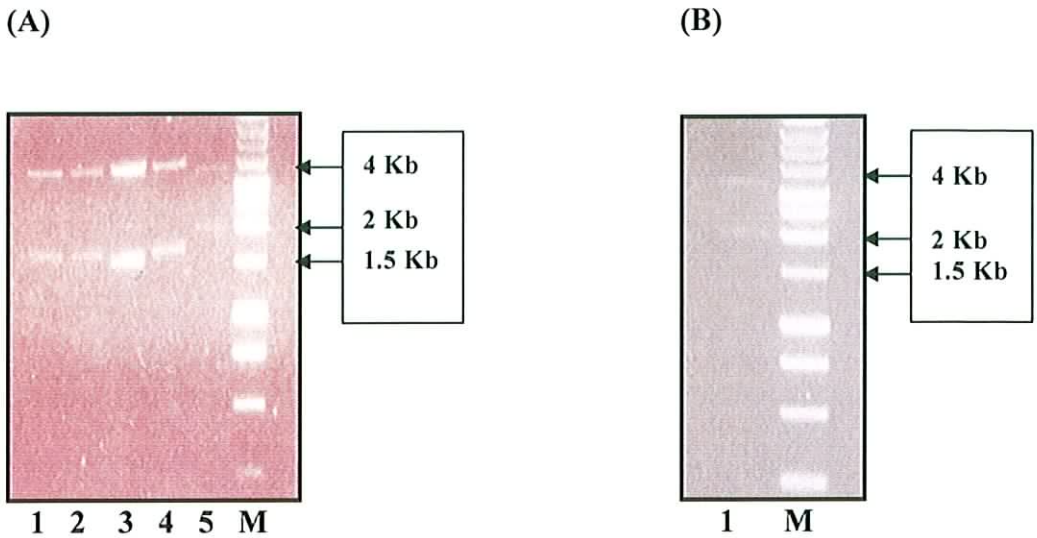

Fig. 5.10: (A) Agarose (0.8%) gel electrophoresis of plasmids containing the *aphA-3* resistance cassette after digestion with Psi I restriction enzyme. The *AKR* gene in these plasmids was amplified from *H. pylori* 26695. Plasmids in lanes 1-4 contain the *aphA-3* in the reverse direction whereas the lane 5 contains a plasmid with the *aphA-3* in the forward direction. **(B)** Agarose (0.8%) gel electrophoresis of a plasmid containing the *aphA-3* resistance cassette after digestion with Psi I restriction enzyme. The *AKR* gene in this plasmid was amplified from *H. pylori* 1061. The *aphA-3* resistance cassette is in the forward direction.

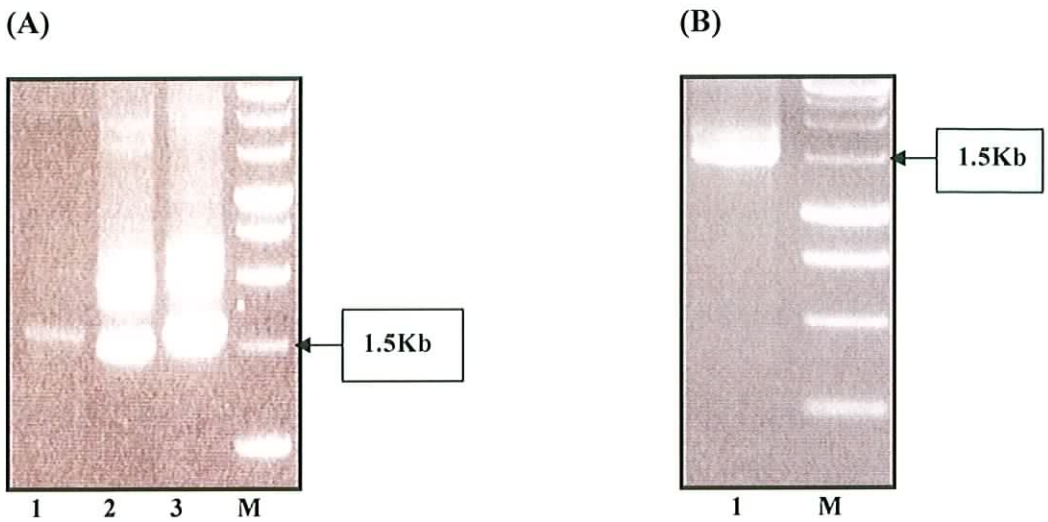

Fig. 5.11: (A) Agarose (0.8%) gel electrophoresis of plasmids containing the *aphA-3* resistance cassette (1.5Kb) after PCR of the *aphA-3* cassette. The *AKR* gene in these plasmids was isolated from *H. pylori* 26695. **(B)** Agarose (0.8%) gel electrophoresis of a plasmid containing the *aphA-3* resistance cassette (1.5Kb) after undergoing a PCR reaction. The *AKR* gene in this plasmid was isolated from *H. pylori* 1061.

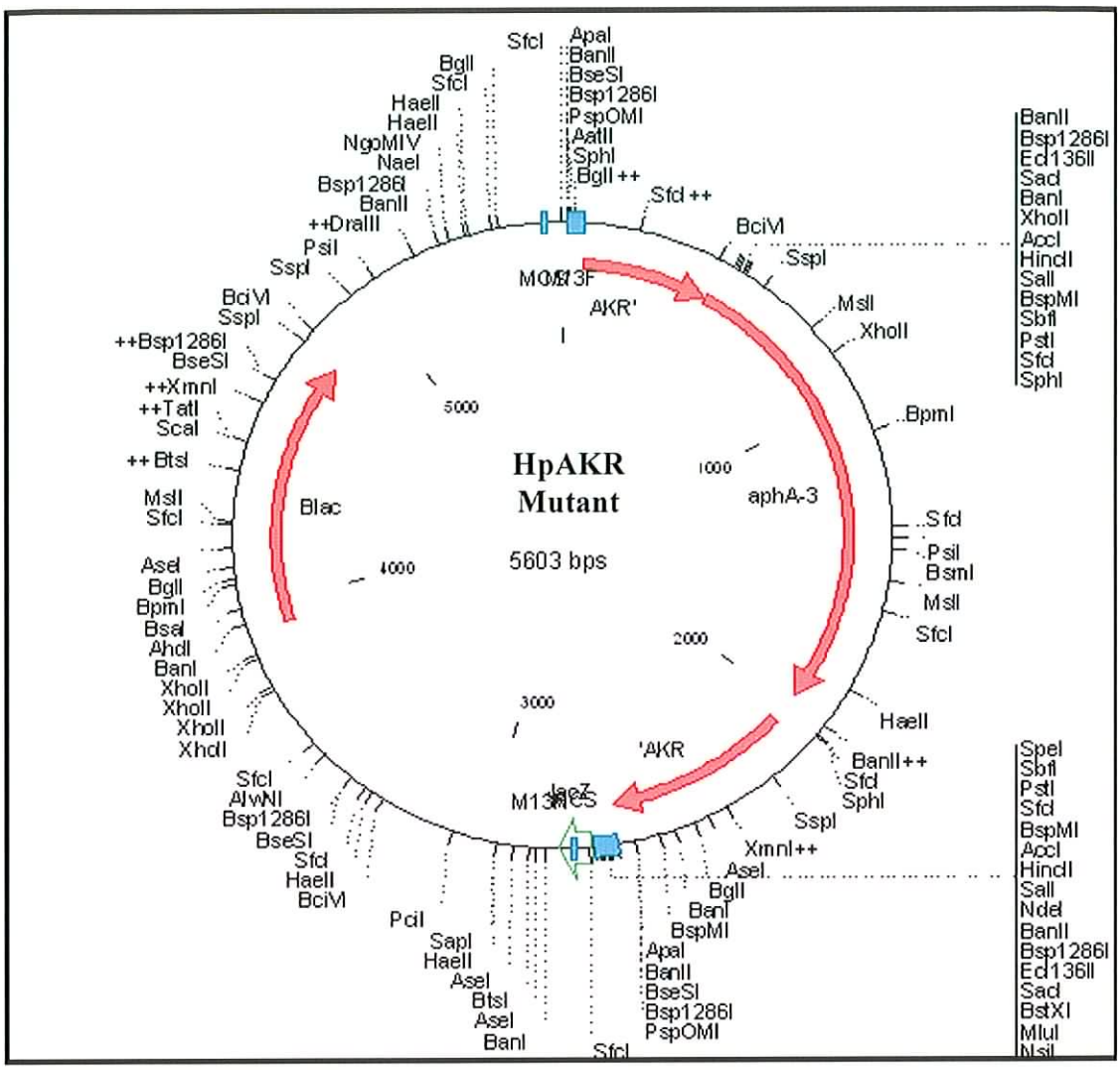

Fig. 5.12: Scientific Educational software simulation of pGEM:HpAKR::*aphA-3* construct with the *aphA-3* in the forward direction. The construct is a total of 5603 bps in size.

5.4 Production and Genotyping of HpAKR Mutant

Naturally competent *H. pylori* cells (strains 1061 and 26695) were transformed with the HpAKR mutant construct (as described in Materials and Methods, Chapter 2; section 2.12.2). Colonies which grew on Columbia agar containing 5% horse blood supplemented with kanamycin (20 µg/ml) were screened by PCR using HpAKR forward and reverse primers (Table 5.2). No *H. pylori* 26695 transformants were obtained using natural transformation or electroporation. The electroporation was carried out as outlined in Materials and Methods, Chapter 2; Section 2.12.3.

For *H. pylori* strain 1061, transformants were obtained and this event was visualized as a 1.5 Kb increase in the size of the *HpAKR* gene, attributed to the recombination of the *aphA-3* disrupted *HpAKR* gene into the chromosomal gene (Fig. 5.13). Of the 20 colonies screened, all contained the inserted *aphA-3* cassette.

To confirm the absence of a functional protein in the HpAKR mutant, cytosolic fractions were prepared from the isogenic HpAKR mutant and wild type strains and probed by Western blotting using affinity purified polyclonal rabbit anti-HpAKR anti serum (as described in Materials and Methods, Chapter 2; Section 2.2). However, the AKR protein could not be detected by Western blotting in either the wild type or HpAKR mutant strains even when large amounts of extract (400 µg) were loaded on the gels (Fig. 5.14).

H. pylori whole cells, from both agar plates and liquid cultures, were also subjected to Western blotting, however, no AKR band was observed in the parental wild type strain.

Even immunoprecipitation using anti-AKR antibodies was insufficient to enrich the AKR yield to make it detectable by Western blotting

This data suggested that the native protein was either present in very low amounts or that it was not recognised by the antiserum. However, the probability of the latter occurring was unlikely since the antiserum was capable of detecting the recombinant HpAKR. Therefore, the ability of aldehydes to induce expression of the protein was then evaluated.

For this purpose the substrate employed was 3-nitrobenzaldehyde. Both the HpAKR mutant and wild type strains were grown in the presence of 3-nitrobenzaldehyde at a concentration of 1.7 mM for 48 h in broth cultures after which time the cells were processed for Western blotting. Prior to blotting, the cell extract was immunoprecipitated with anti-AKR antibodies (affinity purified) to enrich for AKR. Using this approach, the protein was detected in the wild type strain of *H. pylori* but not in the HpAKR isogenic mutant. (Fig. 5.15).

Having established that the HpAKR protein was absent in the HpAKR mutant strain and present in the wild type strain, it was of interest to determine the phenotype of the HpAKR mutant.

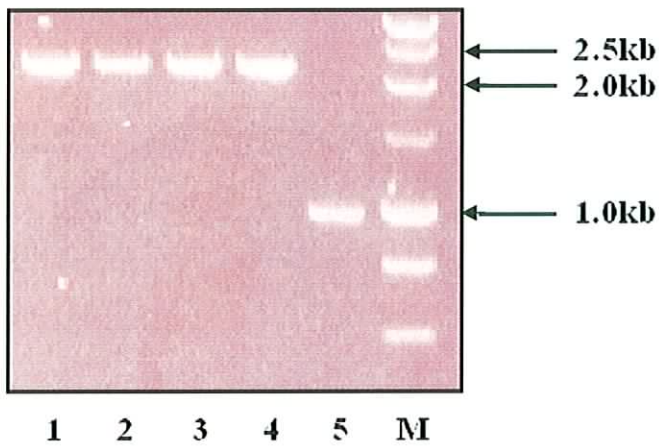

Fig. 5.13: 1% agarose gel indicating the presence of the inserted *aphA-3* cassette in the construct HpAKR mutant. Lanes 1-4 show a 1.5 Kb increase in size of the *HpAKR* gene (chromosomal) due to the presence of the inserted *aphA-3* cassette amplified from *H. pylori* 1061. Lane 5 contains HpAKR, with an approximate size of 990bp, amplified from the parental wild type *H. pylori* 1061. Lane M contains the DNA size marker.

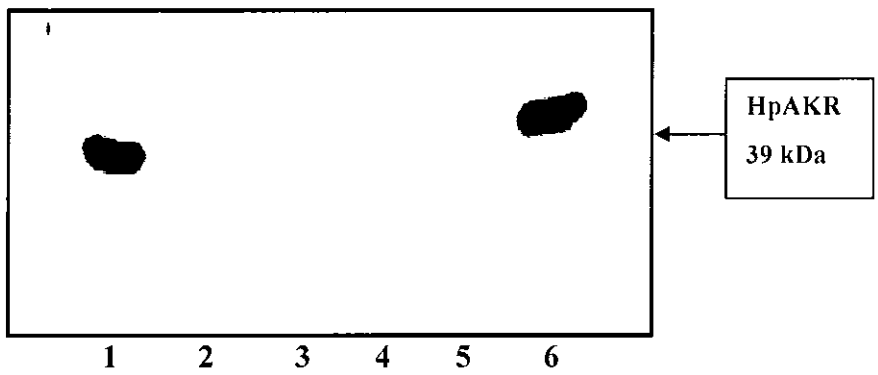

Fig. 5.14: Immunoblot analysis using anti-HpAKR antibodies. Lanes 1 & 6 contain the purified recombinant HpAKR as a positive control. Lanes 2 (100 µg of protein) & 3 (400 µg of protein) contain the HpAKR mutant lysates. Lanes 4 (100 µg of protein) & 5 (400 µg of protein) contain the *H pylori* 1061 parental strain.

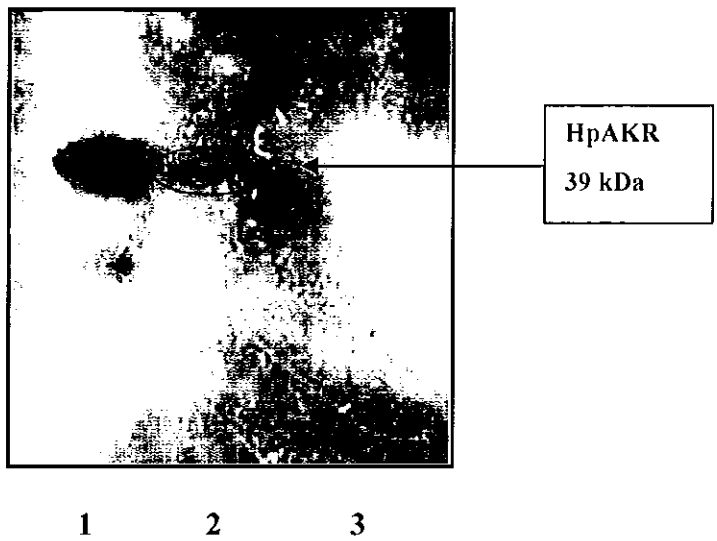

Fig. 5.15: Immunoblot analysis using anti-HpAKR antibodies. Lane 1 contains the purified recombinant HpAKR protein as a control. Lane 2 contains the AKR protein (highlighted in red) from the *H. pylori* 1061 parental strain. Lane 3 contains HpAKR mutant. The presence of the AKR in lane 2 is highlighted.

5.5 Growth Characteristics of HpAKR mutant

The *H. pylori* 1061 (wild type) and HpAKR mutant strains were grown under standard microaerobic conditions in Brain Heart Infusion medium supplemented with FCS (5 %; v/v) at pH 7.0. The optical density of the liquid cultures was monitored at 600 nm every 6 h over a period of 48 h (Fig. 5.16). Growth curves were found to be highly reproducible. All curves were repeated 6 times with similar results.

It is evident from Fig. 5.16 there was no substantial difference in the growth profiles between the HpAKR mutant and wild type strains at pH 7.0 *in vitro*. However, the *H. pylori* 1061 wild type strain exhibited a slightly higher growth rate after 36 h incubation compared to that observed by the HpAKR mutant.

5.6 The Effect of Acid Stress on the Growth Characteristics of the HpAKR Mutant

Previous reports in the literature suggested that the disruption of a region immediately upstream of the *HpAKR* gene resulted in an acid sensitive *H. pylori* (Biljmsa *et al.*, 2000). Therefore the HpAKR mutant was grown under acidic conditions to assess the mutant's ability to survive in the absence of a functional HpAKR at low pHs. The medium was titrated to the chosen pH after the addition of the FCS (5 %, v/v) at 37°C. Prior to inoculation, the medium was pre-equilibrated in cell culture flasks under microaerobic conditions.

At pH 6.0, the growth characteristics of both the wild type and HpAKR mutant strains were similar to those seen at pH 7.0 (Fig. 5.17a).

At pH 5.5, a significant difference in growth was observed between the wild type and HpAKR mutant strains (Fig. 5.17b). The growth rate of the HpAKR mutant was severely compromised beyond 10 h of growth, compared to the wild type.

The growth rate of both the wild type and the mutant were both compromised at pH 5.0 (Fig. 5.17c).

The difference in growth rate between the wild type and HpAKR mutant strains became more apparent as the pH of the medium was reduced. The growth profile of the wild type and the HpAKR mutant reduced dramatically at pH 5.0 when compared to the growth profile observed at pH 7.0.

The ability of *H. pylori* to grow in an acidic environment was believed to be due, at least in part, to the activity of the urease enzyme. The ammonia generated from the urease-mediated hydrolysis of urea helps counteract the acidic pH of the stomach, at least in the microenvironment of the bacterium. Therefore, to assess the effect of urea addition on the acid sensitive phenotype for both the wild type and HpAKR mutant strains, Brucella broth, containing 5% foetal calf serum and DENT at pH 5 and 5.5, was supplemented with 10 mM urea.

The addition of urea to the medium at pH 5.0 (Fig. 5.18a) and pH 5.5 (Fig. 5.18b) resulted in growth profiles similar to those seen at pH 7.0 in the absence of urea.

This was likely due to the increase in pH of the medium after 48 h bacterial growth. In the presence of urea the pH rose from pH 5 or 5.5 to approximately pH 7.0. This pH change did not occur in the absence of urea. Similar findings for acid sensitive *H. pylori* mutants have been previously described (Bijlsma *et al.*, 2000).

Figures 5.18 (a) and (b) also illustrate the growth profiles for both the wild type and HpAKR mutant strains in the absence of urea. This data clearly illustrates a significant increase in growth for both the HpAKR mutant and wild type strains in the presence of urea.

5.7 The Effect of EDTA on the Growth Characteristics of the HpAKR Mutant.

The growth characteristics of the mutant and wild type were also assessed in the presence of the chelating agent EDTA to determine whether or not the HpAKR mutant had different divalent metal cation requirements. Both the wild type and HpAKR mutant exhibited similarly impaired growth in the presence of 0.1 mM EDTA (Fig. 5.19a), with growth levels being reduced by approximately 50% when compared to the growth in the absence of EDTA. However, when the concentration of EDTA was increased to 1mM, the growth of both strains was significantly reduced, with the AKR mutant demonstrating a more sensitive phenotype (Fig. 5.19b).

While a divalent metal ion is not involved in the AKR reaction (Chapter 4 Section 4.9.1), it is interesting that the HpAKR mutant is more sensitive to a metal chelating agent such as EDTA. The reason for this increased sensitivity is not known.

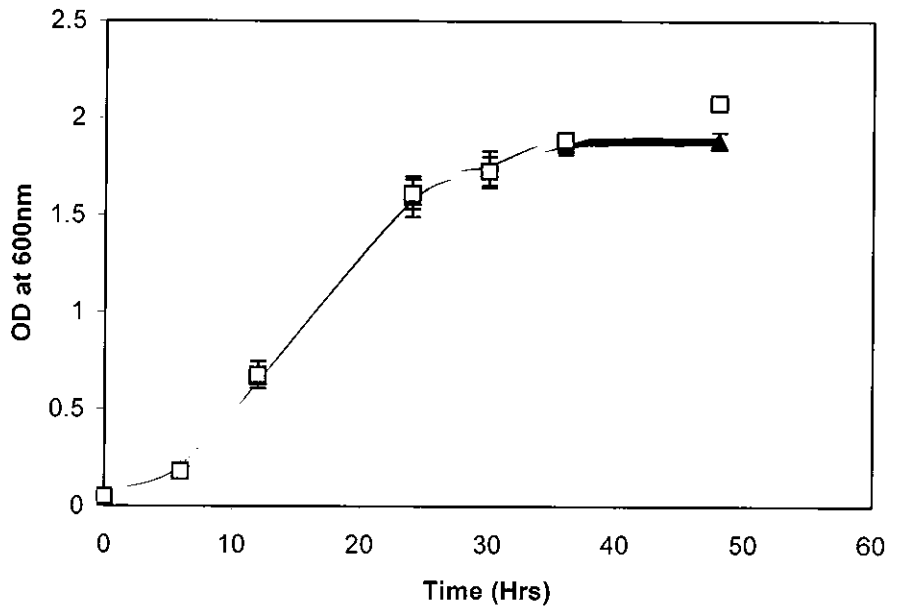

Fig. 5.16: The growth characteristics of both *H. pylori* 1061 wild type (□) and HpAKR mutant (▲) at pH 7.0 in Brucella broth supplemented with 5% foetal calf serum and DENT. Results are shown as the mean ± SEM (n=6).

(A) pH 6.0

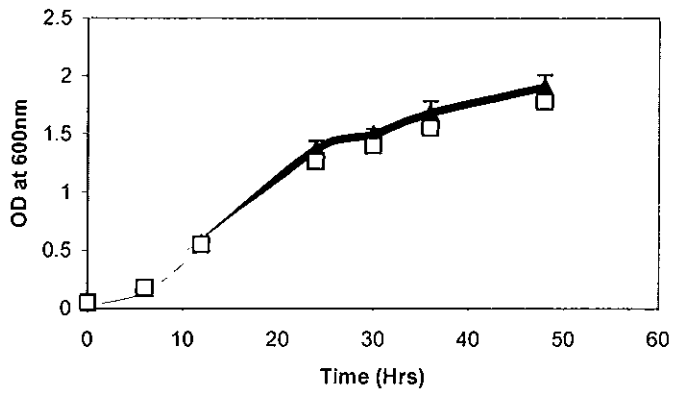

(B) pH 5.5

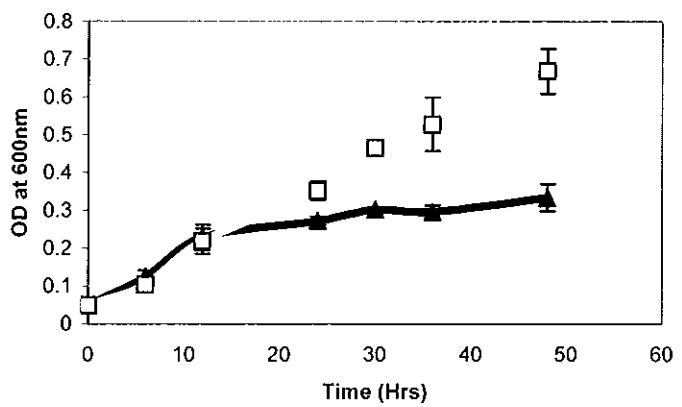

(C) pH 5.0

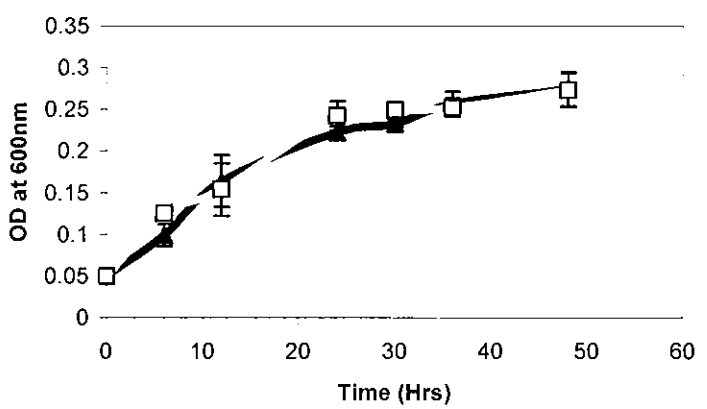

Fig. 5.17: The growth characteristics of both *H. pylori* 1061 wild type (□) and HpAKR mutant (▲) in Brucella broth supplemented with 5% foetal calf serum and DENT. Medium pH; (A) pH 6.0, (B) pH 5.5 and (C) pH 5.0. Results are shown as the mean ± SEM (n=6)

(A) pH 5.5

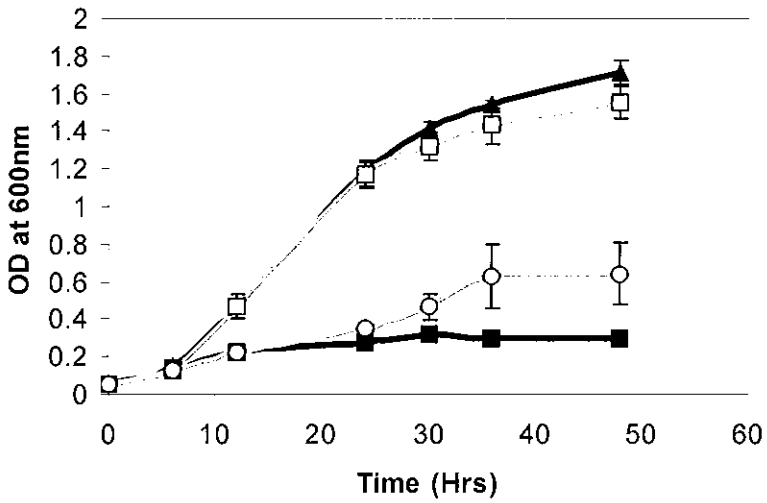

(B) pH 5.0

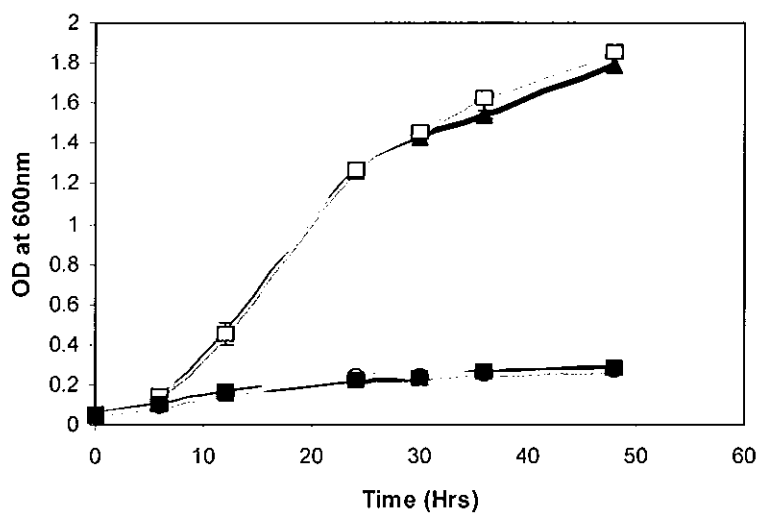

Fig. 5.18: The growth characteristics of both *H. pylori* 1061(□) wild type, HpAKR mutant (▲) in the presence of 10 mM urea and *H. pylori* 1061 (○) wild type, HpAKR mutant (■) in the absence of urea. The Brucella broth was supplemented with 5% foetal calf serum and DENT. Medium pH: (A) pH 5.5 and (B) pH 5.0. Results are shown as the mean ± SEM (n=6).

(A): 0.1 mM EDTA

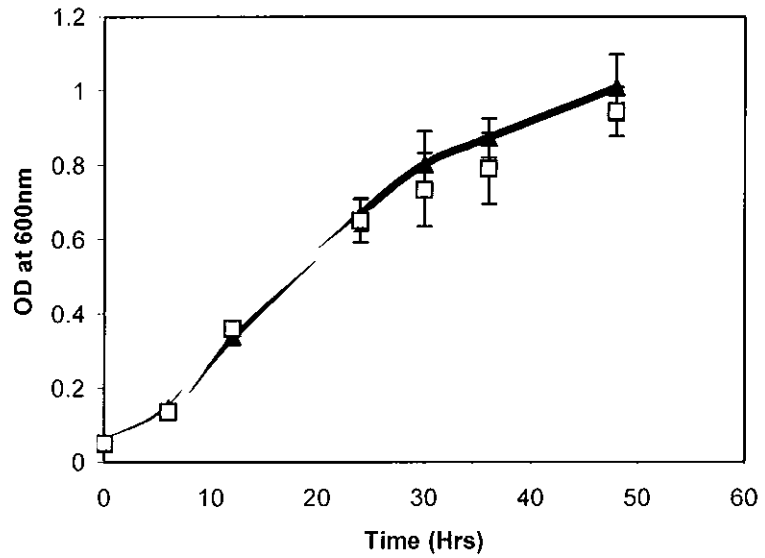

(B): 1 mM EDTA

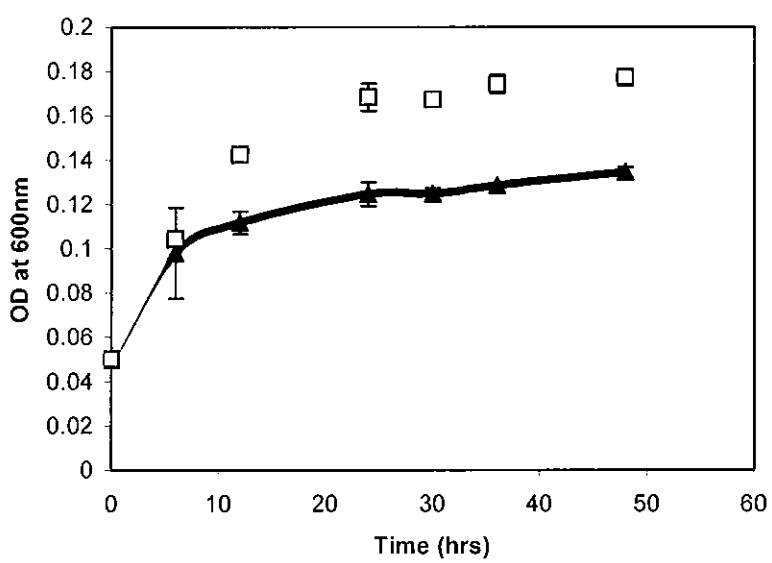

Fig. 5.19: The growth characteristics of both *H. pylori* 1061 wild type (□) and HpAKR mutant (▲) in Brucella broth supplemented with 5% foetal calf serum, DENT and EDTA. Concentration of EDTA in (A) is 0.1 mM and (B) is 1 mM. Results are shown as the mean ± SEM (n=6).

5.8 Growth Characteristics of the HpCAD Mutant Under Neutral and Acidic Conditions

The studies on the growth characteristics of the HpCAD mutant were carried out in collaboration with Dr. Blanaid Mee. The HpCAD mutant was constructed in a similar manner to that for the HpAKR mutant mutant however there was a slight variation in the protocol used. The construction of this mutant can be found in Appendix B. Preliminary studies undertaken by Blanaid Mee are extended in this study.

A report in the literature suggested that HpCAD mRNA is upregulated in response to acid stress conditions (Ang *et al.*, 2001). Therefore to assess this both the HpCAD mutant and wild type strains were exposed to neutral and acidic environments and their growth profiles monitored over a period of 48 h.

Initially, the *H. pylori* 1061 wild type and HpCAD mutant strains were grown under standard microaerobic conditions in Brain Heart Infusion medium supplemented with FCS (5 %; v/v) at pH 7.0. The optical density of the liquid cultures was monitored at 600 nm over a period of 48 h (Fig. 5.20).

It is evident from Fig. 5.20, that the growth profile of the HpCAD mutant is slightly compromised in comparison to the *H. pylori* 1061 parental strain at pH 7.0. The HpCAD mutant exhibits a reduction in growth after 36 h incubation.

For studies under acidic conditions, the medium was titrated to the required pH after the addition of the FCS (5 %, v/v) and at 37°C. A pronounced difference in growth became apparent with reduction in pH of the medium.

At pH 6.0, the growth profile for both the parental strain and HpCAD mutant was similar to that seen at pH 7.0 (Fig. 5.21a). However, at pH 5.5, the growth of the parental strain was impaired whilst the HpCAD mutant continued to grow (Fig. 5.21b). At pH 5.0, the growth profile of both the wild type and HpCAD mutant was impaired. However the growth displayed by the wild type was more compromised than that of the HpCAD mutant (Fig. 5.21c). No change in the pH of the medium was evident after 48 h growth at each pH examined.

It is evident from the data that the absence of the HpCAD protein confers an advantage on the bacterium for growth in acidic environments. However, the decrease in the growth rate of the HpCAD mutant after 36 h was observed at every pH analysed except at pH 5.0. This decrease in growth was not observed in the parental strain. The ability of the HpCAD mutant to grow at a greater rate than the wild type in an acidic environment is surprising.

As was observed for the HpAKR mutant and wild type strains in the presence of urea, the growth profiles observed for both the wild type and HpCAD mutant was similar to those seen at pH 7.0. The HpCAD mutant demonstrated a slight impairment in comparison to the wild type. The decrease in growth after 36 h incubation for the HpCAD mutant was observed again at pH 5.0 (Fig. 5.22a) and pH 5.5 (Fig. 5.22b) in the presence of urea. An increase in pH from pH 5.0 and pH 5.5 to approximately pH 7.0 after 48 h was also evident.

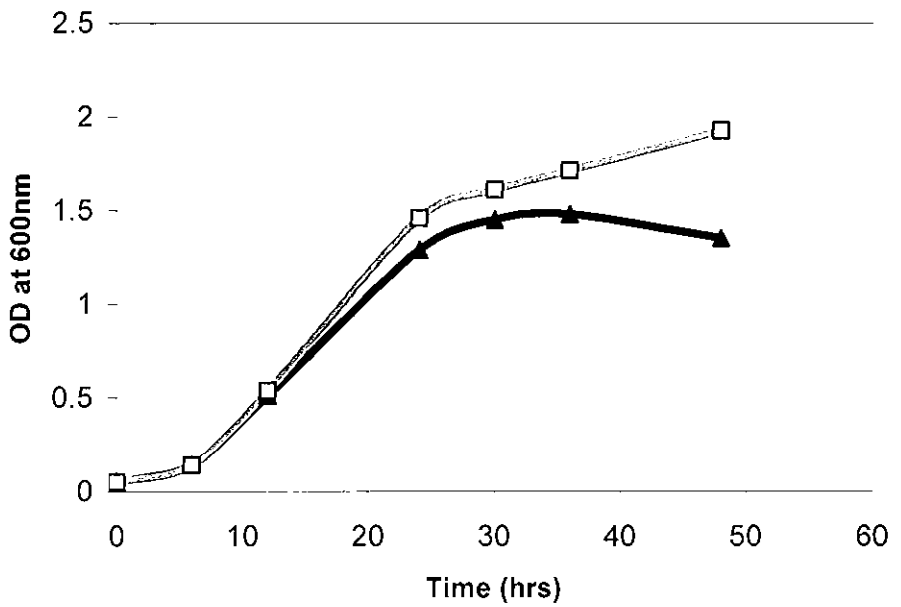

Fig. 5.20: The growth characteristics of both *H. pylori* 1061 wild type (□) and HpCAD knockout mutant (▲) at pH 7.0 in Brucella broth supplemented with 5% foetal calf serum and DENT. Results are shown as the mean ± SEM (n=6).

(A) pH 6.0

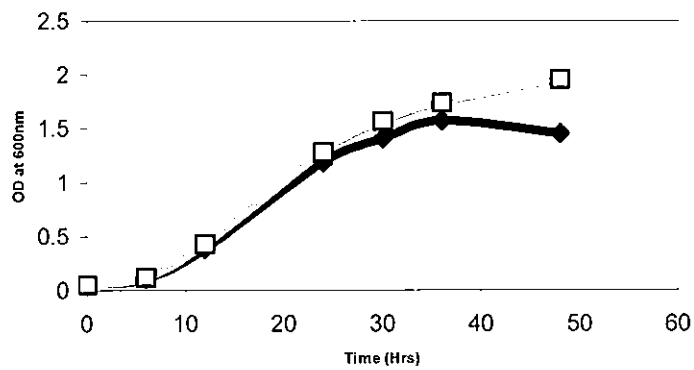

(B) pH 5.5

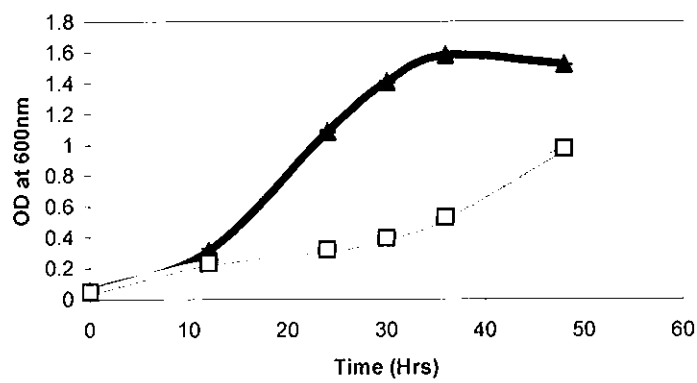

(C) pH 5.0

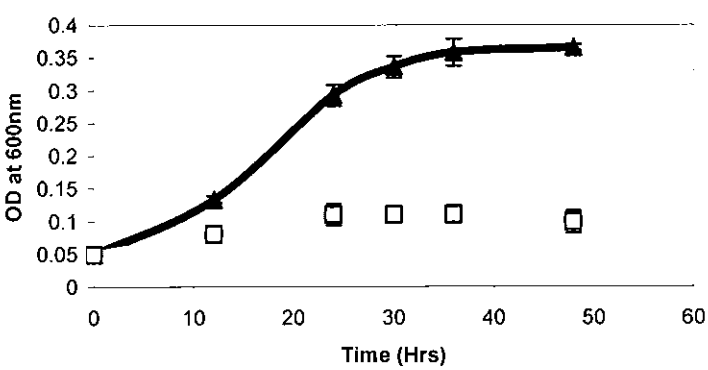

Fig. 5.21: The growth characteristics of both *H. pylori* 1061 wild type (□) and HpCAD knockout mutant (▲) at pH 5.0 in Brucella broth supplemented with 5% foetal calf serum and DENT. Medium pH (A) pH 6.0, (B) pH 5.5 and (C) pH 5.0. Results are shown as the mean ± SEM (n=6).

(A) pH 5.0

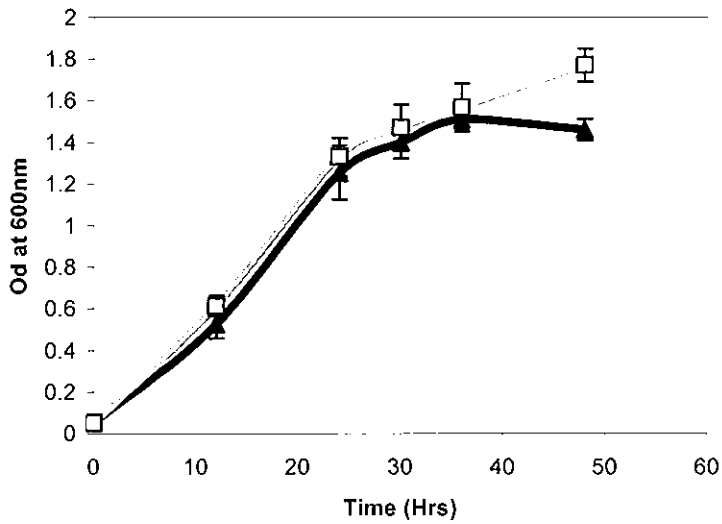

(B) pH 5.5

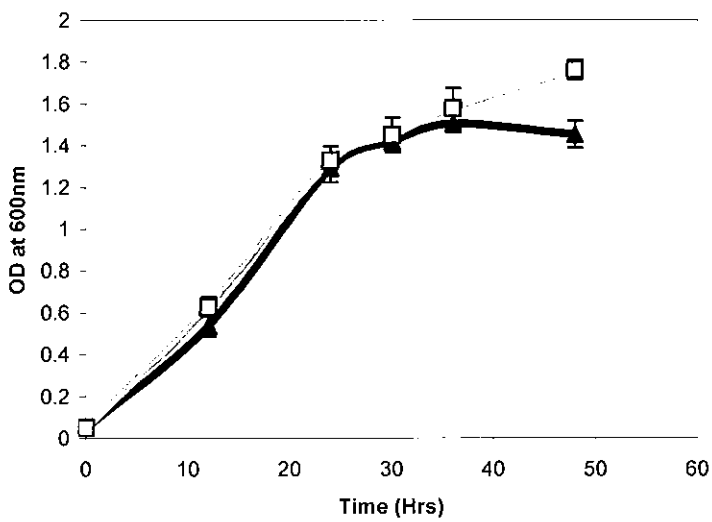

Fig. 5.22: The growth characteristics of both *H. pylori* 1061 wild type (□) and HpCAD mutant (▲) in Brucella broth supplemented with 5% foetal calf serum, DENT and 10 mM urea. Medium pH (A) pH 5.0 and (B) pH 5.5. Results are shown as the mean ± SEM (n=6).

5.9 Discussion

This chapter detailed the construction of an isogenic HpAKR-negative mutant of *H. pylori* and subsequent characterisation of this knockout in terms of its growth characteristics in an acidic environment. A previously constructed HpCAD mutant was also characterised in terms of its acid sensitivity.

HpAKR was disrupted by insertion of a kanamycin resistance cassette (*aphA-3*) within the ORF encoding the enzyme. Natural transformation of *H. pylori* strain 1061 with the HpAKR kanamycin disrupted construct was achieved. Electroporation was attempted in an effort to transform the construct into *H. pylori* strain 26695 however these efforts were unsuccessful. Although *H. pylori* 26695 is naturally competent, attempts to introduce the mutant gene by natural transformation were also unsuccessful. PCR was used to confirm that recombination occurred with the incorporation of the *aphA-3* disrupted *HpAKR* gene into the chromosomal DNA of *H. pylori* 1061. This was seen as a 1.5 Kb increase in the size of the *HpAKR* gene due to the presence of the *aphA-3* cassette.

Attempts were made to confirm the absence of the HpAKR protein by Western blotting. Surprisingly, it proved difficult to detect this protein even when elevated amounts of whole cells were used for SDS-PAGE and Western blotting. This may indicate that HpAKR is present in low copy number in *H. pylori* wild type under these culture conditions. However, data from the Max Planck Institute (http://web.mpiib-berlin.mpg.de/cgi-bin/pdbs/2d-page/extern/index.cgi) indicate that the AKR is present in cytosolic fractions analysed by 2D electrophoresis. Based on the intensity and size of the spot, it is clear that the HpAKR (Fig. 5.23) constitutes only a small proportion of

cellular protein in the organism. This was estimated by comparison to the size of the urease spots, which represents between 6-10% of the total soluble protein (Hu *et al.*, 1992).

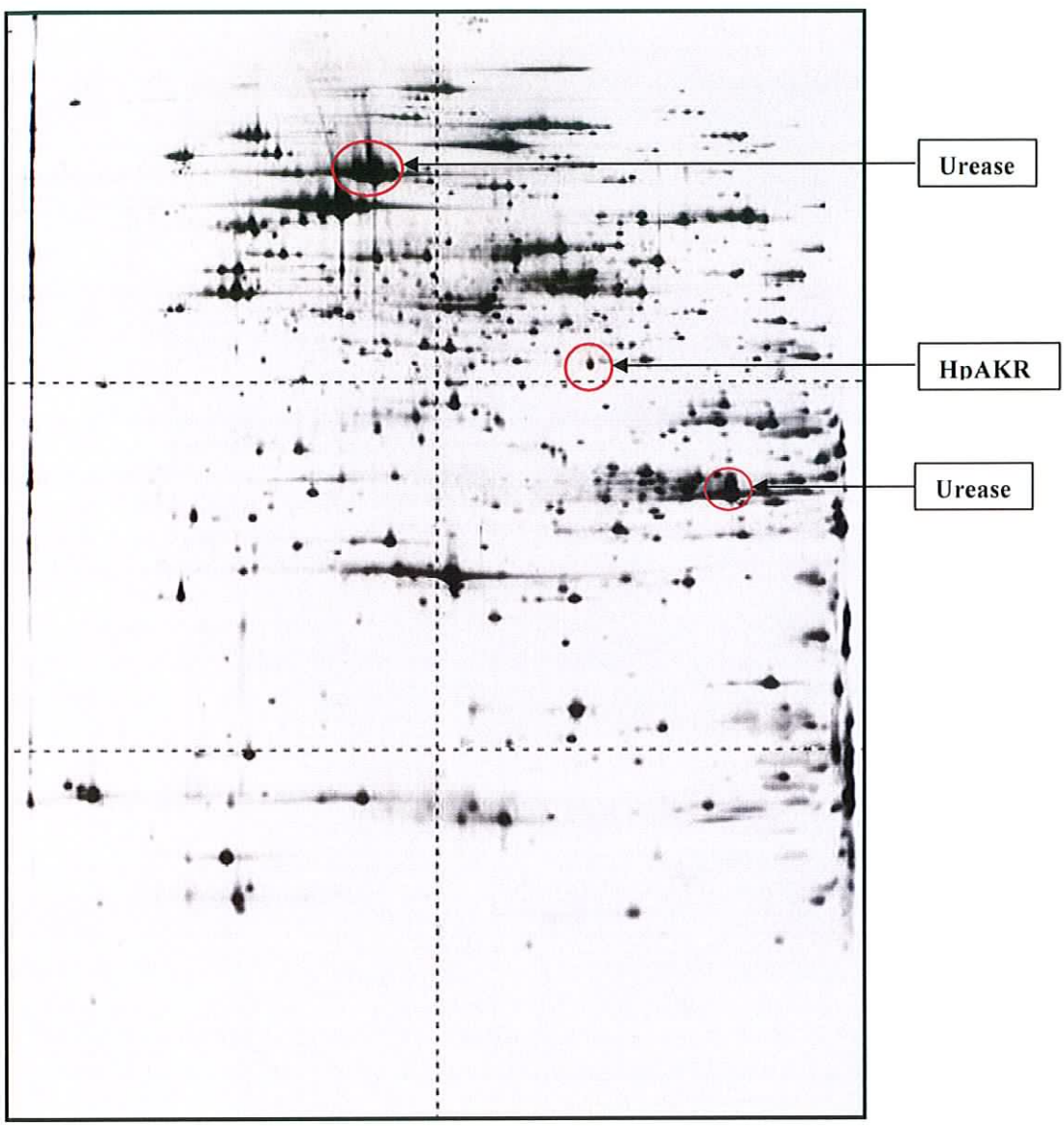

Fig. 5.23: 2-D gel electrophoresis of cellular proteins from *H. pylori 26695*. The spots corresponding to urease and HpAKR are identified.

In an effort to enrich for AKR, a cytosolic extract of *H. pylori* (wild type and mutant) was immunoprecipitated with affinity-purified anti-AKR IgG prior to Western blotting. However, these efforts proved unsuccessful, as the AKR was still undetectable by Western blotting under these conditions

Therefore attempts were made to induce the expression of AKR in *H. pylori* by addition of an HpAKR substrate, 3-nitrobenzaldehyde, to a broth culture of *H. pylori*. When combined with immunoprecipitation, a 37 kDa species was detected in the parental wild type strain but not in the HpAKR mutant strain.

These data indicate that HpAKR is induced in response to the presence of aldehydes, in this case 3-nitrobenzaldehyde, suggesting that HpAKR behaves in a manner analogous to a stress response protein. Under these conditions no HpAKR was observed in the mutant strain. Furthermore, this indicates that chromosomal disruption had occurred and no functional HpAKR was produced by the mutant strain. Other aldo keto reductases have been shown to be inducible also. For example, an active aldose reductase in a rat smooth muscle cell line was induced in the presence of glucose (Spycher et al., 1997).

Previous reports suggested a role for HpAKR in acid adaptation (Bijlsma *et al.*, 2000 and Merrel *et al.*, 2003). This was suggested because disruption of the *H. pylori* genome upstream of the ORF for HpAKR gave rise to an acid sensitive phenotype. It was suggested that this enzyme was involved in acid adaptation since it was located immediately 5' to the insertion point. Interestingly, these workers suggested that the enzyme was required when exposure to acid conditions was chronic (Bijlsma *et al.*, 2000).

The work presented here demonstrates that there was no significant difference in growth rate between the mutant and wild type strain at pH 7.0 or 6.0. Therefore, the deletion of

the *HpAKR* gene did not have any effect on growth of the bacterium under neutral or mildly acidic conditions. However, at pH 5.5, the isogenic mutant of *H. pylori* lacking HpAKR displayed a reduced growth rate compared to that of the parental strain, albeit at a slower rate than observed under neutral conditions. This finding was robust and was repeated several times. Neither the wild type nor parental strain showed significant growth at pH 5.0.

Normal growth profiles of both parental and HpAKR mutant strains were restored when the acidified medium was supplemented with urea. This recovery in growth was due to the activity of the urease enzyme resulting in ammonia production from urea metabolism. There was also a marked increase in medium pH after 48 h growth from pH 5 or 5.5 to approximately pH 7.0. No such pH increase was observed in the absence of urea. Similar findings have been reported by Clyne *et al* (1995) who ascribed a similar pH increase to the production of ammonia as a result of urease activity.

The presence of EDTA also significantly reduced the growth rate of both the wild type and the HpAKR mutant. At a concentration of 1 mM EDTA, the growth of the HpAKR mutant was more impaired than that of the wild type. EDTA has been shown to possess antimicrobial properties especially in gram-negative bacteria. Recent reports suggest that EDTA inhibits peptidoglycan biosynthesis in *H. pylori* (a process which is active in growing bacterial cells), by chelating Mg^{2+} and Mn^{2+}, thus releasing lipopolysaccharide and disintegrating the outer membrane structure (Alakomi *et al.*, 2006 and Nagai et al., 2004). However, this general effect of EDTA on *H. pylori* does not explain the reason for the difference in growth profiles observed between the HpAKR mutant and wild type strains in the presence of EDTA.

Certain members of the alcohol dehydrogenase family require metal ions for activity (Magonet *et al.*, 1992, Dales *et al.*, 1995 and Arslanian *et al.*, 1971). Therefore it is plausible to suggest that the HpCAD enzyme might be inhibited by EDTA. This would be expected to result in the accumulation of toxic aldehydes within the HpAKR mutant when compared to the wild type strain. This aldehyde accumulation might give rise to increased sensitivity to EDTA. Accumulation of aldehydes within the HpAKR mutant could be attributed to the fact there would be only one active oxidoreductase (HpSCADH) in the HpAKR mutant strain, consequently limiting the cells capacity to detoxify aldehydes. In contrast, the wild type strain may be capable of reducing a wider range of aldehydes more efficiently due to the presence of both active HpAKR and HpSCADH enzymes. To lend support to the above theory, it would be necessary to establish whether or not HpCAD is EDTA sensitive. Since members of the classical short chain alcohol dehydrogenases do not typically require metal ions for activity, it is unlikely that EDTA would inhibit this enzyme. Further experiments are required to resolve this issue.

As part of continuing research on alcohol dehydrogenase enzymes, an isogenic HpCAD negative mutant was characterised in terms of its acid sensitivity. Reports in the literature suggest that the HpCAD mRNA is up regulated in response to acid stress (Ang *et al.* 2001, Wen *et al.* 2003 and Merrell *et al*, 2003). Therefore, the absence of a functional HpCAD in the mutant would be expected to impede the growth of the bacterium, especially under acidic conditions. However, the results obtained indicate that the absence of a functional CAD protein in *H. pylori* confers a significant survival advantage to the HpCAD mutant when exposed to acidic environments. This role for HpCAD seems counterintuitive; on the one hand it is upregulated under acid conditions

(Ang *et al.*, 2001) while the data from this study indicate that the presence of HpCAD actually impedes growth under acidic conditions.

Although this is an intriguing observation, additional studies are required to determine both the mechanism and significance of this finding. A key question is whether such a mutant (HpCAD) would have a survival advantage *in vivo* remains to be investigated. During the initial phase of infection when the pathogen is transiently exposed to acidic conditions, it would be expected that the HpCAD mutant would be more adapted to colonising an acidic environment than the wild type. However, as the pathogen is only transiently exposed to strongly acidic conditions in the lumen of the stomach, the apparent survival advantage displayed by the HpCAD mutant *in vitro* may not be significant factor *in vivo* as the bacteria rapidly become adherent to the gastric epithelium where the pH is closer to neutral. (Slonczewski *et al.*, 2000 and Schreiber *et al.*, 2004).

Moreover, *H. pylori* is rarely, if ever, exposed to very low extracellular pH due to the presence of gastric urea which helps maintain both the microenvironment of the bacterium (via urease activity) and the cytoplasmic pH at or near neutral pH (e.g. Stingl *et al.*, 2001). It would be interesting to determine the cytoplasmic pH in the HpCAD mutant under acidic conditions in the absence of urea to explore the possibility that HpCAD may contribute somehow to maintaining intracellular pH. *H. pylori* may never encounter conditions that would be expected to impose selective pressure on the organism to delete the *CAD* gene and confer a survival advantage under acidic conditions.

Another consideration is that HpCAD is not working solely as an alcohol dehydrogenase but has an additional function in this bacterium. It would be of interest

to attempt to identify potential protein complexes with which HpCAD may associate, using co-immunoprecipitation experiments, for example.

A key experiment to determine whether a CAD negative mutant conferred a survival advantage *in vivo* would be to use an animal model of infection to assess colonisation proficiency. Such animal models could be co-infected with both the HpCAD mutant and the parental wild type to determine whether the HpCAD mutant could compete with and/or overgrow the wild type.

Interestingly, irrespective of the culture conditions, the HpCAD mutant failed to grow beyond 36 h of culture (with the exception of growth at pH 5.0). This decline may be due to the accumulation of aldehydes within the bacterium. From the kinetic analysis performed on the recombinant HpCAD enzyme (Mee *et al.*, 2005), it is known that the enzyme can reduce a wide range of aldehydes. Aldehyde detoxification is likely to be essential to the survival of the organism and the present data suggests that the inability of the HpCAD mutant to reduce these aldehydes may result in a reduced lifetime. In this context, it would be of interest to monitor the cytosolic levels of aldehydes over time.

From the kinetic analysis reported in this study (Chapter 4), HpCAD and HpAKR recombinant enzymes do not overlap with regards to their substrate preference. Therefore it is plausible to suggest that certain aldehydes, usually reduced by HpCAD, may not be reduced by the HpSCADH within the bacterium. To ascertain this, a substrate preference profile would need to be determined for the HpSCADH.

Other workers have reported the ability to rescue *H. pylori* grown at reduced pH when the medium was supplemented with urea. Under acidic conditions in the presence of urea, normal growth of both the HpCAD mutant and wild type strains was restored. The growth curves of the parental and HpCAD mutant strain were similar to those seen at pH 7.0 in the absence of urea. An increase in pH of the growth medium from pH 5.0 or pH 5.5 to pH 7.0 was also observed. These data support the view that a HpCAD mutant would not have sustained a selective growth advantage *in vivo*, since the stomach is a rich source of urea.

In conclusion, a *H. pylori* isogenic HpAKR-negative mutant has been constructed and characterised to evaluate its contribution to growth under acid conditions. The acid stress studies demonstrated that an intact AKR is required for *H. pylori* survival under acidic conditions *in vitro* and thus it may represent a novel determinant of infectivity. It would be of great interest to infect an animal model with the HpAKR mutant to determine whether colonisation of the gastric mucosa would occur to establish the *in vivo* function of HpAKR. Similarly, as the ability of *H. pylori* to grow better in an acid environment without the *HpCAD* gene has the potential to produce a more pathogenic strain of the bacterium. It would be of interest to use animal infection studies to determine what contribution this mutation would have on infectivity *in vivo*. However, the aldehyde detoxifying activity of HpCAD may be essential to the long-term survival of the bacterium *in vivo*, as appears to be the case *in vitro*. Consequently, any short-term survival advantage that may be conferred on *H. pylori* CAD mutant *in vivo* may be outweighed by the disadvantage of losing an important aldehyde metabolising enzyme.

Chapter 6

Cloning, Expression, Purification & Preliminary Characterisation of a Short Chain Alcohol Dehydrogenase

6.0 Cloning, Expression, Purification & Preliminary Characterisation of a Short Chain Alcohol Dehydrogenase

6.1 Introduction

Alcohol dehydrogenases (ADHs) display a wide variety of substrate specificities and play an important role in a range of physiological processes (Van der Oost *et al.*, 2001). Most of the classes of ADHs can be divided up into subgroups based on their co-factor specificity. The NAD^+-dependent alcohol dehydrogenases can be further divided into the long chain or zinc-containing ADHs, the short chain ADHs and the iron containing ADHs (Van der Oost *et al.*, 2001).

Short chain alcohol dehydrogenases (SDR) are monomeric NAD(P)(H)-dependent enzymes of typically 250 amino acid residues (Kallberg *et al.*, 2001 and Jornvall *et al.*, 1999). Their substrate spectrum includes steroids, alcohols, sugars, aromatic compounds and xenobiotics (Kallberg *et al.*, 2001 and Van der Oost *et al.*, 2001). The criteria for SDR classification are the occurrence of specific sequence motifs, arranged in a specific manner. These motifs comprise of Rossman-fold elements for nucleotide binding and specific residues at the active site including the highly conserved triad of Ser, Tyr, and Lys residues (Kallberg *et al.*, 2001). Historically, SDRs were believed only to be present in prokaryotes and insects. However, in recent years, the characterisation of the human 15-hydroxyprostaglandin dehydrogenase illustrated that SDRs are actually present in a braoder range of eurkaryotes (Jornvall *et al.*, 1999). Other common elements amongst the SDRs are the N-terminal coenzyme binding site consensus sequence of GXXXGXG and an active site consensus sequence of YXXXXK (Jornvall *et al.*, 1999). Even though the primary sequence identity can be as low as 15-30%, the

3D folds are quite similar except at the C-terminal regions (Fig. 6.1) (Kallberg *et al.*, 2002).

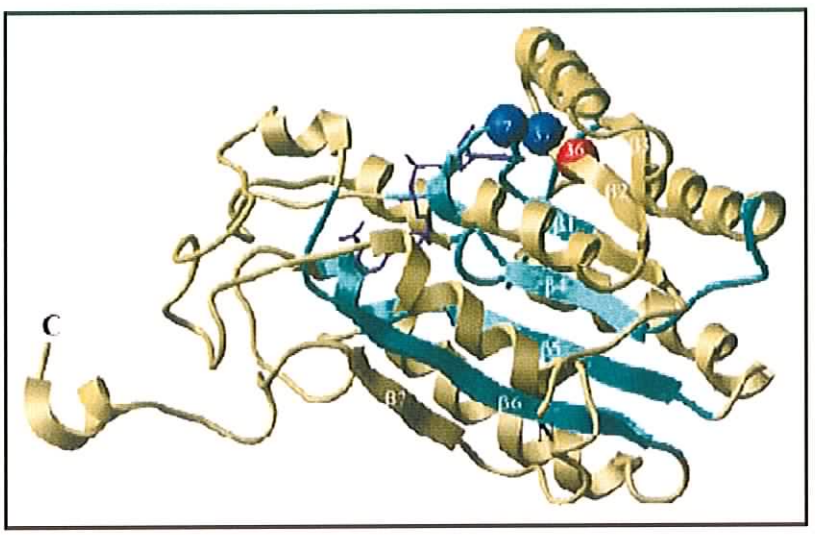

Fig. 6.1: General 3D structure of short chain alcohol dehydrogenases. (Kallberg *et al.*, 2002).

The SDRs can be divided into two large families, "classical" and "extended", with different Gly-motifs in the co-enzyme-binding regions and different chain lengths ranging from 250 residues for the classical SDRs to 350 in extended SDRs (Fig. 6.2). There are few highly conserved residues throughout the SDRs however several sequence motifs are distinguishable within families.

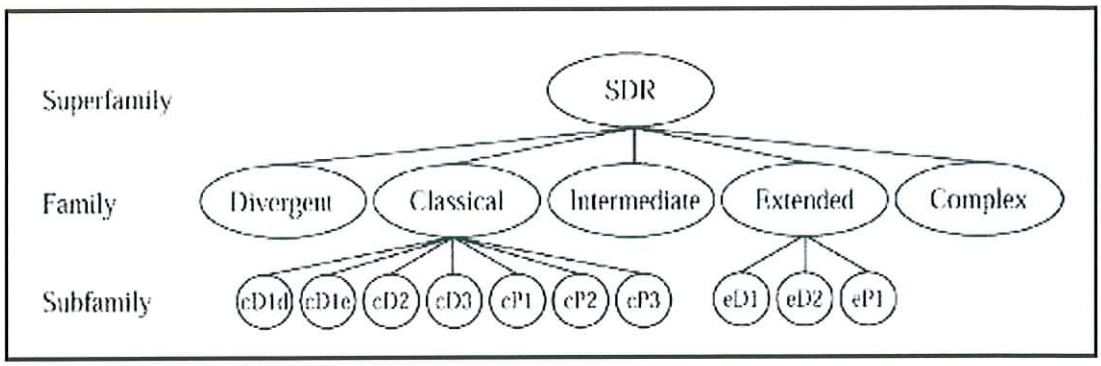

Fig. 6.2: The two levels of classification within the SDR family. At the first level the superfamily is divided into five families. At the second level, the members of classical and extended families are separated into seven and three subfamilies, respectively, based upon the pattern of the co-enzyme binding site residues (Kallberg *et al.*, 2002).

The sequenced genome of *H. pylori* 26695 identified a single putative *short chain alcohol dehydrogenase* gene (Hp0357), annotated in the TIGR (www.tigr.org) database. This will be referred to as HpSCADH from this point on. Since there is such a high level of diversity found in the SDRs, both on a genomic and a biochemical level, it is not possible to suggest a particular function based on the amino acid sequence comparison to other characterised SDRs. Therefore, to gain a better understanding of the role of this enzyme, HpSCADH was cloned, expressed in *E. coli* and an initial characterisation was performed in terms of its catalytic activity.

6.2 BLAST Analysis

A protein BLAST analysis (carried out on March 2007) revealed the highest sequence similarity with other putative short chain alcohol dehydrogenases and oxidoreductases from several different bacterial families. A ClustalW sequence alignment was constructed using the sequences with the highest identity (Table 6.1) Greatest identity to the HpSCADH was observed in *Helicobacter pylori* HPAG1 (96% identity), *Helicobacter pylori* J99 (96% identity), *Actinobacillus pleuropneumoniae* (62% identity), *Aeromonas hydrophila* (60% identity), short-chain alcohol dehydrogenase from *Haemophilus influenzae* (57% identity), oxidoreductase from *Haemophilus influenzae* (57% identity), and a probable NADP-dependent dehydrogenase from *Haemophilus influenzae* (57% identity).

6.3 Cloning of the *H. pylori* Short-chain Alcohol Dehydrogenase

6.3.1 Primer Design, PCR and Cloning of *HpSCADH* Gene

Oligonucleotides used for the amplification of the *HpSCADH* gene were designed using the putative *short chain alcohol dehydrogenase* gene sequence from *Helicobacter pylori* 26695, available at www.TIGR.org. The primers (Table 6.2) were designed to introduce an Nde I and BamH I restriction enzyme cleavage site at the N-terminus and C-terminus, respectively (Fig 6.3).

The entire *HpSCADH* gene was amplified by PCR using genomic DNA from *H. pylori* 26695 as template (genomic DNA was prepared as described in Materials and Methods, Chapter 2; section 2.11.2). PCR amplification of the *HpSCADH* gene from *H. pylori* 26695 is shown in Fig. 6.4. All PCR products were the expected size 750bp (as expected from the TIGR database).

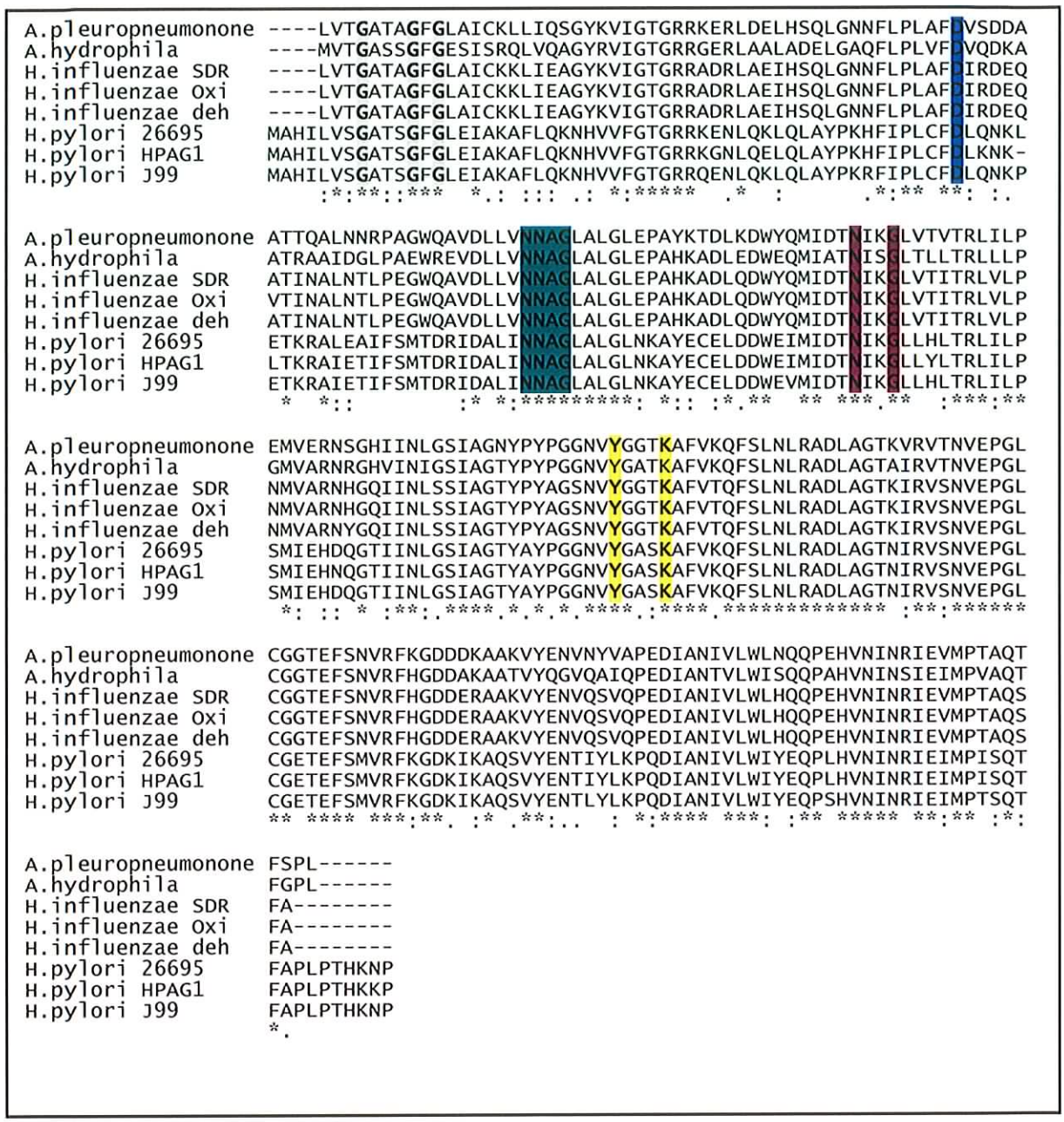

Table 6.1: ClustalW alignment illustrating the homology of related proteins to HpSCADH. Sequence similarity is indicated by (*) exact matches, (:) strong similarity, (.) weak similarity. SDR: Short chain reductase, Oxi: Oxidoreductase, Deh: dehydrogenase. N-terminal co-factor binding site (GxxxGxG) highlighted in grey, the active site (YxxxK) highlighted in yellow, a mid region conservation site (NNAG) highlighted in green, NxxG (highlighted in purple) is part of the active site and aspartic acid (highlighted in blue).

Primer direction	Primer sequence
Forward	5'-CGC-CAT-ATG- GCG CAC ATT-3' **Nde I**
Reverse	5'- CGC-GGA-TCC AGG GTT TTT ATG GGTG-3' **BamH I**

Table 6.2: Oligonucleotide primers designed for the amplification of the *HpSCADH* gene from *H. pylori* 26695.

CGCCATATGGCGCACATTTTAGTTAGCGGGGCGACTTCAGGGTTTGGATTAGAAATCGC
TAAAGCGTTTTTACAAAAAAACCATGTGGTTTTTGGCACAGGGAGGCGAAAAGAGAATTT
ACAAAAATTGCAACTCGCTTACCCTAAGCATTTCATTCCCTTGTGTTTTGATCTTCAAAAC
AAGCTTGAAACTAAGCGAGCGTTAGAGGCTATTTTTTCCATGACGGATCGCATTGACGC
TCTGATCAATAACGCCGGCTTAGCACTAGGCTTGAACAAGGCTTATGAATGCGAGTTAG
ACGACTGGGAAATCATGATAGATACGAATATCAAGGGGTTGTTGCATCTCACCCGCTTG
ATCTTGCCCTCTATGATAGAGCATGACCAAGGGACTATCATCAATCTTGGTTCTATCGCT
GGCACTTACGCCTATCCTGGAGGGAATGTCTATGGAGCGAGCAAGGCGTTTGTGAAAC
AATTTTCTTTAAATTTGCGAGCGGATTTGGCTGGCACTAACATTAGAGTGAGTAATGTTG
AACCCGGTTTGTGCGGCGAAACCGAATTCAGCATGGTGCGTTTTAAAGGCGATAAAATC
AAAGCCCAATCCGTCTATGAAAACACCATCTACCTCAAACCACAAGATATTGCTAACATC
GTGCTATGGATTTATGAACAACCCTTGCATGTCAATATCAACCGCATAGAAATCATGCCT
ATAAGCCAAACTTTCGCTCCCCTACCCACCCATAAAAACCCTTAA

Figure 6.3: Gene Sequence for HpSCADH. Primers used for the amplification of the gene are underlined. The inserted Nde I restriction enzyme cleavage site is highlighted in yellow. The inserted BamHI restriction enzyme cleavage site is highlighted in red.

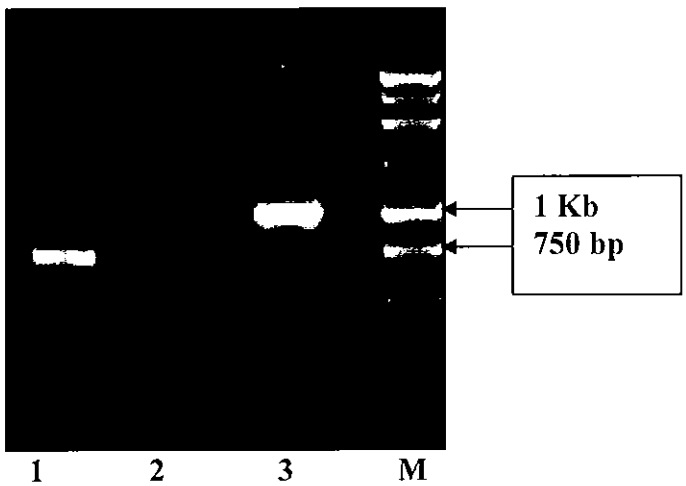

Fig. 6.4: Agarose (1 %) gel electrophoresis of the PCR products obtained by amplification of the *HpSCADH* gene from *H. pylori* strains 26695 using High Fidelity *Taq* polymerase (Roche) in lane 1. Lane 2 contains a negative control (contains no DNA) and lane 3 contains amplified HpCAD as the positive control. Lane M contains the DNA ladder. Amplification was carried out as described in Materials and Methods, section 2.6.4.

6.3.2 Generation of pET-HpSCADH Construct

The restriction sites introduced during primer design were also present in the multiple cloning site of the plasmid pET16(b) and would therefore allow for directional insertion. Following sequential restriction digests with Nde I and BamH I (Fig. 6.5). The amplified HpSCADH was directionally ligated into the cloning pET 16(b) plasmid. The resulting construct was designated pET-HpSCADH.

The transformants were again selected on the basis of ampicillin resistance conferred by the pET plasmid and screened for insertion of the amplified *HpSCADH* gene into the plasmid. Three constructs with an increase in size of approximately 750 bp were identified. Prior to DNA sequencing, PCR analysis was carried out on these three constructs using the SCADH primers (Table 6.2), in order to confirm the presence of the inserted *HpSCADH* gene (Fig. 6.6).

6.4 Expression and Purification of HpSCADH

6.4.1 Induction and Expression of HpSCADH protein

The pET-HpSCADH construct containing the cloned *HpSCADH* gene was transformed into *E. coli* BL21(DE3) *pLysS* for overexpression. Transformants were selected on the basis of dual ampicillin (50μg/ml) and chloroamphenicol (20 μg/ml) resistance. The transformants were screened to ensure uptake of the pET-HpSCADH construct (Material and Methods, Chapter 2, section 2.7.3). The HpSCADH synthesis in the *E. coli* BL21(DE3)*pLysS* cells harbouring the pET-HpSCADH construct was induced by addition of 1mM IPTG. IPTG was added when the bacterial culture reached an OD at 600nm of 0.6. Following addition of IPTG, the cells were incubated for 3 h at 37 °C and then a further 12 h at room temperature (to reduce the formation of inclusion bodies) before harvesting.

6.4.2 Purification of HpSCADH Protein

In general, a 600 ml culture of pET-HpSCADH transformed *E. coli* BL21(DE3)*pLysS* was prepared prior to purification of the protein. The His-tag, composed of 10 histidine residues, present on the N-terminus of the expressed HpSCADH protein facilitated one-step affinity purification on a nickel-charged iminodiacetic acid column. The purity of fractions collected was assessed using SDS-PAGE analysis. SDS gels were stained with Coomassie brilliant blue and showed a single band with a molecular mass of approx 27 kDa (Fig. 6.7).

The purified HpSCADH protein was dialysed against 50 mM KH_2PO_4 (pH 7.5). However, the majority of the protein precipitated out of solution. The addition of 5 mM DTT to the buffer had little effect on preventing precipitation. Optimisation of the purification for HpSCADH protein is currently being carried out by Carmel Cremin (Ph.D student, DIT). Table 6.3 outlines possible agents that may improve the stability of the HpSCADH.

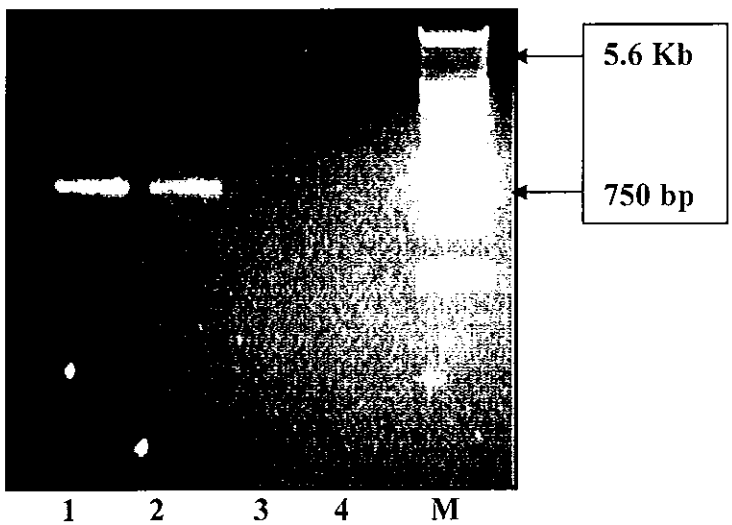

Fig. 6.5: 1% Agarose gel of *HpSCADH* gene and pET16b vector cut with *Nde1* and *BamH1* restriction enzymes. Lane 1 contains HpSCADH uncut. Lane 2 contains SCADH cut with BamH I and Nde I. Lane 3 contains pET16b uncut. Lane 4 contains pET16b cut with BamH I and Nde I. Lane M contains DNA ladder.

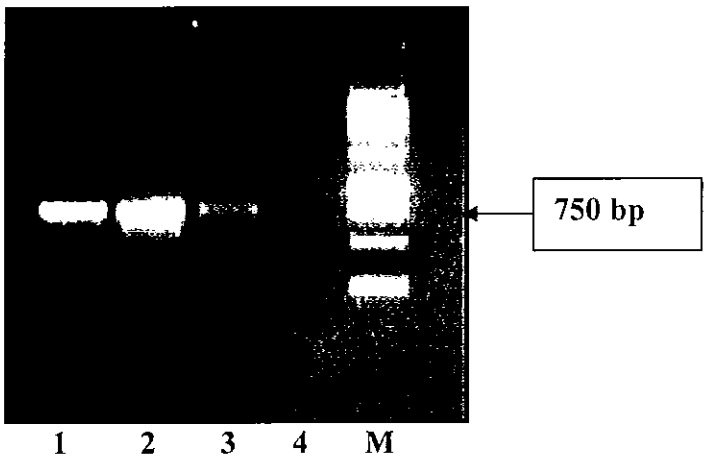

Fig. 6.6: 1% Agarose gel of amplified SCADH from transformants containing the pET-HpSCADH construct. Lanes 1-3 contain the amplified *HpSCADH* gene (750 bp). Lane 3 contains more than one product from the PCR and therefore was not used. Lane 4 contains the negative control. Lane M is the size marker.

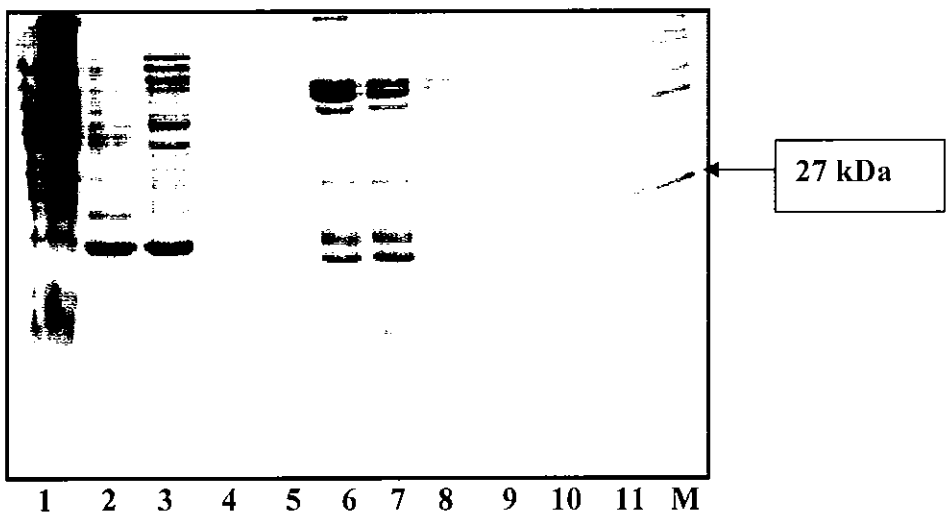

Fig. 6.7: 15% SDS-PAGE indicating the purity of recombinant HpSCADH eluted from the nickel-charged iminodiacetic acid column. Lane 1-3 shows the nickel column wash. Fractions 9-11 show a predominant species for the HpSCADH protein with an approximate molecular mass of 27 kDa after staining with Coomassie brilliant blue. Lane M contains the molecular weight markers.

Type of agent	Additive	Recommended conc range
Kosmotropes	$MgSO_4$	0-0.4M
	$(NH_4)_2SO_4$	0-0.3M
	NH_2SO_4	0-0.2M
	CS_2SO_4	0-0.2M
Weak Kosmotropes	NaCl	0-1M
	KCl	0-1M
Amino Acids	Glycine	0.5-2%
	L-arginine	0-5M
Sugars & polyhyrdic Alcohols	Sucrose	0-1M
	Glucose	0-2M
	Lactose	0.1-0.5M
	Ethylene glycol	0-60% v/v
	Xylitol	0-30%w/v
	Mannitol	0-15% w/v
	Inositol	0-10% w/v
	Sorbitol	0-40% w/v
	Glycerol	5-40% v/v
Detergents	Tween 80	0-0.2% w/v
	Tween 20	0-120 μM
	Nonidet P-40	0-1%

Table 6.3: List of potential agents that are used for stabilising protein (Bondos *et al.*, 2003)

6.5 Substrate Analysis of HpSCADH

The HpSCADH demonstrated activity towards 0.2 mM benzyl alcohol (Fig. 6.8) when assayed spectrophotometrically in a reaction mixture containing 0.2 mM benzyl alcohol, 0.2 mM NADP and 50 mM potassium phosphate buffer (pH 7.5). The assay was carried out at 37°C and carried out for 300 s.

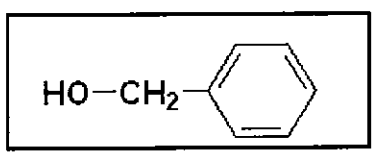

Fig. 6.8: Structure of benzyl alcohol

Michaelis constants were not calculated for the HpSCADH. However, the activity observed in the presence of benzyl alcohol shows that the enzyme is active as an alcohol dehydrogenase. Optimisation of the purification is required to ensure that there is sufficient protein in solution for kinetic analysis to be preformed using various alcohol and aldehyde substrates.

6.6 Discussion

This chapter describes the cloning, expression and preliminary characterisation of the HpSCADH. The BLAST analysis indicates that this protein shares a high amino acid identity (up to 96%) with other putative prokaryotic SCADHs. As expected there was a high sequence identity between various strains of *H. pylori* HPAG1 (96%) and J99 (96%).

The greatest identity from other non-*Helicobacter* prokaryotes was obtained for SCADHs from *Actinobacillus pleuropneumoniae* (62%), *Aeromonas hydrophila* (60%), short-chain alcohol dehydrogenase from *Haemophilus influenzae* (57%), oxidoreductase from *Haemophilus influenzae* (57%), and NADP-dependent dehydrogenase from *Haemophilus influenzae* (57%). However, these enzymes are putative and are not characterised in term of their biochemical activity. Therefore comparison of amino acid sequence to potentially assign a role that the *HpSCADH* gene may play within *H. pylori* is not possible.

The sequence alignment constructed (Table 6.1) illustrates that all short chain alcohol dehydrogenases/reductases conserved motifs are conserved in HpSCADH and the putative SCADHs identified by BLAST analysis. Such motifs (Table 6.1) include a N-terminal co-factor binding site (GxxxGxG) highlighted in grey (Jornvall *et al.*, 1999, van der Oost *et al.*, 2001), the active site (YxxxK) highlighted in yellow (Jornvall *et al.*, 1999, Kallberg *et al.*, 2001, Hasseleert *et al.*, 1996), and a mid region conservation site that stabilises the β-strand with the central β-sheet and positions the sheet (NNAG) highlighted in green (Terada *et al.*, 2000, Kallberg *et al.*, 2001).

From the sequence alignment (Table 6.1), HpSCADH can now be classified as a classical short chain alcohol dehydrogenase based on the following:

- The conserved motif NxxG (highlighted in purple) is part of the active site in classical SCADH.
- The presence of the aspartic acid at position 54 is part of the co-factor binding site (hightlighted in blue).
- HpSCADH is 250 residues in length, which is typical for the classical SCADHs (Kallberg *et al.*, 2002).

The *HpSCADH* gene was cloned into pET 16(b) vector and the pET:HpSCADH construct was transformed into *E. coli*. The protein was efficiently expressed in the presence of 1 mM IPTG. The purification and characterisation of HpSCADH protein is ongoing (Carmel Cremin, PhD student, DIT). Stabilisation of the protein is required to maintain high yields of the purified enzyme reproducibly to complete the kinetic profile of the enzyme. The addition of DTT to the dialysis buffer made little difference in preventing protein precipitation indicating that the oxidation of thiol groups is not a factor in the instability of the protein. Table 6.3 lists several agents used for the stabilisation of proteins however these agents would need to be assessed to ensure that they do not interfere with the enzyme's activity.

Sufficient quantity of purified enzyme was obtained to allow for preliminary spectrophotometric assays. The enzyme was shown to be active with benzyl alcohol as a substrate. This study demonstrates that the putative assignation on the TIGR database is correct and that the HpSCADH protein is active as a short chain alcohol dehydrogenase. Further studies with this enzyme are ongoing in this laboratory.

Chapter 7

General Discussion

7.0 General Discussion

This thesis describes the cloning, expression, purification and kinetic characterisation of an aldo keto reductase from *Helicobacter pylori* (HpAKR). The construction and characterisation of *H. pylori* isogenic HpAKR and HpCAD negative mutants are also described. Finally, the cloning, expression, purification and initial characterisation of a short chain alcohol dehydrogenase (HpSCADH) is described. Optimisation of the purification and substrate specificity studies of HpSCADH are part of ongoing research in this laboratory.

7.1 Cloning, Expression and Characterisation of HpAKR.

The pET cloning system was utilised as it provided an efficient system for expression and purification of the target HpAKR protein. The amount of AKR expressed was sufficient (6-8 mg) to assess substrate specificity for a wide range of aldehyde substrates. DNA sequencing of the cloned *HpAKR* gene, indicated the presence of nucleotide differences, at positions 425, C→G and 426, T→C from the sequence of this gene as published on the TIGR database. This difference gave rise to a protein with an amino acid change at residue 153, from leucine to alanine. This difference was observed on 3 separate occasions. The recombinant HpAKR was capable of aldehyde reducing activity even with this amino acid difference. Analysis of the HpAKR sequence showed that the alanine residue is not present on or close to any known conserved region of the AKRs (Jez *et al.*, 1997). It was therefore felt that it was unlikely to significantly affect activity of the enzyme.

The kinetic data illustrate that HpAKR has a preference for aromatic aldehydes. The K_m values estimated are relatively high. This suggests that HpAKR may be required to

operate over a wide range of aldehyde concentrations. The high K_m values would minimise the possibility of enzyme saturation. The K_{cat} for the general aldo keto reductase substrate, 4-nitrobenzaldehyde, was 416.9 S^{-1}. This K_{cat} was approximately 380 fold higher than that for the human succinic semialdehyde reductase (Schaller *et al.*, 1999), 175 fold higher than that for the *Saccharomyces cerevisae* AKR (Kuhn *et al.*, 1995), 35 fold higher than the pyridoxal reductase from *Schizosaccharomyces pombe*, (Nakano *et al.*, 1999) and 14 fold higher than that for the 2-methylbutyraldehyde reductase from *Saccharomyces cerevisiae* (Ford *et al.*, 2002). Thus, of the range of AKR enzymes studied to date it is clear that HpAKR is noteworthy for its high turnover. This high turnover may be further related to the need for the enzyme to catalyse reactions over a wide range of substrate concentrations.

As mentioned previously, HpAKR was assigned membership of the 13th AKR family and was named AKR13C1. The other two family members, *YakC* protein from *S. pombe* (AKR13A1) and the AKR from *Xyella fastidiosa* (AKR13B1), have also been characterised. Comparison of the three family members is difficult due to the limited kinetic data available for AKR13A1 and AKR13B1. However, the other family members demonstrated a more limited substrate specificity profile than HpAKR. The Michaelis constants estimated for HpAKR clearly indicate that the enzyme reduces a wider range of aldehydes with a higher efficiency ($K_{cat}/_{Km}$) than the other members of the AKR13 family. It is noteworthy that AKR13B1 is capable of reducing glyceraldehyde unlike the other two family members, HpAKR and AKR13A1 (Rosselli *et al.*, 2006).

7.2 Comparison of Oxidoreductases in *H. pylori*

The *H. pylori* cinnamyl alcohol dehydrogenase (HpCAD) was the first oxidoreductase to be characterised in this laboratory (Mee *et al.*, 2005). As expected, the HpCAD demonstrated a substrate preference for cinnamyl alcohol and cinnamyl aldehyde as well as coniferyl alcohol and coniferyl aldehyde although there was an approximately 4-fold decrease in activity for the latter substrates.

It is worth noting that both HpAKR and HpCAD reduced aromatic aldehydes such as benzaldehyde. Both enzymes demonstrated a high efficiency for this substrate and it was the only aldehyde, of those studied that was reduced by both enzymes. HpAKR did not display activity towards any of the other aldehydes employed in the HpCAD study (Mee *et al.*, 2005) indicating that there was little redundancy between these proteins.

The activity exhibited by the two enzymes reveals that the organism may possess more than one pathway by which a broad range of aldehydes can be reduced and thus has implications for the theory proposed by other workers, that toxic aldehydes might contribute to the pathogencity of *H. pylori* (See Chapter 1, Section 1.1.5).

7.3 Acid Stress of *H. pylori* Isogenic HpAKR Negative Mutant.

A direct disruption of the *HpAKR* gene was undertaken to gain insight into the functional role the protein plays in the bacterium. A previous report in the literature had suggested the *HpAKR* gene might play a role in acid adaptation. It was also suggested that HpAKR was required when exposure to an acidic environment was chronic (Bijlsma *et al.*, 2000). Since a direct disruption of the *HpAKR* gene was not carried out previously, a definite functional role in acid adaptation could not be confirmed. Therefore, in this study the isogenic HpAKR negative mutant was exposed to

environments at different pH values and growth profiles over a period of 48 h were examined.

The findings from this study illustrate that HpAKR is essential for the growth of *H. pylori* in an acidic environment. Differences in growth profiles at pH 5.5 clearly indicate that the growth of the HpAKR mutant is severely compromised (Fig. 5.17b), in comparison with the wild type strain. The difference in growth rates at this pH is thought to be especially significant since the pH of the gastric mucosa is believed to be between pH 4.0 and 6.5 (Bijlsma *et al.*, 2002) and it has been suggested that the bacteria are exposed to the occasional acid shock as low as pH 2.0 (Bijlsma *et al.*, 2002 and Schreiber *et al.*, 2005).

The addition of urea to the acidic medium resulted in a restoration of "normal" growth profile and an increase in pH, to approximately pH 7.0, which was attributed to the production of ammonia as a result of urease activity.

These findings indicate that inhibition of HpAKR may represent a potential therapeutic target in the treatment of *H. pylori* infection. The departure from Michaelis-Menten kinetics observed by the recombinant HpAKR in the presence of sodium valproate is an interesting insight that could ultimately influence the design of inhibitors for the protein.

7.4 Acid Stress of *H. pylori* Isogenic HpCAD Negative Mutant

It was reported in the literature that HpCAD was up regulated 24-fold on exposure to acidic conditions (Ang *et al.*, 2001). The isogenic HpCAD negative mutant was also exposed to different acidic environments and growth monitored. From this study, it became apparent that the absence of the HpCAD conferred a growth advantage on the HpCAD mutant at acidic pH. The growth of the wild type strain was compromised at pH 5.5 while the HpCAD mutant showed a higher growth rate at this pH (Fig. 5.21b).

It is not yet clear how the absence of the CAD enzyme could yield a more acid tolerant phenotype. Several aspects need to be considered in relation to these findings. For example, it may be that CAD is involved indirectly in modulating intracellular pH. This could be investigated by measuring the intracellular pH of *H. pylori* in the HpCAD mutant under different acidic conditions. Any deviation in intracellular pH homeostasis observed, when compared to the wild type could then be attributed to HpCAD.

Interestingly, knocking out the *CAD* gene resulted in a reduction in growth rate at each pH tested after 36 h in *culture* with the exception of growth at pH 5.0. The reason for this is not known however it is possible that by knocking out the CAD protein, an accumulation of aldehydes, normally reduced to the less toxic alcohols, by this enzyme, might be exerting a toxic effect on the bacterium.

To probe the role that HpAKR and HpCAD play, an animal model of infection would be of great interest. Since HpAKR plays such an important role in acid adaptation, an animal model would indicate whether the HpAKR mutant could withstand the initial acid shock in the stomach and colonise the gastric mucosa. With regard to the HpCAD mutant, determining the severity and duration of the *H. pylori* infection would be essential since the absence of the *CAD* gene appears to confer a growth advantage on *H. pylori*, at least *in vitro*. *In vivo,* where there is ample gastric urea available to neutralise the microenvironment of the bacterium, it would be of interest to assess whether this growth advantage would be found for the HpCAD mutant. Co-infection of an animal model with both the HpCAD mutant with the parental strain would also demonstrate the ability of the HpCAD mutant to outgrow the parental strain.

7.5 Preliminary Characterisation of *H. pylori* SCADH

Preliminary studies on the *H. pylori* short chain alcohol dehydrogenase (HpSCADH) have been carried out. The purification is being optimised as part of ongoing research in this laboratory. This study confirms that the HpSCADH is an active alcohol dehydrogenase.

7.6 Future Work

Future work in this laboratory will concentrate on the characterisation of the short chain alcohol dehydrogenase along with a knockout of this protein. Generation of a mutant lacking a combination of some or all of these oxidoreductases in *H. pylori* will determine which of these enzymes are essential to the survival of the bacterium. Animal studies would provide important information regarding the ability of these isogenic mutants to colonise the gastric mucosa *in vitro*.

References

Alakomi HL, Paananen A, Suihko ML, Helander IM, and Saarela M. 2006. Weakening Effect of Cell Permeabilizers on Gram-Negative Bacteria Causing Biodeterioration. Applied and Environmental Microbiology **72**: 4695-4703.

Ando T, Israel DA, Kusugami K, and Blaser MJ. 1999. HP0333, a member of the dprA family, is involved in natural transformation in *Helicobacter pylori*. Journal of Bacteriology **181**: 5572-5580.

Andrzejewska J, Lee SK, Olbermann P, Katzowitsch E, Linz B, Achtman M, Kado CI, Suerbaum S, and Josenhans C. 2006. Characterisation of the Pilin Orthology of the *Helicobacter pylori* Type IV *cag* Pathogenicity Apparatus, a Surface-Associated Protein Expressed during Infection. Journal of Bacteriology **188**: 5865-5877.

Ang S, Lee CZ, Peck K, Sindici M, Matrubutham U, Gleeson MA, and Wang JT. 2001. Acid-induced gene expression in *Helicobacter pylori*: study in genomic scale by microarray. Infection and Immunity **69**: 1679-1686.

Arslanian MJ Pascoe, and Reinhold JG. 1971. Rat Liver Alcohol Dehydrogenase: Purification and Properties. Biochemical Journal **125**: 1039-1047.

Athmann C, Zeng N, Kang T, Marcus EA, Scott DR, Rektorschek M, Buhmann A, Melchers K, and Sachs G. 2000. Local pH elevation mediated by the intrabacterial urease of *Helicobacter pylori* cocultured with gastric cells. Journal of Clinical Investigation **106**: 339-347.

Bijlsma JJE, Lie-A-Ling M, Nootenboom IC, Vandenbroucke-Grauls CMJE, and Kusters JG. 2000. Identification of the loci essential for growth of *Helicobacter pylori* under acidic conditions. Journal of Infectious Disease **182**: 1566-1569.

Bijlsma JJE, Waidner B, van Vliet AHM, Hughes NJ, Hag S, Bereswill S, Kelly DJ, Vandenbroucke-Grauls CMJE, Kist M, and Kusters J. 2002. The *Helicobacter pylori* Homologue of the Ferric Uptake Regulator is Involved in Acid Resistance. Infection and Immunity **70**: 606-611.

Billard P, Menart S, Fleer R, and Bolotin-Fukuhara M. 1995. Isolation and characterization of the gene encoding xylose reductase from Kluyveromyces lactis. Gene **162**: 93-97.

Bondos SE, and Bickenell. 2003. Detection and prevention of protein aggregation before, during , and after purification. Analytical Biochemistry **316**: 223-231.

Bradford MM. 1976. A rapid and sensitive method for the quantitation of microgram quantities of protein utilizing the principle of protein-dye binding." Anal Biochem **72**: 248-254.

Busler VJ, Torres VJ, McClain S, Tirado O, Friedman DB, and Cover TL. 2006. Protein-protein Interaction among *Helicobacter pylori* Cag Proteins. Journal of Bacteriology **188**: 4787-4800.

Chang Q, Harter TM, Rikimaru LT, and Petrash JM. 2003. Aldo-keto reductase as modulators of stress response. Chemico-Biological Interactions **143-144**: 325-332.

Clyne M, Labigne A, and Drumm B. 1995. *Helicobacter pylori* required an acidic environment to survive in the presence of urea. Infection and Immunity **63**: 1669-1673.

Colrat S, Latche A, Guis M, Pech JC, Bouzayen M, J, Fallot, and Roustan JP. 1999. Purification and characterisation of a NADPH-dependent aldehyde reductase from Mung Bean that detoxifies Eutypine, a toxin from *Eutypa lata*. Plant Physiologuy. **119**: 621-626.

Covacci A, Telford JL, Del Giudice G, Parsonnet J, and Rappuoli R. 1999. *Helicobacter pylori* virulence and genetic geography. Science **284**1328-1333.

Cromlish JA, and Flynn TG. 1983. Purification and Characterisation of Two Aldose Reductase Isoenzymes from Rabbit Muscle. Journal of Biological Chemistry **258**: 3416-3424.

Crowe SE. 2005. *Helicobacter* infection, chronic inflammation, and the development of malignancy. Current Opinion in Gastroenterology **21**: 32-38.

De Jongh KS, Schofield PJ, and Edwards MR. 1987. Kinetic mechanism of sheep liver NADPH-dependent aldehyde reductase. Biochemical Journal **242**: 143-150.

Dzieniszewski J, and Jarosz M. 2006. Cuidelines in the Medical Treatment of *Helicobacter pylori* Infection. Journal of Physiology and Pharmacology **3**: 143-154.

Ellis EM. 2002. Microbial aldo-keto reductases. FEMS Microbiology Letters **216**: 123-131.

Ellis EM, and Hayes JD. 1995. Substrate specificity of an aflatoxin-metabolising aldehyde reductase. Biochemical Journal **312**: 535-541.

Ellis EM, Judah DJ, Neal GE, and Hayes JD. 1993. An Ethoxyquin-Inducible Aldehyde Reductase from Ra Liver that Metablioses Aflatoxin B_1 defines a subfamily of aldo-keto reductases. Proceeding of the National Academy of Sciences **90**: 10350-10354.

Ferrero RL, Cussac V, Courcoux P and Labigne A. 1992. Construction of Isogenic Urease-Negative Mutants of *Helicobacter pylori* by Allelic Exchange. Journal of Bacteriology. **174**: 4212-4217.

Ford G, and Ellis EM. 2002. Characterisation of Yprlp from *Saccharomyces cerevisiae* as a 2-methylbuytaldehyde reductase. Yeast **19**: 1087-1096.

Foynes S, Dorrell N, Ward SJ, Stabler RA, McColm AA, Rycroft AN, and Wren BW. 2000. *Helicobacter pylori* possesses two CheY response regulators and a histidine kinase sensor, CheA, which are essential for chemotaxis and colonization of the gastric mucosa. Infection and Immunity **68**: 2016-2023.

Garza-Gonzalez E, Bosques-Padilla FJ, Perez-Perez GI, Flores-Gutierrez JP, and Tijerina-Menchaca R. 2004. Association of gastric cancer, HLA-DQA1, and infection with *Helicobacter pylori* CagA+ and VacA+ in a Mexican population. Journal of Gastroenterology **39**: 1138-1142.

Gavidia I, Perez-Bermudez P, and Seitz HU. 2002. Cloning and expression of two novel aldo keto reductases from Digitalis purpurea leaves. European Journal of Biochemistry **269**: 2842-2850.

Gobert AP, Mersey BD, Cheng Y, Blumberg DR, Newton JC, and Wilson KT. 2002. Cutting edge: urease release by *Helicobacter pylori* stimulates macrophage inducible nitric oxide synthase. Journal of Immunology **168**: 6002-6006.

Goodwin A, Kersulyte D, Sisson G, Veldhuyzen van Zanten SJ, Berg DE, and Hoffman PS. 1998. Metronidazole resistance in *Helicobacter pylori*is due to null mutations in a gene (rdxA) that encodes an oxygen-insensitive NADPH nitroreductase. Molecular Microbiology **28**: 383-393.

Grant AW, Steel G, Waugh H, and Ellis EM. 2002. A novel aldo-keto reductase from *Escherichia coli* can increase resistance to methylglyoxal toxicity. FEMS Microbiology Letters **218**: 93-99.

Habrych M, Rodriguez S, and Stewart JD. 2002. Purification and identification of an Escherichia coli beta-keto ester reductase as 2,5-diketo-D-gluconate reductase YqhE. Biotechnology Progress **18**: 257-261.

Haeseleert F, Huang J, Lebioda L, Saari JC, and Palczewski K. 1998. Molecular Characterisation of a novel Short-Chain Dehydrogenase /Reductase that Reduces All-*trans*-rentinal. Journal of Biological Chemistry **273**: 21790-21799.

Hardin FJW, and R.A. 2002. *Helicobacter pylori:* review and Update. Hospital Physician **38**: 23-31.

Harlow ELD. 1998. Antibodies: A Laboratory Manual. Cold Spring Harbor Laboratory Press. Cold Spring Harbor: NY.

Hinshelwood A, McGarvie G, and Ellis EM. 2003. Substrate specificity of mouse aldo-keto reductase AKR7A5. Chemical Biological Interacteractions **143**: 263-269.

Hinshelwood A, McGarvie G, and Ellis EM. 2002. Characterisation of a novel mouse liver aldo-keto reductase AKR7A5. FEBS Letters **523**: 213-218.

Hu LT, Foxall PA, Russell R, and Mobley HL. 1999. Purification of recombinant *Helicobacter pylori* urease apoenzyme encoded by ureA and ureB. Infection and Immunity **60**: 2657-2666.

Hyndman D, Bauman DR, Heredia VV and Penning TM. 2003. The aldo-keto reductase superfamily homepage. Chemico-Biological Interactions **143-144**: 621-631.

Ishikura S, Horie K, Sanai M, Matsumoto K, and Hara A. 2005. Enzymatic properties of a member (AKR1C19) of the aldo-keto reductase family. Biological & Pharmaceutical Bulletin **28**: 1075-1078.

Itoh N, Asako H, Banno K, Makino Y, Shinihara M, Dairi T, Wakita R, and Shimiz M. 2004. Purification and characterisation of NADPH-dependent aldo-keto reductase specific for ß-keto esters from Penicillium citrinum, and production of methyl (S)-4-bromo-3-hydroxybutyrate. Applied Microbiological Biotechnology **66,**: 53-62.

Jacobson K, Chiba N, Chen Y, Barrientos M, James C, Riddell RH, and Hunt RH. 2001. Gastric acid secretory response in *Helicobacter pylori*-positive patients with duodenal ulcer disease. Candian Journal of Gastroenterology **15**: 29-39.

Janas B, Czkwianianc E, Bak-Romaniszyn L, Bartel H, Tosik D, and Planeta-Malecka I. 1995. Electron microscopic study of association between coccoid forms of *Helicobacter pylori* and gastric epithelial cells. The American Journal of Gastroentrology **90**: 1829-1833.

Jez J, and Penning TM. 2001. The Aldo-Keto Reductase (AKR) superfamily: an update. Chemico-Biological Interactions **130-132**: 499-525.

Jez JM, Bennett MJ, Schlegel BP, Lewis M and Penning TM. 1997. Comparative anatomy of the aldo-keto reductase superfamily. Biochemical Journal **326**: 625-636.

Jornvall H, Hoog JO, and Persson B. 1999. SDR and MDR: completed genome sequences show these protein families to be large, of old origin, and of complex nature. FEBS Letters **445**: 261-264.

Judah DJ, Hayes JD, Yang JC, Lian LY, Roberts GCK, Farmer PB, Lamb JH, and Neal GE. 1993. A Novel Aldehyde Reductase with Activity towads a metabolite of aflatoxin B1 is expressed in rat liver during carcinogenesisand following administration of an anti-oxidant. Biochemical Journal **292**: 13-18.

Kaihovaara P, Salmela KS, Roine RP, Kosunen TU, Salaspuro M. 1994. Purification and characterization of *Helicobacter pylori*alcohol dehydrogenase. Alcoholism: Clinical and Experimental Research **18**: 1220-1225.

Kallberg Y, Opperman U Jornvall H and Persson B. 2002. Short-Chain dehydrogenase/reductase (SDRs): Co-enzyme -based functional assigments in completed genomes. European Journal of Biochemistry **269**: 4409-4417.

Kallberg Y, Oppermann U, Jornvall H and Persson B. 2001. Short-chain dehydrogenase/reductase (SDR) relationship: A large family with eight clusters common to human, animal and plant genomes. Protein Science **11**: 636-641.

Kanazu T, Shinoda M, Nakayama T, Deyashiki Y, Hara A, and Sawada H. 1991. Aldehyde reductase is a major protein associated with 3-deoxyglucosone reductase activity in rat, pig and human livers. Biochemical Journal **279**: 903-906.

Karaca C, Guler N, Yazar A, Camlica H, Demir K, and Yildirim G. 2004. Is lower socio-economic status a risk factor for *Helicobacter pylori* infection in pregnant women with hyperemesis gravidarum? Turkish Journal of Gastroenterology **15**: 86-89.

Keenan J, Day T, Neal S, Cook B, Perez-Perez G, Allardyce R and Bagshaw P. 2000. A role for the bacterial outer membrane in the pathogenesis of *Helicobacter pylori*infection. FEMS Microbiology Letters **182**: 259.

Knight LP, Primiano T, Groopman JD, Kensler TW, and Sutter TR. 1999. cDNA cloning, expression and acticty of second human aflatoxin B1-metabloising member of the aldo-keto reductase superfamily, AKR7A3. Carcinogenesis **20**: 1215-2223.

Ko J, Kim I, Yoo S, Min B, Kim K, and Park C. 2005. Conversion of methylglyoxal to acetol by *Escherichia coli* aldo-keto reductases. Journal of Bacteriology **187**: 5782-5789.

Krah A, Miehlke S, Pleissner KP, Zimmy-Arndt U, Kirsch C, Lehn N, Meyer TF, Jungblut PR, and Aebischer T. 2004. Identification of candidate antigens for serologic detection of *Helicobacter pylori*- infected patients with gastric carcinoma. International Journal of Cancer **108**: 456-463.

Kubiseski TJ, and Flynn G. 1995. Studies on human aldose reductase probing the role of arginine 268 by site directed mutagenesis. The Journal of Biological Chemistry **270**: 16911-16717.

Kuhn A, Zyl C, Tonder AV and Prior BA 1995. Purification and partial characterisation of an aldo-keto reductase from *Saccharomyces cerevisiae*. Applied and Environmental Microbiology: 1580-1585.

Kuipers EJ, Israel DA, Kusters JG, and Blaser MJ. 1998. Evidence for a conjugation-like mechanism of DNA transfer in *Helicobacter pylori*. Journal of Bacteriology **180**: 2901-2905.

Kusters JG, van Vliet AHM, and Kuipers EJ. 2006. Pathogenesis of *Helicobacter pylori* Infection. Clinical Microbiology Reviews **19**: 449-490.

Laemmli UK. 1970. Cleavage of structural proteins during the assembly of the head of bacteriophage T4. Nature **227: 680-685**.

Lee JK, Koo BS, and Kim SY. 2003. Cloning and Characterisation of the *xyl1* Gene, Encoding an NADH-Preferring Xylose Reductase from *Candida parapsilosis*, and its Functional Expression in *Candida tropicalis*. Applied and Environmental Microbiology **69**: 6179-6188.

Leunk RD, Johnson PT, David BC, Kraft WG, and Morgan DR. 1988. Cytotoxic activity in broth-culture filtrates of Campylobacter pylori. Journal of Medical Microbiology **26**: 93-99.

Li Y, Wandinger-Ness A, Goldenring JR, and Cover TL. 2004. Clustering and redistribution of late endocytic compartments in response to *Helicobacter pylori* vacuolating toxin. Molecular Biology Cell **15**:1946-1959.

Machielsen R, Uria AR, Kengen SWM, and Van der Oost J. 2006. Production and characterisation of a thermostable alcohol dehydrogenase that belongs to the aldo-keto reductase superfamily. Applied and Environmental Microbiology **72**: 233-238.

Magonet E, Hayen P, Delforge D, Delaive E, and Remacle J. 1997. Importance of the Structural Zinc-Atom for the Stability of Yeast Alcohol Dehydrogenase. Biochemical Journal **287**: 361-365.

Marais A, Mendz GL, Hazell SL, and Megraud F. 1999. Metabolism and genetics of Helicobacter pylori: the genome era. Microbiol Mol Biol Rev **63**: 642-674.

Marshall B. 2002. *Helicobacter pylori*: 20 years on. Clinical Medicine **2**: 147-152.

Marshall BJ, and Warren JR. 1984. Unidentified curved bacilli in the stomach of patients with gastritis and peptic ulceration. Lancet **1**: 1311-1315.

Marshall BJ, Armstrong JA, McGechie DB, and Glancy RJ. 1985. Attempt to fulfil Koch's postulates for pyloric *Campylobacter*. The Medical Journal of Australia **142**: 436-439.

Martin HJ, Breyer-Pfaff U, Wsol V, Venz S Block S, and Maser E. 2006. Purification and Characterisation of AKR1B10 from Human Liver: Role in Carbonyl Reduction of Xenobiotics. Drug Metabolism and Disposition **34**: 464-470.

Martino MC, Stabler RA, Zhang ZW, Farthing MJ, Wren BW, Dorrell N. 2001. *Helicobacter pylori* pore-forming cytolysin orthologue TlyA possesses *in vitro* hemolytic activity and has a role in colonization of the gastric mucosa. Infection and Immunity **69**: 1697-1703.

Maruyama R, Nishizawa M, Itoi Y, Ito S, and Inoue M. 2002. The enzyme with benzil reductase activity conserved from bacteria to mammals. Journal of Biotechnology **94**: 157-169.

Matsumoto K, Endo S, Ishikura S, Matsunaga T, Tajima K, El-Kabbani O, and Hara A. 2006. Enzymatic properties of a member (AKR1C20) of the Aldo-Keto Reductase Family. Biological & Pharmaceutical Bulletin **29**: 539-542.

Matsunaga T, Shintani S and Hara A. 2006. Multiplicity of Mammalian Reductases for Xenobiotic Carbonyl Compound. Drug Metabolism Pharmacokinetics **21**: 1-18.

Matysiak-Budnik T, Karkkainen P, Methuen T, Roine RP, Salaspuro M. 1995. Inhibition of gastric cell proliferation by acetaldehyde. Journal of Pathology **177**: 317-322.

McGee DJ, Radcliff FJ, Mendz GL, Ferrero RL, and Mobley HL. 1999. *Helicobacter pylori* rocF is required for arginase activity and acid protection *in vitro* but is not essential for colonization of mice or for urease activity. Journal of Bacteriology **181**: 7314-7322.

Mee B, Kelleher D, Frias J, Malone R, Tipton KF, Henehan GT, and Windle HJ. 2005. Characterization of cinnamyl alcohol dehydrogenase of *Helicobacter pylori*. An aldehyde dismutating enzyme. FEBS Journal **272**: 1255-64.

Menaker RJ, Sharaf AA, and Jones NL. 2004. *Helicobacter pylori* infection and gastric cancer: host, bug, environment, or all three? Current Gastroenterology Report **6**: 429-435.

Merrel DS, Goodrich ML, Otto G, Tompkins LS, and Falkow S. 2003. pH Regaulated Gene Expression of the Gastric Pathogen *Helicobacter pylori*. Infection and Immunity **71**: 3529-3539.

Mine T, Muraoka H, Saika T, and Kobayashi I. 2005. Characteristics of a clinical isolate of urease-negative *Helicobacter pylori* and its ability to induce gastric ulcers in Mongolian gerbils. Helicobacter **10**: 125-131.

Morita T, Huruta T, Ashiuchi M, and Yagi T. 2002. Characterization of recombinant YakC of *Schizosaccharomyces pombe* showing YakC defines a new family of aldo-keto reductases. Journal of Biological Chemistry **132**: 635-641.

Murata- Kamiya N, and Kamiya H. 2001. Methylglyoxal, an endogenous aldehyde, crosslinks DNA polymerase and the substrate DNA. Nucleic Acid Research **29**: 3433–3438.

Nagai T, and Oita S. 2004. Anti-*Helicobacter pylori*activty of EDTA. Journal of General Appllied Microbiolgy **50**: 115-118.

Nakano M, Morita T, Yamamoto T, Sano H, Ashiuchi M, Masui R, Kuramitsu S, and Yagi T. 1999. Purification, molecular cloning and catalytic activity of *Schizosaccharomyces pombe* pyridoxal reductase. Journal of Biological Chemistry **274**: 23185-23190.

Nirag C, Siegal GP, Klemm K, Atkinson BF, and Jhala DN. 2003. Infiltration of *Helicobacter pylori* in the Gastric Mucosa. American Journal of Clinical Pathology **119**: 101-106.

Prinz C, Hafsi N, and Voland P. 2003. *Helicobacter pylori* virulence factors and the host immune response: implications for therapeutic vaccination. TIM **11**: 134-138.

Prinz C, Schwendt S, and Voland P. 2006. *H. pylori* and Gastric Cancer: Shifting the global burden. World Journal of Gastroenterology **12**: 5458-5464.

Roine RP, Salmela KS, Hook-Nikanne J, Kosunen TU and Salaspuro M. 1992. Alcohol dehydrogenase mediated acetaldehyde production by Helicobacter pylori--a possible mechanism behind gastric injury. Life Science **51**: 1333-1337.

Rosselli LK, Oliveira LP, Azzoni AR, Tada SFS, Catani CF, Saraiva AM, Soares JS, Medrano FJ, Torriani IL, and Souza AP. 2006. A new member of the aldo-keto reductase family from the plant pathogen *Xylella fastidiosa*. Archives of Biochemistry and Biophysics **453**: 143-50.

Salaspuro V and Salaspuro M. 2004. Synergistic effect of alcohol drinking and smoking on *in vivo* acetaldehyde concentration in saliva. International Journal of Cancer **111**: 480-483.

Salmela KS, Roine RP, Koivisto T, Hook-Nikanne J, Kosunen TU, Salaspuro M. 1993. Characteristics of *Helicobacter pylori*alcohol dehydrogenase. Gastroenterology **105**: 325-330.

Salmela KS, Sillanaukee P, Itala L, Vakevainen S, Salaspuro M, and Roine RP. 1997. Binding of acetaldehyde to rat gastric mucosa during ethanol oxidation. Journal of Laboratory Clinical Medicine **129**: 627-33.

Sambrook JF and Maniatis EF. Ed. 1989. Molecular Cloning. A laboratory Manual, 2nd Edition, Cold Spring Harbor Laboratory Press Cold Spring Harbor NY.

Sanli G, Dudley JI, and Blaber M. 2003. Structural Biology of the Aldo-Keto Reductase Family of Enzymes. Cell Biochemistry and Biophysics **38**: 79-101.

Schaller M, Schaffhauser M, Sans N, and Wermuth B. 1999. Cloning and Expression of Succinic Semialdehyde Reductase from Human Brain. European Journal of Biochemistry **265**: 1056-1060.

Schreiber S, Bucker R, Groll C, Azevedo-Vethacke M, Garten D, Scheid P, Friedrich S, Gatermann S, Josenhans C, and Suerbaum S. 2005. Rapid loss of motility of *Helicobacter pylori* in the gastric lumen *in vivo*. Infection and Immunity **73**: 1584-1589.

Schreiber S, Konradt M, GRoll C, Scgeid P, Hanauer G, Werling HO, Josenhans C, and Suerbaum S. 2004. The Spatial Orientation of *Helicobacter pylori* in the Gastric Mucus. PNAS **101**: 5024-5029.

Sekar V 1987. A rapid screening procedure for the identification of recombinant bacterial clones. BioTechniques **5**: 11-13.

Selbach M, Moese S, Hauck CR, Meyer TF, and Backert S. 2002. Src Is the Kinase of the *Helicobacter pylori* CagA Protein *in vitro* and *in vivo*. Journal of Biological Chemistry **277**: 6775-6778.

Shimatani T, Inoue M, Iwamoto K, Hyogo H, Yokozaki M, Saeki T, Tazuma S, Horikawa Y, and Harada N. 2005. Gastric acidity in patients with follicular gastritis is significantly reduced, but can be normalized after eradication for *Helicobacter pylori*. *Helicobacter pylori* **10**: 256-265.

Shirin H, Levine A, Shevah O, Shabat-Sehayek V, Aeed H, Wardi J, Birkenfeld S, Eliakim R, and Avni Y. 2005. Eradication of *Helicobacter pylori* Can Be Accurately Confirmed 14 Days after Termination of Triple Therapy Using a High-Dose Citric Acid-Based C Urea Breath Test. Digestion **71**: 208-212.

Slonczweski JL, McGee DJ, Phillips J, Kirkpatrick C, and Mobley HLT. 2000. pH-Dependent Protein Profiles of *Helicobacter pylori* Analysed by 2-Dimensional Gels. *Helicobacter* **5**: 240.

Smeets LC, Bijlsma JE, Boomkens SY, Vandenbroucke-Grauls CM and Kusters JG. 2000. *comH*, a novel gene essential for natural transformation of *Helicobacter pylori*. Journal of Bacteriology. **182**: 3948-3954.

Spycher SE, Tabataba-Vakili S, O'Donnell VB, Palomba L, and Azzi A. 1997. Aldose reductase induction: a novel response to oxidative stress of smooth muscle cells. The Federation of American Societies for Experimental Biology **11**: 189-198.

Srivastava SK, Ramana KV, and Bhatnagar A. 2005. Role of Aldose Reductase and Oxidative Damage in Diabetes and the Consequent Potential for Therapeutic Options. Endocrine Reviews **26**: 380-392.

Stingl K, Uhlemann EM, Deckers-Hebestreit G, Schmid R, Bakker EP, and Altendorf K. 2001. Prolonged Survival and Cytoplasmic pH Homeostasis of *Helicobacter pylori* at pH 1. Infection and Immunity **69**: 1178-1180.

Terada T, Sugihara Y, Nakamura K, Sato R, Inazu N, and Maeda M. 2000. Cloning and Bacterial Expression of Monomeric Short-Chain Dehydrogenase (Carbonyl Reductase) from CHO-K1 cells. European Journal of Biochemistry **267**: 6849-6857.

Thiele GM, Duryee MJ, Willis MS, Sorrell MF, Freeman TL, Tuma DJ, Klassen LW. 2004. Malondialdehyde-acetaldehyde (MAA) modified proteins induce pro-inflammatory and pro-fibrotic responses by liver endothelial cells. Comparative Hepatology **3**: Suppl 1: S25.

Todaka T, Yamano S, and Toki S. 2000. Purification and characterisation of NAD-dependent morphine-6-dehydrogenase from hamster liver cytosol, a new member of the aldo-keto reductase superfamily. Archives of Biochemistry and Biophysics **374**: 189-197.

Tomb JF, White O, Kerlavage AR, Clayton RA, Sutton GG, Fleischmann RD, Ketchum KA, Klenk HP, Gill S, Dougherty BA, Nelson K, Quackenbush J, Zhou L, Kirkness EF, Peterson S, Loftus B, Richardson D, Dodson R, Khalak HG, Glodek A, McKenney K, Fitzegerald LM, Lee N, Adams MD, Hickey EK, Berg DE, Gocayne JD, Utterback TR, Peterson JD, Kelley JM, Cotton MD, Weidman JM, Fujii C, Bowman C, Watthey L, Wallin E, Hayes WS, Borodovsky M, Karp PD, Smith HO, Fraser CM, and Venter JC. 1997. The complete genome sequence of the gastric pathogen *Helicobacter pylori*. Nature **388**: 539-547.

Towbin H, Staehelin T, and Gordon J. 1979. Electrophoretic transfer of Protein from Polyacrylamide Gels to Nitrocellulose sheets: Procudure and some applications. PNAS **79**: 4350-4354.

Tsuda M, Karita M, Morshed MG, Okita K, and Nakazawa T. 1994. A urease-negative mutant of *Helicobacter pylori* constructed by allelic exchange mutagenesis lacks the ability to colonize the nude mouse stomach. Infection and Immunity **62**: 3586-3589.

Van der Oost J, Voorhorst WGB, Kengen SWM, Geerlng ACM, Wittenhorst V, Gueguen Y and de Vos M. 2001. Genetic and biochemical characterisation of a short chain alcohol dehydrogenase from the hyperthermophilliv archaeon *Pyrococcus furiosus*. European Journal of Biochemistry **268**: 3062-3068.

Verduyn C, Van Kleef R, Frank J, Schreuder H, Van Dijken JP, and Scheffers WA. 1985. Properties of the NAD(P)H-dependent Xylose Reductase from the Xylose-Fermenting yeast *Pichia Stipitis*. Biochemical Journal **226**: 669-677.

Visapaa JP, Gotte K, Benesova M, Li J, Homann N, Conradt C, Inoue H, Tisch M, Horrmann K, Vakevainen S, Salaspuro M, Seitz HK. 2004. Increased cancer risk in heavy drinkers with the alcohol dehydrogenase 1C*1 allele, possibly due to salivary acetaldehyde. Gut **53**: 871-876.

Wang KX and Wang XF. 2004. Cloning and sequencing of cagA gene fragment of *Helicobacter pylori* with coccoid form. World Journal of Gastroenterology **10**: 3511-3513.

Wen Y, Marcus EA, Matrubutham U, Gleeson MA, Scott DR, and Sachs G. 2003. Acid-adaptive genes of *Helicobacter pylori*. Infection and Immunity **71**: 5921-5939.

Wermuth B, Burgisser H, Bohern K, and Von Wartburg JP. 1982. Purification and characterisation of human-brain aldose reductase. European Journal of Biochemistry **127**: 279-284.

Willen R, Carlen B, Wang X, Papadogiannakis N, Odselius R, and Wadstrom T. 2000. Morphologic conversion of *Helicobacter pylori* from spiral to coccoid form. Scanning (SEM) and transmission electron microscopy (TEM) suggest viability. Upsala Journal of Medical Sciences **105**: 31-40.

Yabe-Nishimura C. 1998. Aldose Reductase in Glucose Toxicity: A potential Targt for the Prevention of DiabeticComplications. Pharmacological Reviews **50**: 21-31.

Yum DY, Lee BY, and Pan JG. 1999. Identification of the yqhE and yafB genes encoding two 2, 5-diketo-D-gluconate reductases in *Escherichia coli*. Applied and Environmental Microbiology **65**: 3341-3346.

Zhang Y, and Lee H. 1997. Site-directed mutagenesis of the cysteine residues in the *Pichia stipitis* xylose reductase. FEMS Microbiology Letters **147**: 227-232.

Appendix A

Reagents and Buffers

SDS-PAGE/ Protein Purification Reagents

10 x Phosphate Buffered Saline (PBS)

Reagent	Volume/Quantity
$Na_2HPO_4.2H_2O$ (8 mM)	14.24 g
KH_2PO4 (1.5 mM)	2.04 g
NaCl (137 mM)	80.0 g
KCl (2.7 mM)	2.0 g
• Adjust pH to 7.4 and made up to 1 L final volume	

Bradford Reagent

Reagent	Volume/Quantity
Coomassie Brilliant Blue G	100 mg
96% Ethanol	50 ml
0.85% orthophosphoric acid	100 ml
• Made up to 1 L final volume with distilled water and filtered prior to use	

5X Reducing Sample Buffer

Reagent	Volume/Quantity
Glycerol	5 ml
β-mercaptoethanol	6.25 ml
20 % SDS	5 ml
1.0 M Tris (pH 6.8)	1.25 ml
0.2 % Bromophenol Blue	0.3 ml
• Make up to 25 ml with distilled water.	

Resolving Gel Buffer

Reagent	Volume/Quantity
Tris base	18.165 g
Distilled water	100 ml
• Adjust pH to 8.8 with concentrated HCl.	

Stacking Gel Buffer

Reagent	Volume/Quantity
Tris base	12.11 g
Distilled water	100 ml
• Adjust pH to 6.8 with concentrated HCl.	

10% Ammonium Persulphate (APS)

Reagent	Volume/Quantity
APS	50 mg
Distilled water	1 ml
• Prepared fresh prior to use.	

Water-Saturated Butanol

Reagent	Volume/Quantity
n-Butanol	50ml
Distilled water	50ml
• Solution was mixed vigorously and upper phase used.	

10X Running Buffer

Reagent	Volume/Quantity
Tris base	30 g
Glycine	114 g
SDS	5.0 g
Distilled water	1000 ml
• Diluted 1:10 prior to use.	

Coomassie Blue R-250 Gel Stain

Reagent	Volume/Quantity
Coomassie Brilliant Blue R-250	0.5 g
Methanol	200 ml
Glacial acetic acid	35 ml
Distilled water	265 ml

Destain Solution

Reagent	Volume/Quantity
Methanol	400 ml
Glacial acetic acid	70 ml
Distilled water	530 ml

Immunoblotting

Blocking Solution (5%)

Reagent	Volume/Quantity
Skimmed dried milk powder	5 g
PBS	100 ml

0.1% PBS-Tween Washing Solution

Reagent	Volume/Quantity
Tween 20	1 ml
PBS	1000 ml

Primary and Secondary Antibody Diluent Solution (5%)

Reagent	Volume/Quantity
Skimmed dried milk powder	5 g
PBS	100 ml

Transfer Buffer

Reagent	Volume/Quantity
Tris base	2.9 g
Glycine	1.45 g
SDS	0.185 g
Methanol	100 ml
• Make up to 500ml with distilled water	

Ponceau S Protein Detection

Reagent	Volume/Quantity
Ponceau S	0.2 % (w/v)
TCA	3 % (v/v)
• Staining was carried out until bands were visible and destaining was performed by several washes in deionised water	

Membrane Stripping Buffer

Reagent	Volume/Quantity
Tris base pH 6.8 (62.5 mM)	6.25 ml
β-mercaptoethanol (100 mM)	0.68 ml
SDS (2%)	20 ml
• Make up to 100 ml final volume with distilled water.	

Enhanced Chemillumenscence

Developing Solution

Reagent	Volume/Quantity
Iodophenol	4 mg
Luminol (Sodium Salt)	12 mg
DMSO	0.5 ml
0.1 M Tris (pH 8.8)	50 ml
H_2O_2	18 µl

Prokaryotic Cloning

Luria-Bertani (LB) Broth Medium

Reagent	Volume/Quantity
Gibco® LB Powder	37 g
Distilled water	1000 ml

Antibiotic Selection

Antibiotics	Concentration	Preparation
Ampicillin	100 mg/ml	Prepared in distilled water, sterile filtered (0.2 μ), aliquoted and stored at – 20°C.
Kanamycin	30 mg/ml	
Chloramphenicol	50 mg/ml	Prepared in ethanol, aliquoted and stored at – 20°C.

Plasmid Screening Solutions

Solution II

Reagent	Volume/Quantity
NaOH (1 M)	1 ml
SDS (10%)	0.5 ml
Sterile water	3.5 ml
Prepare fresh before use.	

Lysis Solution

Reagent	Volume/Quantity
Solution II (above)	4 ml
Gel loading buffer	0.9 ml
Sterile water	1.1 ml

Solution III

Reagent	Volume/Quantity
Formic acid (1.8 M), Potassium Acetate (3 M)	3 µl

Competent Cell Preparation Buffers

Washing Buffer

Reagent	Volume/Quantity
1M Tris (pH 8.0)	10 ml
1M $CaCl_2$	50 ml
1M $MgCl_2$	10 ml
Distilled water	930ml

Freezing Buffer

Reagent	Volume/Quantity
Glycerol	15 ml
1M Tris (pH 8.0)	1 ml
1M $CaCl_2$	5 ml
1M $MgCl_2$	1ml
Distilled water	78 ml

Agarose Gel Electrophoresis

TAE Buffer (10X)

Reagent	Volume/Quantity
Tris base	24.2 g
Glacial Acetic Acid	5.71 ml
EDTA, pH 8.0 (0.5 M)	20 ml

Gel Loading Dye (6 x)

Reagent	Volume/Quantity
Xylene cyanol (0.25%)	0.125 g
Bromophenol Blue (0.25%)	0.125 g
Glycerol (30%)	15 g
• Make up to a final volume of 50ml with distilled water.	

Ethidium Bromide (EB) Stock

Reagent	Volume/Quantity
Ethidium Bromide	100 mg
PBS	20 ml

2-D Gel Electrophoresis

Rehydration Stock Solution

Reagent	Volume/Quantity
Urea (8 M)	12 g
CHAPS (2 % w/v)	0.5 g
Bromophenol Blue	trace
• Make up to a final volume of 25 ml with double distilled water. Store in 1 ml aliquots at –20°C. • Before use add 2.8 mg DTT and 5 µl IPG buffer per1 ml aliquot of rehydration stock solution	

SDS Equilibration Buffer

Reagent	Final conc	Volume / Quantity
Tris-HCl (1.5 M, pH 8.8)	50 mM	6.7ml
Urea	6 M	72.07 g
Glycerol (87 % v/v)	30 % (v/v)	69 ml
SDS	2 % (v/v)	4.0 g
Bromophenol Blue	trace	trace
• Make up to a final volume of 25 ml with double distilled water. Store in 20 ml aliquots at –20°C • Before use add 100 mg DTT per 10 ml SDS equilibration buffer		

***H. pylori* Growth Media**

Cryogenic Preservative Freezing medium

Reagent	Volume/Quantity
Brain Heart Infusion Media	1 ml
Glycerol	20 % (v/v)
Horse Serum	7 % (v/v)

Columbia Blood Agar Medium

Reagent	Volume/Quantity
Columbia Agar base	4.1 g
Sterile Horse Blood	7 ml
DENT Supplement	400 µl/100 ml broth

Appendix B

Construction of an Isogenic HpCAD-Negative Mutant of *H. pylori*

B.1 Primer Design, PCR and *Xcm* I Restriction Digests

This appendix outlines the construction of the HpCAD mutant.

All bacterial strains and plasmids used for the construction of the HpAKR mutant were used to construct the HpCAD mutant (see Chapter 5, Table 5.1). The following primers were used for the amplification of the HpCAD (Table B.1).

The PCR products were cut with the restriction enzyme *Xcm* I to ascertain whether the target restriction site was present or absent to allow for the insertion of the *aphA-3* cassette. The restriction site was found to be present only in the HpCAD amplified from *H. pylori* 26695. The PCR amplification was repeated using different template genomic DNA preparations from different strains of *H. pylori* and identical results were obtained.

All subsequent DNA manipulations to generate a HpCAD isogenic mutant were carried out using the HpCAD product amplified from *H. pylori* 26695, as it alone possessed the target *Xcm* I site.

Gene	Primer direction	Primer sequence
HpCAD	Forward	5'– ATG AGA GTT CAA TCT AAA – 3'
HpCAD	Reverse	5'– TTA ATC AAA CGA TTT TTT CAT A – 3'

Table B.1: Primers used for the cloning and construction of HpAKR isogenic mutant.

B.1.1 Insertion of Amplified HpCAD into pGEM-T Easy and *Psi* I Restriction Digestion

The *HpCAD* gene was amplified by PCR using a Taq polymerase without proofreading capacity to generate a product with A' overhangs. The HpCAD amplicon was ligated into the pGEM T Easy vector within the LacZ gene (Refer to Chapter 5, section 5.2.2) (Fig. B.2).

B.1.2 *Xcm* I Restriction Digest of pGEM:HpCAD Construct

The unique *Xcm* I restriction site was the target for insertion of the kanamycin resistance cassette (*aphA-3*). Restriction with *Xcm* I produced a linearised pGEM:HpCAD construct, visualised by an increase in the molecular size of the construct on an agarose gel (Fig. B.3).

The amplification of the *aphA-3* cassette from the pJMK30 plasmid is outlined in chapter 5, section 5.3.2. The primers used for this amplification are outlined in chapter 5, Table 5.3. Prior to the ligation of the *aphA-3* cassette into the *Xcm* I restricted pGEM:HpCAD construct, the overhangs created from the *Xcm* I digested were removed by T4 DNA Polymerase. The construct was transformed into *E.coli* DH5α.

B.1.3 Determination of *aphA-3* Orientation within pGEM:HpCAD::*aphA-3* Construct

The *E. coli* DH5α transformants were selected on the basis of dual antibiotic resistance; ampicillin (50µg/ml) selected for the pGEM-T Easy marker and kanamycin (20µg/ml) selected for insertion of the *aphA-3* cassette.

As both the *aphA-3* insert and linearised pGEM:HpCAD construct had blunt ends, the orientation of the inserted cassette was determined by PCR and subsequently confirmed by DNA sequencing.

During the PCR, the HpCAD forward and reverse primers were used in tandem with standard Kana-L and *aphA-3* primers are detailed below (Table B.2).

These primers were designed to point outwards from the inserted *aphA-3* cassette and consequently when coupled with the HpCAD primers, they provided a useful method to determine the orientation of the cassette. Sci. Ed. software was utilised to predict the fragment sizes of the PCR amplified regions within the pGEM-T Easy construct using different primer combinations. The software also ruled out the amplification of regions using alternative primer combinations (as primers appeared in the same orientation) and thus provided a means of interpreting the resulting PCR fragment sizes.

Five plasmids were isolated from transformed colonies, which had grown on dual antibiotic plates (ampicillin/kanamycin). In all cases the *aphA-3* cassette was found to have inserted in the reverse orientation. The reverse orientation of the *aphA-3* cassette was established using a combination of HpCAD forward and Kana-L primers, which amplified a region of approx 300 bps; the predicted size of this region was 326 bps (Fig. B.4). While a combination of HpCAD forward and AphA3 primers failed to yield a product, this was unsurprising as the reverse orientation of the *aphA-3* primer on the cassette is in the same orientation as the HpCAD forward primer (Fig. B.4)

The resulting pGEM:HpCAD construct containing the inserted kanamycin cassette (*aphA-3*) in the reverse orientation was named pGEM:HpCAD::*aphA-3*. Scientific Educational software was used to simulate a graphical image of the pGEM:HpCAD::*aphA-3* construct (Fig. B.5). This will be referred to as HpCAD mutant from this point.

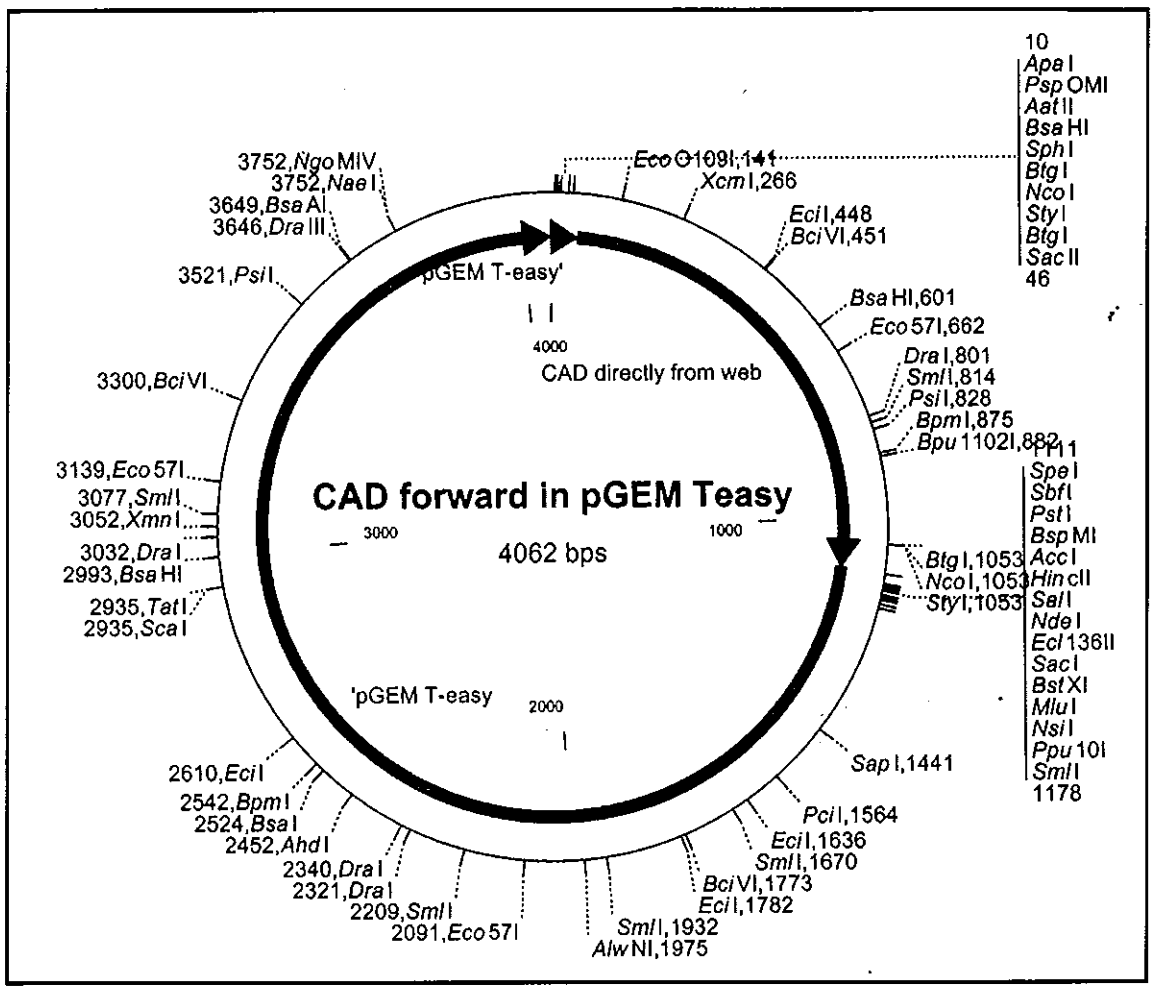

Fig. B.2: The pGEM:HpCAD construct. Scientific Educational software simulation of HpCAD in the forward orientation in pGEM-T Easy vector. The *Psi* I restriction sites are located at positions 828 and 3521

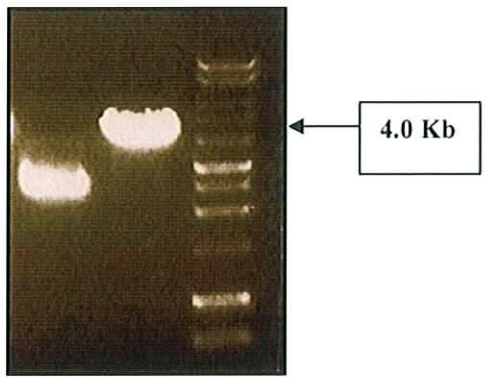

Fig. B.3: Agarose (1 %) gel electrophoresis of *Xcm* I restriction digest of pGEM:HpCAD construct; Lane 1 shows the uncut construct. Lane 2 shows the *Xcm I* digested construct.

Gene	Primer sequence
Kana-L primer	5'-TTA CCT ATC ACC TCA AAT GG-3'
AphA-3 primer	5'-CTG GAT GAA TTG TTT TAG TAC-3'

Table B.2: PCR primers used in combination with HpCAD forward and reverse primers to determine the orientation of the *aphA-3* cassette within the pGEM:HpCAD::*aphA-3* construct.

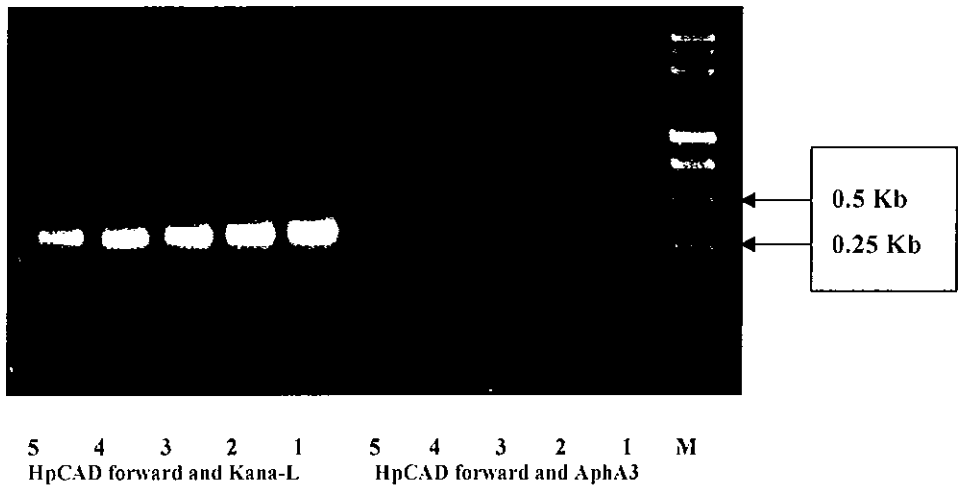

Fig. B.4: Agarose (1 %) gel electrophoresis of the 326 bp region PCR amplified between HpCAD forward and Kana-L primers identifying reverse orientation of kanamycin cassette (*aphA-3*).

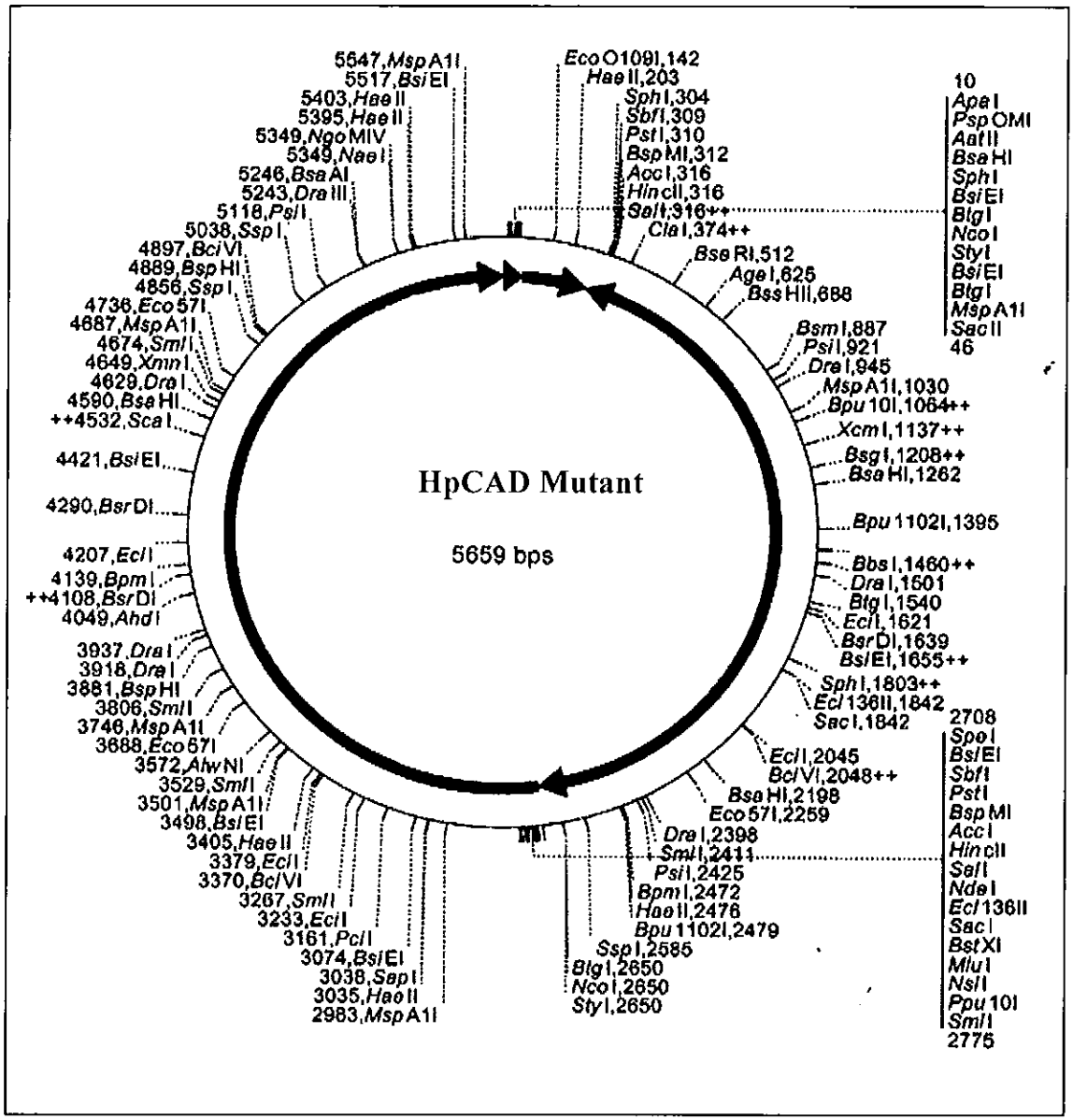

Fig. B.5: Image of HpCAD mutant construct generated using Scientific Educational software

B.1.4 Generation of HpCAD Mutant

Naturally competent *H pylori* (26695 and 1061) cells were transformed with the HpCAD mutant construct, outlined in Chapter 5, section 5.6. As with the HpAKR mutant transformation, transformants were only obtained for *H. pylori* 1061. Again, the event was visualised as a 1.5 Kb shift upwards in the size of the *HpCAD* gene, attributed to the incorporation of the *aphA-3* into the chromosomal gene (Fig. B.6)

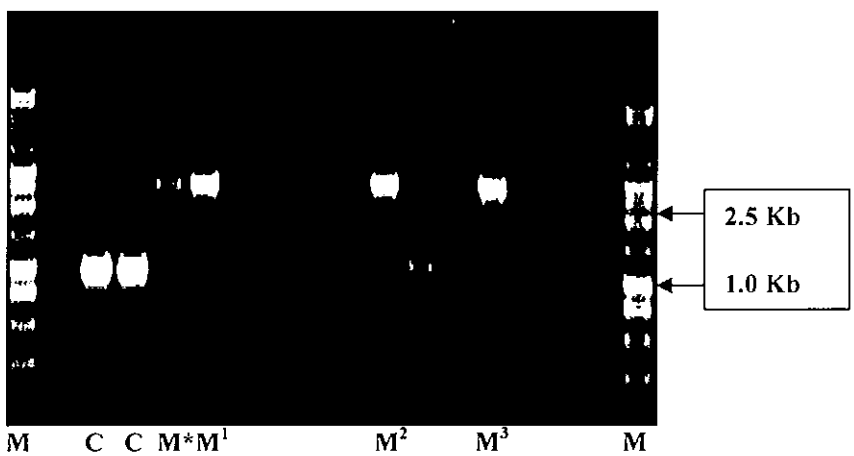

Fig. B.6: Agarose (1 %) gel electrophoresis showing incorporation of the kanamycin cassette (*aphA-3*) into chromosomal DNA of *H. pylori* (strain HpCAD mutant strain); amplification of the HpCAD from the wild type (*H. pylori* 1061) acted as a control (C). Clones M^{1-3} were chosen for further study, (M^{*} was not chosen for further study). Lanes M contain the DNA ladder.